

THESIS FOR THE DEGREE OF LICENTIATE OF ENGINEERING

Time-dependent relaxation of charge and energy  
in electronic nanosystems

JENS SCHULENBORG

Department of Microtechnology and Nanoscience (MC2)

*Applied Quantum Physics Laboratory*

CHALMERS UNIVERSITY OF TECHNOLOGY

Göteborg, Sweden 2016

Time-dependent relaxation of charge and energy in electronic nanosystems  
JENS SCHULENBORG

© JENS SCHULENBORG, 2016

Thesis for the degree of Licentiate of Engineering  
ISSN 1652-0769  
Technical Report MC2-331

Applied Quantum Physics Laboratory  
Department of Microtechnology and Nanoscience (MC2)  
Chalmers University of Technology  
SE-412 96 Göteborg  
Sweden  
Telephone: +46 (0)31-772 1000

**Cover:**

Sketch of an interacting single-level quantum dot, level-shifted to reveal a fundamental relation in the transient heat current.

Printed by Chalmers Reproservice  
Göteborg, Sweden 2016

Time-dependent relaxation of charge and energy in electronic nanosystems  
Thesis for the degree of Licentiate of Engineering

JENS SCHULENBORG

Department of Microtechnology and Nanoscience (MC2)  
Applied Quantum Physics Laboratory  
Chalmers University of Technology

## ABSTRACT

The study of the *dynamics* of strongly confined, interacting open quantum systems has attracted great interest over the past years, due to potential applications in nanoelectronics, metrology as well as quantum information. Most recent experimental and theoretical research in this field has shifted attention towards *electronic heat currents*, recognizing their potential for practical purposes as well as for tests of fundamental theories, and also aiming to control the inevitable heat dissipation of any dynamically operated electronic device.

Using the generalized master equation framework and a novel second quantization approach in Liouville space, the research articles discussed in this thesis contribute to the theory of dynamics in electronic nanosystems in two related ways. On the one hand, we study the voltage-switch induced *transient* electronic charge and heat current out of a single-level quantum dot with strong local Coulomb interaction into a tunnel-coupled reservoir. The first paper discusses how to measure the decay rates governing the transient response of the quantum dot to the voltage switch; the second paper shows how the induced tunneling processes lead to energy dissipation, in time and in the presence of many-body charging effects. On the other hand, we identify a fundamental relation which represents a *generalization of hermiticity* for the effective Liouvillian governing the dissipative, nonunitary dynamics of a large class of tunnel-coupled, *open* fermionic quantum systems. Offering a more *systematic* way to characterize time-dependent decay, two initially surprising observations in the transient heat current out of the quantum dot studied in the papers turn out to be prime manifestations of this relation, and are shown to be of general nature: the existence of a decay rate that only depends on the coupling itself, and the signature of electron-electron *attraction* in the transient dynamics of systems with *repulsive* Coulomb interactions.

**Keywords:** open quantum system, nonunitary dynamics, generalization of hermiticity, electronic nanosystem, quantum dot, voltage switch, transient response, relaxation rate, rate detection, heat current, Coulomb charging energy



## ACKNOWLEDGEMENTS

First and foremost, I would like to thank my supervisor Janine Splettstößer for giving me the opportunity to work as a Ph.D. candidate on a nice project in a nice place, and for her continuous moral and scientific support. Special thanks also go to my co-supervisor Maarten Wegewijs and his current postdoc Roman Saptsov. Without the countless fruitful discussions, and without their ingenious work on the causal superfermion approach and on the derivation of the central formula of this thesis, this work would not have been possible in the present form.

I also would like to thank Maarten<sup>1</sup>, Roman and Maciek Misiorny for their hospitality during my visit at the FZ Jülich in September 2014, and Michael Hell for a very inspirational discussion during his visit at our institute. Furthermore, I thank everyone to whom I had the pleasure of presenting my talks and posters. These sessions were very helpful in refining my understanding of my own project. Of course, I also thank Angelo di Marco and Joren Vanherck for their valuable suggestions on improving this thesis.

Finally, I apologize to everyone that was forced to, and thank everyone that was willing to bear spending time with me. The reader should also note that Giovanni Viola has asked to be mentioned here.

---

<sup>1</sup>Due to the lumped sum of Dutch cookies Maarten has supplied to the author of this footnote, Maarten is officially excused for not having been aware of the author's arrival.



## LIST OF PUBLICATIONS

This thesis presents a summary and an extension to the following two appended papers:

- [I] J. Schulenburg, J. Splettstoesser, M. Governale, and L. D. Contreras-Pulido, “Detection of the relaxation rates of an interacting quantum dot by a capacitively coupled sensor dot”, *Phys. Rev. B* **89**, 195305 (2014).
- [II] J. Schulenburg, R. B. Saptsov, F. Haupt, J. Splettstoesser, and M. R. Wegewijs, “Fermion-parity duality and energy relaxation in interacting open systems”, *ArXiv e-prints* (2015), arXiv:1508.06145.

We always refer to these publications as paper I and paper II, according to the labeling in the list above.



# CONTENTS

<b>Abstract</b>	<b>iii</b>
<b>Acknowledgements</b>	<b>v</b>
<b>List of publications</b>	<b>vii</b>
<b>Contents</b>	<b>ix</b>
<b>1 Introduction</b>	<b>1</b>
1.1 General scientific context . . . . .	1
1.2 Charge dynamics of nanoscale devices . . . . .	3
1.3 Electronic heat currents in nanosystems . . . . .	8
1.4 Organization of this thesis . . . . .	12
<b>2 Time-dependent decay in open fermionic quantum systems</b>	<b>13</b>
2.1 General model . . . . .	13
2.2 The quantum state of the open system . . . . .	16
2.3 Transient open system dynamics after an instantaneous switch . . . . .	18
2.4 The Liouville space of the open system . . . . .	20
2.5 Master equation and transport quantities . . . . .	22
2.6 Time-dependent decay for weakly coupled systems . . . . .	23
2.6.1 Born-Markov approximation . . . . .	24
2.6.2 Time scales, modes and amplitudes . . . . .	25
2.6.3 Statistical interpretation of the reduced dynamics . . . . .	27
2.7 Time evolution beyond the Born-Markov approximation . . . . .	29
<b>3 The fermion-parity duality</b>	<b>33</b>
3.1 Time scales, modes and amplitudes in closed and open systems . . . . .	33
3.2 Mode-amplitude duality for open fermionic systems . . . . .	35
3.3 The fermion-parity mode . . . . .	39
3.4 The amplitude of the fermion-parity mode . . . . .	41
3.4.1 The parity amplitude covector . . . . .	41
3.4.2 The stationary state of the dual model . . . . .	43
3.4.3 The decay process represented by the parity mode . . . . .	44
3.5 Summary . . . . .	46
<b>4 Time-dependent energy relaxation of an interacting quantum dot</b>	<b>47</b>
4.1 Model . . . . .	47
4.2 Reduced density operator of the quantum dot . . . . .	49

4.3	The inverted stationary state . . . . .	51
4.4	Transient heat transport . . . . .	53
<b>5</b>	<b>Detecting the fermion-parity rate</b>	<b>57</b>
5.1	Sensor quantum dot detector . . . . .	57
5.2	Time-resolved readout of the quantum dot dynamics . . . . .	59
5.3	Capacitive detector backaction . . . . .	61
<b>6</b>	<b>Conclusion</b>	<b>65</b>
6.1	Summary . . . . .	65
6.2	Open questions . . . . .	66
	<b>Appendices</b>	<b>67</b>
<b>A</b>	<b>Coupling kernel in the Born-Markov approximation</b>	<b>69</b>
A.1	Superfermions and tunneling Liouvillian . . . . .	69
A.2	Lowest order coupling kernel in the time and frequency domain . .	71
A.3	The unique stationary state . . . . .	75
<b>B</b>	<b>Current kernels</b>	<b>79</b>
B.1	Particle current . . . . .	79
B.2	Heat current in the Born-Markov, single-channel limit . . . . .	80
<b>C</b>	<b>Influence of the fermion-parity mode</b>	<b>85</b>
	<b>References</b>	<b>89</b>
	<b>Appended papers</b>	<b>101</b>
	<b>Paper I</b>	<b>103</b>
	<b>Paper II</b>	<b>119</b>

# 1 Introduction

## 1.1 General scientific context

At its core, the general topic of this thesis and the two appended papers I and II – the *relaxation behavior* of *open* systems – relates to two fundamental properties of practically any realistic physical system of interest in experiments or in applications. First, almost all systems are open, that is, they couple in some form to their environment, which could be a measurement device, an electromagnetic field, or simply the matter surrounding the device. Second, for a device to be useful, an external agent must, sooner or later, modify or operate it in some time-dependent, periodic or aperiodic fashion: an experimentalist tunes and measures a sample, a transistor on a chip is switched on and off to control an electrical current. Any such operation inevitably drives the open system away from the stable stationary state it could maintain in the presence of its environment, and the response of the system is to relax to a new stationary state, typically by dissipating energy into the environment. It is this relaxation process which is of interest here.

The controlled time-dependent operation of a device under the influence of relaxation becomes particularly interesting – and is still a matter of active experimental and theoretical research – once the functionality of this device relies on the *quantum mechanical properties* of individual particles or excitations. This is exactly the case for the class of systems this work addresses: *electronic* nanoscale devices, in particular single-electron transistors (SETs) [1–7] or nanoscale capacitors [8–13]. Driven by the continuous downscaling in the computer industry and the potential perspective of building quantum computers [14], such open *quantum* systems have gained much interest for potential applications. Most importantly, they allow to time-dependently control the emission, absorption and detection *individual* electrons or spins [12, 13, 15–25].

One property of relaxation that is highly relevant for this type of time-dependent manipulation of electronic nanosystems is the simple fact that relaxation does not take place instantly, but rather on a typical relaxation time. Namely, once the time between two subsequent operations on the device becomes as small as this relaxation time, the *transient behavior* of the system, that is, the detailed time-dependence of the relaxation process, plays a crucial role. On the negative side, the relaxation time yields an upper bound on the frequency at which a certain device can work reliably, meaning here the frequency at which it can, e.g., emit or absorb single electrons. However, on the positive side, the transient dynamics

can also be an additional source of experimentally extractable information, since the relaxation behavior typically reflects properties which characterize the device of interest. Time-dependently driven open quantum systems are therefore also a topic of more fundamental research, studying, e.g., non-Markovian dynamics [26–36], qubit gate control [37–39], or the role of fluctuations [13, 23, 40, 41].

A second general consequence of relaxation is that the energy dissipated in the decay process heats up the environment. In fact, this is already relevant for commercially available technology, such as CPUs that are typically operated at high frequencies and thus need to be cooled in order to remain functioning. However, for the nanoscale systems of interest here, heat dissipation is of particular interest. For practical applications, it is important that these devices rely on charge and energy quantization effects which typically only play a role at temperatures much lower than room temperature. Apart from motivating the development of more efficient external cooling methods to maintain such temperatures, this has been one driving force behind the research on so-called *nanoscale heat engines* [42–50]. Such engines can in principle be integrated directly into nanoscale circuits in order to convert parts of the thermal energy of electrons into directed electrical currents. From a more fundamental point of view, the possibility of time-dependent manipulation of individual electrons also naturally leads to questions about the *time-dependent heat current* which is carried by such individual electrons. This concerns, e.g., how heat flow through a nanoscale heat engine can be controlled time-dependently [51–57], but also how the energy of individual particles relaxes as a function of time [58, 59], and in how far such transient electronic heat currents contain more information about the physical system than the charge currents.

As we detail below, the appended papers I and II contribute in several ways to the above described, ongoing research on the time-dependent behavior of electronic nanosystems. From the point of view of applications, paper I theoretically studies how to use a single-electron detector in order to *measure* the typical relaxation times of a nanoscale capacitor with strong level quantization and Coulomb interaction. While readout of *charge* relaxation rates for such devices has already been implemented experimentally [60], the paper shows that a detector that is capacitively coupled to the capacitor has in fact access to an additional, not yet measured time scale which contains further information about the time-dependent relaxation of the system [61, 62]. Paper II studies the time resolved *electronic heat dissipation* of the same nanoscale capacitor, and demonstrates that due to the decay of the Coulomb charging energy, it is exactly this additional time scale that paper I suggests to measure which becomes highly relevant for the heat current. From a more theoretical point of view, paper II also identifies a fundamental relation that dictates the nonunitary decay dynamics of a large class of fermionic open quantum systems, in a way that is analogous to how hermiticity of the Hamiltonian dictates the time evolution of closed quantum systems. Since it is

the transient heat dissipation of the nanoscale capacitor which most naturally exposes the physical consequences of this relation, paper II further motivates recent endeavors to experimentally realize time-resolved measurements of energy quanta carried by individual particles [58, 59].

## 1.2 Charge dynamics of nanoscale devices

The basic building blocks of any classical electrical circuit are characterized by an electrical resistance  $R$ , a capacitance  $C$ , and also an inductance  $L$ . On a *macroscopic* level, these key quantities derive entirely from the geometry, as well as from the phenomenological properties of the circuit elements and their materials. Together,  $R$ ,  $C$  and  $L$  determine the time scales for the dynamic response of the electrical current to some externally applied voltages or a non-stationary charge distribution in the circuit. A simple example is the classical RC-element: a capacitance  $C$  and the electrical resistance  $R$  that is connected to the capacitor yield the typical time scale on which the capacitor is charged or discharged, known as the RC-time  $\tau_{RC} = R \cdot C$ .

However, once the electrical circuit is downsized to the nanoscale, this simple picture has to be modified in several ways. One effect arises when a capacitance  $C$  of a device becomes small enough that the Coulomb energy  $E_C = e^2/2C$  to charge the system with an individual electron<sup>1</sup> exceeds the energy provided by the applied voltage or thermal fluctuations<sup>2</sup>. Namely, as illustrated in the upper panel of Fig. 1.1(a) and first shown for small metallic tunnel junctions by Fulton et al. [1], the system can reach a state in which transport to and from the device is completely blocked; the system exhibits what is known as *Coulomb blockade*. This effect causes the device to be charged or discharged in discrete steps of individual electrons when the electrochemical potential of the device is decreased or increased compared to the potential of the connected circuit.

Another important point is that once the lateral dimensions of a nanoscale device are on the order of the typical electron wave length in the circuit, the charging dynamics are determined by an effective charge relaxation resistance and electrochemical capacitance [8–10]. These quantities differ from their classical counterparts by taking into account the effect of the electronic density of states of the components in the system. In other words, the capacitance and resistance directly reflect the quantum mechanical nature of the device: the nanoscale device becomes a *quantum device*. A specific example of such a quantum device is explained in more detail in the lower panel of Fig. 1.1(a) and in Fig. 1.1(b): the semiconductor based, gate-defined *quantum dot* [64–68], which laterally confines electrons in all 3 dimensions and therefore exhibits pronounced level-quantization

<sup>1</sup>In the constant interaction approximation.

<sup>2</sup>This typically corresponds to lateral dimensions  $\lesssim 100$  nm.

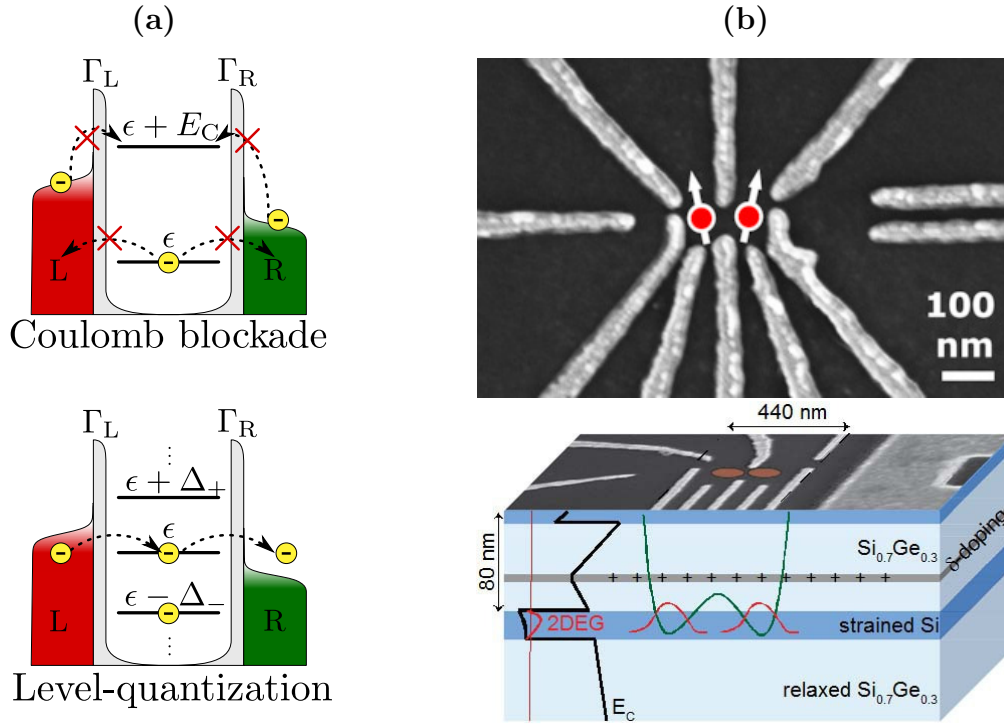


**Figure 1.1:** (a): Illustration of Coulomb blockade (top panel) and level quantization (bottom panel) in an electronic nanodevice. In each case, the system couples via tunnel barriers  $\Gamma_L$  and  $\Gamma_R$  to a left (L) and right (R) lead with biased chemical potentials  $\mu_L > \mu_R$ . In case of Coulomb blockade, the additional charging energy  $E_C$  completely blocks transport in and out of the system. For large level splittings,  $\Delta_{\pm} > \mu_L - \mu_R$ , and a single level  $\epsilon$  in the bias window  $\mu_L > \epsilon > \mu_R$ , it is mainly (apart from level broadening due to the coupling) electrons with this specific energy  $\epsilon$  that can tunnel through the quantum dot. (b): Example of heterostructure based, gate-defined quantum dots. The top panel shows a micrograph of two gate defined quantum dots. The white regions indicate gate electrodes that generate an electrostatic potential beneath the surface of the shown sample, the red circles mark electrons which are, in this case, spin aligned and occupy two adjacent quantum dots. The lower panel illustrates how the electrons are confined. The movement perpendicular to the sample surface is restricted by the electrochemical potential landscape of the stacked SiGe/Si layers, trapping electrons in a 2 dimensional electron gas (2DEG) within the thin Si layer. Inside this 2DEG, the electrons are further confined to “zero-dimensional” quantum dots via the electrostatic potentials generated by the gate electrodes on top of the sample surface. **Source:** [63].

effects. This kind of quantum dot is particularly interesting for this work, as it can be easily integrated into an electrical nanocircuit, and since the applied gate potentials enable a *time-dependent control* of the physical properties of the quantum dot. Most importantly, the typical energy splitting  $\Delta$  in the discrete, quantum mechanical level spectrum of these systems can be tuned to be as large, or even much larger than the Coulomb charging energy  $E_C$  [69]. This allows such a device to not only be charged by individual electrons, but furthermore makes it

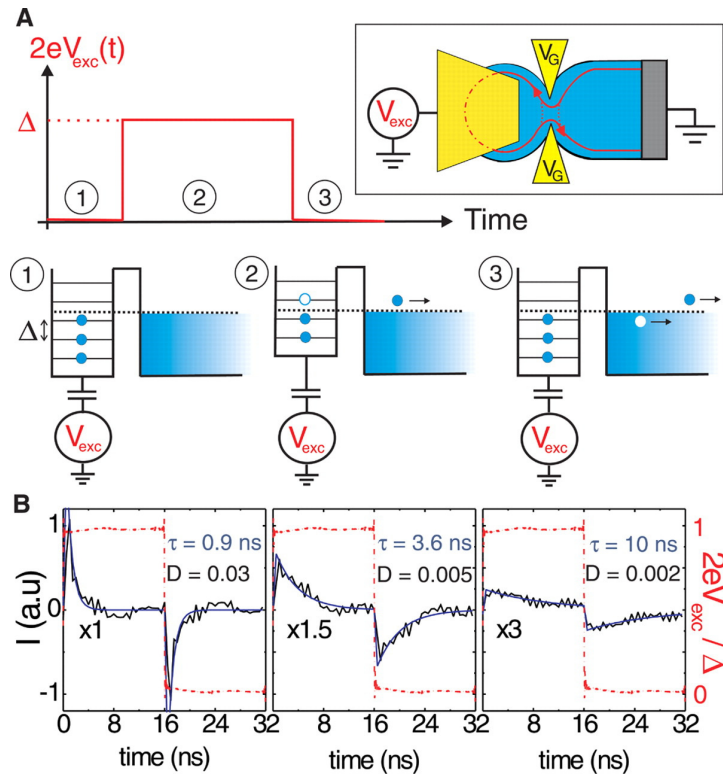


**Figure 1.2:** Panel A shows a quantum capacitor [11] that is used as a single electron source [12]. An ac top gate voltage  $V_{exc}$  is applied to a GaAs heterostructure based quantum dot in order to shift its discrete energy level spectrum. Thereby, the device emits single electrons at a fixed energy and spin via a quantum point contact (QPC) which acts as tunnel barrier between the dot and the outside reservoir, and whose conductance is voltage-controlled by  $V_G$ . The energy-splitting inside the quantum dot is denoted by  $\Delta$ . Panel B shows, for different QPC conductances  $D$ , experimentally obtained time traces of the applied voltage pulses and the transient response of the quantum dot to these pulses, as indicated by the average time-dependent charge current  $I(t)$  out of the dot. The measured exponential decay is governed by the typical response time  $\tau$  of the system. **Source:** [12].

possible to filter particles with a *specific and tunable energy*<sup>1</sup> [4–6, 68].

The key application of the quantization effects in nanoscale devices which we aim to address here is the dynamically controlled emission and absorption of single electrons via *electron tunneling*. This has already led to technologies such as the single-electron transistor [1–7] or the quantum capacitor [11–13], and opens up new perspectives for, e.g., quantum information processing [12, 19] or metrological purposes such as the redefinition of the Ampère [24, 70–73].

The basic principle is illustrated in Fig. 1.2, showing the quantum dot based single-electron capacitor which was first experimentally studied by Gabelli et al. [11], and later used as a single-electron source by Fève et al. [12]. At some

<sup>1</sup>Within the uncertainty given by the level broadening due to higher order coupling effects.

initial time  $t_0$ , the discrete spectrum of the quantum dot is rapidly shifted by an external gate potential, such that one singly-occupied<sup>1</sup> energy level is lifted above the Fermi edge of the tunnel-coupled reservoir<sup>2</sup>. As a response to this shift, the particle tunnels out of the dot on a time scale given by the typical charge relaxation time of the quantum dot. At some later time  $t > t_0$ , the dot potential is shifted back and the dot is recharged.

The successful operation of such single-electron sources requires knowledge about the transient quantum dot behavior: if the circuit is, e.g., operated at a frequency that is too high compared to the decay times, the electrons do not have enough time to leave or enter the dot. Experimentally, the relevant relaxation times can be determined with detectors which are sensitive enough to detect single electrons, and which possess a bandwidth that is high enough to perform *time-resolved measurements* [15–22, 24]. For the given example in [12], decay times on the order of a few nanoseconds have been obtained [Fig. 1.2]. A theoretical understanding can be developed by describing the response to an instantaneous level shift with a master equation and Fermi’s Golden rule [74]. This relies on the fact that for the systems of interest here and in the appended papers, the *tunnel coupling is assumed to be weak*, meaning that the typical tunneling rates are sufficiently small compared to the frequencies of thermal fluctuations in the coupled environment. Publications by Splettstößer et al. [75] and Contreras et al. [61] have applied this master equation approach to the situation shown in Fig. 1.3. In this system, the level-splitting  $\Delta$  is large enough that only a *single* spin-degenerate<sup>3</sup> level is relevant for the emission and absorption of electrons, but still small compared to the bandwidth  $\Delta E_B$  of the environment (wide-band limit). Furthermore, the on-site Coulomb repulsion  $U$  is assumed to be both weak enough to allow for double occupation, but large enough to see Coulomb blockade effects [1]. Altogether, such single-level systems are thus operated in the regime  $\Delta E_B \gg \Delta \gg U \gg T$ .

The first important result of [75], which has subsequently been verified experimentally [60], is that if the electronic level position of the dot is tuned into the Coulomb blockade regime [Fig. 1.3], the charge relaxation rate is enhanced<sup>4</sup> compared to the rate for levels outside of this regime, as a consequence of the spin-degeneracy. An even more striking result from [61] is, however, that the time-dependent quantum dot occupation probabilities are governed by an additional decay rate, which, unlike the charge and spin rate, is independent of the temperature, the level position, and the Coulomb interaction strength; it in fact only depends on the properties of the tunnel barrier itself. The paper [61] has shown observables whose time-dependent averages decay at this rate, and has

<sup>1</sup>Note that a strong magnetic field is applied in the described experiment.

<sup>2</sup>The quantum dot in fact tunnel couples to a quantum hall edge channel.

<sup>3</sup>In contrast to [12], the system in [61, 75] does not include a magnetic field.

<sup>4</sup>By contrast, the spin relaxation rate is reduced.

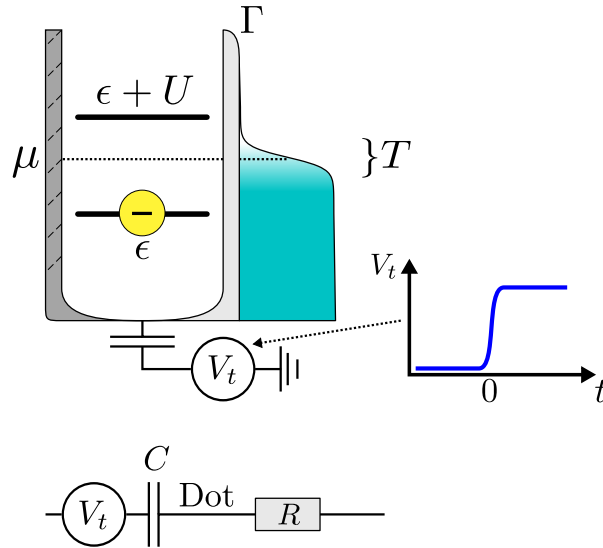


**Figure 1.3:** Sketch of a quantum dot capacitor as considered by [61, 75]. Only a single spin-degenerate level  $\epsilon$  that can be tuned time-dependently with the external gate potential  $V_t$  is available for charging via a tunnel-coupled reservoir. Since an additional electron also needs to pay the Coulomb charging energy  $U$  to occupy the dot if the level is already singly occupied, the level position shown in the figure leads to Coulomb blockade. Note that the system can also be considered as a quantum RC-circuit: the dot constitutes one plate of the capacitor  $C$ , and the tunnel barrier as well as the reservoir yield the circuit resistance  $R$ .

furthermore suggested a method to measure the rate using the above mentioned single-electron detection techniques. Yet, the paper has left it open how exactly this measurement should be implemented, and what the actual *physical meaning* of this rate and its remarkable protection against any changes of most of the system parameters is. Subsequent works from Saptsov et al. [62, 76] have related the rate to the fundamental quantum mechanical principle of *fermion-parity superselection*<sup>1</sup> [77–80], thereby showing that the rate exists even for strong tunnel couplings and non-Markovian time evolution, and furthermore coining the expression “fermion-parity rate”. However, a satisfactory explanation for the *physical meaning* of this rate still has not been provided.

The two appended papers I, II and this thesis attempt to shed more light onto this problem. From the more applied point of view, paper I picks up the suggestion from [61] to measure the fermion-parity rate by modeling a concrete setup of a detector that is capacitively coupled to the quantum dot discussed in [61, 75]. The paper establishes a protocol that is suitable to extract this rate, and also accounts for capacitive backaction effects exerted from the detector onto the dot to be measured. In other words, the paper demonstrates that the fermion-parity

<sup>1</sup>The fermion-parity superselection principle prohibits any physical quantum state to be in a quantum superposition of a many-body state with an even fermion number, and another many-body state with an odd fermion number.

rate has a *measurable* influence.

Publication II more fundamentally shows that the fermion-parity rate is a prime manifestation of a newly found, general duality relation between the decay modes and the corresponding excitation amplitudes in the dynamics of a large class of open fermionic systems, including the quantum dot capacitor considered in [61, 62, 75, 76]. This relation essentially restricts the degrees of freedom in the *nonunitary* decay dynamics of dissipative, open quantum systems in a way that is analogous to how hermiticity of closed system Hamiltonians guarantees the dynamics of closed systems to be unitary. As publication II and chapter 3 of this thesis explain, this restriction in the dynamics not only dictates the existence of the fermion-parity rate and its sole dependence on the tunnel barrier properties. In fact, it also offers new insights into the interpretation of this so far elusive rate.

The second essential point presented in paper II is that whereas the charge relaxation dynamics of the single-level quantum dot capacitor are not influenced by the parity rate, the decay of the transient *heat current* carried by the tunneling electrons is in fact even *dominated* by this rate. To appreciate the relevance of paper II and the parity rate, it is thus also crucial to understand why electronic heat currents are generally of interest in such nanoscale devices. In the following section 1.3, we discuss this topic in more details.

## 1.3 Electronic heat currents in nanosystems

A formidable challenge for both the practical application as well as the fundamental physical understanding of electronic nanodevices is to study and control the *heat* that is dissipated with each operation cycle. While heating is already a major problem for current technology such as CPUs, it becomes an even higher obstacle for nanodevices which operate time-dependently on single electrons, as described in the previous section 1.2. One issue is that in order to exploit the effects of level-quantization and Coulomb blockade, one needs to make sure that the electronic<sup>1</sup> temperature  $T$  of the device always remains small compared to the typical level-splitting  $\Delta$  and charging energy  $E_C$ , meaning  $E_C, \Delta \gg T$ . For the quantum dot devices of interest here, this corresponds to temperatures which are at least below  $T \lesssim 100$  K, but in many cases rather on the order of  $T \sim$  K or even less [69]. External cooling with modern cryostats is often capable of maintaining the necessary temperatures, but it requires a lot of money and resources.

Next to this very practical problem, there are further reasons why heat currents are especially interesting for the electronic nanosystems addressed here. The main

---

<sup>1</sup>Electrons generally dissipate their energy via several relaxation channels, namely scattering with phonons, photons or other electrons. What is, however, critical for the operation principle of electronic devices, and what is characterized by the electronic temperature, is the thermal excess energy that is carried by the electrons themselves.

point is that time-dependent operation on individual electrons also implies a time-dependent flow of energy that is carried by these individual electrons. This gives rise to very basic questions: How can one measure and even define the energy of a single electron in an open system with quantum correlations and many-body interactions? How is heat time-dependently dissipated by these electrons in a relaxation process, and in what way are such transient energy dynamics relevant for nanosystems that rely, e.g., on energy filtering [Fig. 1.1(a)]? Despite the fundamental nature of these questions, many of them are also relevant for applications, since they in fact relate to the more practical issue of controlling heat dissipation as an undesired source of perturbation for electronic nanosystems. A prominent example which illustrates this, and which we therefore discuss more in detail in the following, are so-called *nanoscale heat engines* [48–50, 81–84].

The idea of such heat engines is to employ the same type of quantum device that is shown in Sec. 1.2, and that is used to control the flow of single charges, in order to convert the thermal energy of electrons into electrical energy. One advantage of nano heat engines is that they could in principle be integrated directly into the nanocircuits which need to be cooled. However, the main reason why these devices have originally been studied [42–47], and why they have recently attracted attention [50, 85–89], is that their efficiency can benefit from the quantization of charge and energy. Similarly to classical thermoelectric materials, one uses that thermal gradients  $\Delta T = T_{\text{hot}} - T_{\text{cold}}$  induce directed charge currents  $I$ . These currents carry away energy contained in the input heat current  $J$  from the hot source which in principle yields usable electrical output power  $P = I \cdot V$  against a load voltage  $V$ . The performance of nanoscale heat engines is also characterized by the same quantities that are relevant for classical thermoelectrics: the maximum output power  $P_{\text{max}}$  and the efficiency  $\eta = P/J$  compared to the Carnot efficiency  $\eta_C = 1 - T_{\text{cold}}/T_{\text{hot}}$ , in particular at maximum output power,  $\eta_{\text{max}} = P_{\text{max}}/J$  [90, 91]. The crucial difference is that due to the effect of level-quantization and Coulomb blockade, these indicators can in general not anymore be determined by considering currents as a *linear response* in the applied temperature- and electric field gradients [92–97]. As a result, the efficiency is not anymore determined, and hence, restricted by the figure of merit  $ZT = \sigma S^2 T / \lambda$ , relating the Seebeck coefficient  $S$  to the electrical and thermal conductivities  $\sigma$  and  $\lambda$  [96].

Currently studied nanoscale heat engines operate autonomously under *stationary conditions* – and hence mostly maintenance free. An important example for this work, which indeed shows an enhanced efficiency, is the three-terminal *Coulomb blockade heat engine* that was theoretically proposed by R. Sánchez et al. [85] and experimentally realized by Thierschmann et al. [89]. Figure 1.4 and its caption explain the working principle: a single-level<sup>1</sup> quantum dot is tunnel-coupled to one hot reservoir at temperature  $T_h$  – the heat source – and capaci-

---

<sup>1</sup>We stress again that a single-level dot is effectively realized by having a large level splitting  $\Delta$  compared to the temperature(s)  $T$  in the environment.

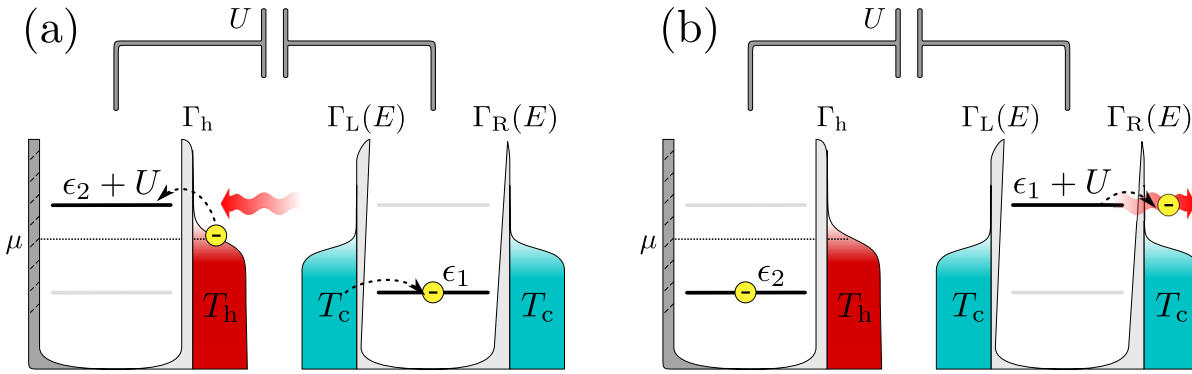


**Figure 1.4:** Illustration of the Coulomb blockade heat engine studied in [85, 89]. Two (spinless) electronic levels  $\epsilon_1$  and  $\epsilon_2$  are capacitively coupled with coupling strength  $U$ , and tunnel-coupled to reservoirs at different temperatures  $T_h > T_c$ . The tunnel barriers to the two cold reservoirs are asymmetric and energy-dependent, such that electrons at energy  $\epsilon_1$  preferably tunnel from the left reservoir, and electrons at energy  $\epsilon_1 + U$  mostly tunnel to the right reservoir. The levels are tuned such that only one of the two dots can be stably occupied, due to the mutually induced Coulomb blockade. The working principle is as follows: given that an electron has entered level 1 from the left, the hot reservoir might thermally excite electrons which have enough energy to pay the additional charging energy  $U$  required to tunnel to level 2 (a). This then causes the electron on level 1 to tunnel out, mostly to the right reservoir due to the asymmetric tunnel barriers (b). Altogether, the charging energy is transferred from the hot to the cold reservoir, and a directed charge current is generated.

tively coupled to another single-level quantum dot which tunnel couples to two cold reservoirs at temperature  $T_c$ . Both level-positions are tuned such that they mutually induce Coulomb blockade via the capacitive coupling. Hence, if a thermally excited electron tunnels from the hot reservoir to the coupled quantum dot, there is a finite probability that an electron occupying the dot coupled to the cold reservoir is pushed out, thereby taking away the charging energy. If the couplings to the two cold baths are furthermore asymmetrically energy-dependent, this yields a *directed* current into the cold reservoir.

Although this heat engine operates only at *stationary* conditions, there are several reasons why it is still interesting for this work. First, the system is formally identical<sup>1</sup> to the detector setup studied in paper I. If such a heat engine is integrated into a circuit which is driven time-dependently, the dynamic capacitive backaction effects<sup>2</sup> studied in paper I will become relevant. Second, it is already noted [50, 85] that whereas the device can in principle reach Carnot efficiency, the output power is relatively small (single-electron tunneling), and the Carnot limit is only assumed at zero output power  $P = 0$ . While improved devices with higher output powers have been studied [86–88], this nevertheless emphasizes the

<sup>1</sup>Apart from the spin-degeneracy and the on-site interaction in the dot to be measured.

<sup>2</sup>We here refer to the dynamics of the open system state; the interaction itself is described *electrostatically*.

desire to have more means or knobs to play with in order to increase the thermo-electric performance. Energy harvesting from phonons [98–101] or other bosonic excitations [50, 102, 103] is one option; another way is time-dependent control.

A heat engine that is time-dependently driven by an external agent loses, by definition, its advantage of operating autonomously, and the work done by the time-dependent driving is also expected to lead to additional heat dissipation. The benefit of time-dependent control is, however, that it also breaks time translational invariance. Under stationary conditions, the transport properties and the performance, as indicated by, e.g., the figure of merit  $ZT$ , are restricted by microscopic time-reversal symmetry [104]. By contrast, the transport behavior and the efficiency of time-dependently driven heat engines are no longer restricted in this way. What is now crucial for us is the following: in order to benefit from time-dependent control in nanoscale heat engines, one also has to understand transient electronic *heat* currents, for the same reason why transient *charge* dynamics are important for the time-dependent control of single charges [Fig. 1.1].

Theoretical investigations of time-dependent heat currents and work extraction in electronic nanosystems, in particular quantum capacitors, have gained popularity since the last decade [51–57]. One recently published example is a study of a *dynamic* linear response theory [57]. It predicts that for a single electronic level  $\epsilon$  coupled to two leads at different temperatures, step-like control of the level-position  $\epsilon(t)$  can increase the efficiency by a factor of up to 4 compared to the efficiency under stationary conditions. Nevertheless, this line of investigation still faces major challenges. Apart from the fact that experiments have only just begun to explore time-resolved measurements of energies carried by single charges in an electronic circuit [58, 59], there are also more fundamental problems to be solved. In *strongly tunnel-coupled* open systems, it is already difficult to *find a definition* of the time-dependent heat current that is consistent with thermodynamic laws [105, 106]. If furthermore *strong local interactions* are present, even *weakly* coupled devices with a clear definition of time-dependent heat currents become of fundamental interest, since the dissipation of many-body charging energies leads to a breakdown of the *tight-coupling* picture: the time-dependent electronic heat current is not anymore given by a constant energy quantum that is carried by *each* electron, and hence not anymore proportional to the charge current [50].

Paper II addresses the latter issue, by studying the level-shift induced, transient electronic heat current out of a single-level quantum dot with strong local interactions,  $U/T \gg 1$ , into a weakly tunnel-coupled fermionic bath. The paper shows that the dominating time scale for the dissipation of the Coulomb energy is *not* the charge relaxation rate which exclusively governs the charge current, but instead the fermion-parity rate [61, 62] that we have mentioned at the end of section 1.2. This result is expected to be relevant for time-dependent heat control in any nanodevice which is based on strong level-quantization and strong local interaction effects leading to Coulomb blockade.

Publication II furthermore emphasizes that the transient heat current most naturally exposes the fundamental *duality relation* that the paper has identified in the transient response of a large class of fermionic open systems. The paper therefore suggests and motivates further experimental studies on time-dependent single-electron heat currents: their inherent dependence on many-particle effects through the dissipation of the interaction energy allows to probe a general symmetry relation in the *dynamics* of many-body physics – something that is completely invisible to single-particle observables such as the charge current.

## 1.4 Organization of this thesis

Having pointed out the scientific context and value of the appended papers I and II, the purpose of the remainder of this thesis is, on the one hand, to review the theoretical background knowledge necessary to understand these papers. On the other hand, we also intend to summarize as well as slightly expand on the main results of the papers. The topical focus of this thesis is clearly on the implications of paper II; paper I is considered and reviewed as far as its insights relate to this general focus. The detailed structure is as follows.

First, chapter 2 gives an overview over the generalized master equation approach which we employ to theoretically study time-dependent decay in open fermionic quantum systems. With details being discussed either in the appendices to this thesis and the papers, or in the cited references, the chapter mainly focuses on explaining the crucial steps from a very general starting point – the definition of an open system and its time-dependent quantum state – towards a concrete motivation for the study presented in chapter 3: the mode-amplitude duality relation identified in paper II. The paper derives this duality under very general assumptions for a broad class of models, but demonstrates its usefulness for the *concrete* physical problem of time-dependent electronic heat dissipation from a single-level quantum dot. Chapter 3 explains in detail how the duality and its application provide theoretical insights in a more general, less model specific context. As such, chapter 3 can be regarded as an extension of the first part of paper II.

Chapter 4 mainly summarizes the second part of paper II, which shows specific results for the transient electronic heat current out of the single-level quantum dot, and which links these results to the duality relation. However, since the paper gives only a brief description of the model and the used methods, the chapter begins with a background theory part which is more detailed in those aspects that were either short or omitted entirely in paper II. Finally, chapter 5 gives a review of the decay rate detection protocol discussed in paper I. Since this paper contains, in contrast to paper II, already a very detailed background theory part as well as some more formal discussions, chapter 5 relies mostly on intuitive, pictorial illustrations and explanations. It furthermore incorporates, to a small extent, later obtained insights from paper II and chapter 3 into the discussion.

## 2 Time-dependent decay in open fermionic quantum systems

This work mainly focuses on the time resolved charge and heat transport through nanoscale quantum capacitors [8, 51–59, 61, 75, 107, 108], and this chapter introduces the basic theory that is required to understand the time evolution of these open quantum systems. The main emphasis is on systems that couple *weakly*, in a sense defined below, to their environment via quantum tunneling, as this case is of main interest in the appended papers I and II. However, a large part of the more general theoretical insights presented in chapter 3 applies to dynamical problems emerging in a *broad* variety of modern and relevant fields of physics, ranging from qubit dynamics [37–39] to cold fermionic gases [109–112]. In order to appreciate this generality, parts of the following treatment are extended beyond the weak coupling theory. We start by establishing the class of time-dependent models for open systems that we aim to discuss.

### 2.1 General model

The model picture of open fermionic quantum systems addressed in this work is sketched in Fig. 2.1. The figure shows a central region  $C$  and a number of contacts in its environment, both occupied by electrons or, more generally, fermionic quasi-particles. The central region and the contacts shall be spatially defined by the electrochemical potential landscape, indicated by the gray shades. The contacts are characterized by areas of roughly constant potentials  $\mu_r$ , and are separated from the central region by potential barriers  $\Gamma_r$  that are thin enough to allow for quantum tunneling. The externally tunable gate potentials  $V_g$  in Fig. 2.1 shape the potential landscape together with the underlying ion lattice and possible magnetic fields, thereby allowing to define the open system and the thin tunnel barriers. Typical experimental realizations are, e.g., two dimensional electron gases within GaAs or SiGe heterostructures that are electrostatically confined by the gate electrodes, see Fig. 1.1(b).

In this work, we study how the quantum state describing only the electrons or fermionic quasi-particles occupying the open system  $C$  evolves in time under exchange of (quasi-)particles with the environment via tunneling. We are not interested in any coupling between these particles and phononic or photonic excitations. The effect of the external fields is accounted for implicitly via their

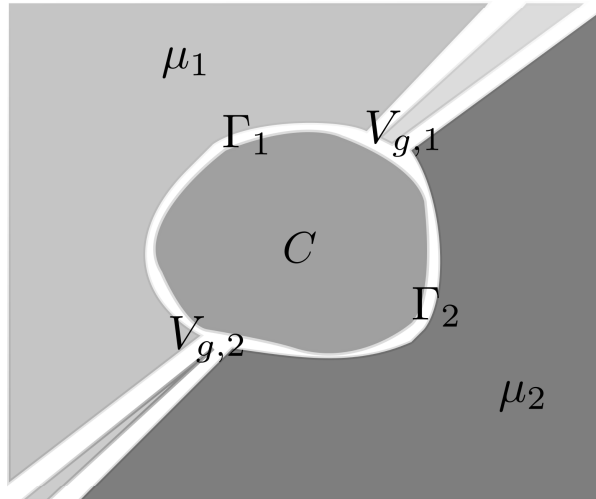


**Figure 2.1:** *Simplified picture of the potential landscape for the class of open fermionic quantum system investigated in this work. The open system is the central region  $C$  which is coupled via tunnel barriers  $\Gamma_r$  to several fermionic reservoirs  $r$  at electrochemical potential  $\mu_r$ . The potential landscape as indicated by the gray and white shades is externally tunable via gate potentials  $V_g$ .*

static effect on the potential landscape, and consequently, on the energy eigenstates of the fermionic system. With these assumptions, the Hamiltonian of the full system,  $H^{\text{tot}}$ , can generally be decomposed into a local part, an environment contribution, and the tunnel coupling:

$$H^{\text{tot}} = H + H^{\text{R}} + H^{\text{T}}. \quad (2.1)$$

The local dynamics of the open subsystem is governed by  $H$ .

$$H = \sum_j \epsilon_j d_j^\dagger d_j + H^{\text{int}}. \quad (2.2)$$

The first term introduces creation ( $d_j^\dagger$ ) and annihilation operators ( $d_j$ ) for fermionic (quasi-)particles in the single-particle states  $|j\rangle$ . These states are energy eigenstates of only the part of the full single-particle Hamiltonian which acts on the subspace of basis states localized within the open subsystem; the states  $|j\rangle$  in fact *define* the open system. The energy associated with  $|j\rangle$  is denoted  $\epsilon_j$ , fully characterized in terms of the multi-index  $j = l_j, \sigma_j, \dots$  labeling the orbital  $l$ , the spin  $\sigma = \uparrow, \downarrow$  with respect to a fixed quantization axis, and further possible degrees of freedom.

The interaction term  $H^{\text{int}}$  can in principle include arbitrary multi-particle interactions between the fermions occupying the open system, that is, the states  $|j\rangle$ . Most importantly, we take into account the two-particle Coulomb interaction between charged electrons or quasi-particles.

The Hamiltonian  $H^R$  describes the environment as a number of reservoirs  $r$  for effectively non-interacting fermions whose dynamics are governed by the reservoir Hamiltonians  $H^r$ :

$$H^R = \sum_r H^r = \sum_{\mathbf{k}i} \epsilon_i(\mathbf{k}) c_{\mathbf{k}i}^\dagger c_{\mathbf{k}i}. \quad (2.3)$$

Equation (2.3) includes creation ( $c_{\mathbf{k}i}^\dagger$ ) and annihilation operators ( $c_{\mathbf{k}i}$ ) for quasiparticles in all the single-particle states  $|\mathbf{k}i\rangle$  which are orthogonal to the open system states  $|j\rangle$ , and hence *define* the environment. These states have eigenvalues  $\epsilon_i(\mathbf{k})$  with respect to the part of the full single-particle Hamiltonian that acts *solely* on the environment. They are a function of the Bloch vector  $\mathbf{k}$  and the multi-index  $i = r_i, n_i, \sigma_i, \dots$ , labeling fermions in reservoir  $r$  with band index  $n$ , spin  $\sigma$ , and any further degree of freedom necessary to distinguish the states.

Finally, even though the states  $|j\rangle$  and  $|i\rangle$  are orthogonal, neither of them are eigenstates of the *full* single-particle Hamiltonian, that is, the full potential landscape including the tunnel barriers. In other words, the Hamiltonian couples these states via tunneling:

$$H^T = \sum_{\mathbf{k}ij} \tau_{\mathbf{k}ij} c_{\mathbf{k}i}^\dagger d_j + \text{H.c.}, \quad (2.4)$$

where  $\tau_{\mathbf{k}ij}$  is the amplitude for tunnel events between any single-particle state  $|j\rangle$  in the open system, and the single-particle state  $|\mathbf{k}i\rangle$  in the environment. These amplitudes define the characteristic frequency scales

$$\Gamma_{ijj'}(E) = 2\pi \sum_{\mathbf{k}} \delta(E - \epsilon_i(\mathbf{k})) \tau_{\mathbf{k}ij} \tau_{\mathbf{k}ij'}^* \quad (2.5)$$

at which the tunneling through the corresponding tunnel barriers takes place. Note that we have set  $\hbar = 1$ . The systems of interest in paper I and II are in the *weak coupling regime*, which can now be defined as the limit in which the typical tunneling times  $\sim 1/\Gamma$  are much longer than the typical memory time of the reservoirs, given by their typical inverse temperature  $\sim 1/T$ . Formally, weak coupling thus means  $\Gamma/T \ll 1$ .

Nevertheless, the class of open fermionic quantum systems defined by the total Hamiltonian  $H^{\text{tot}}$  [Eq. (2.1)] in principle also includes strongly coupled non-equilibrium environments, possibly described at low temperatures, and complex multi-level open systems with arbitrary local fermionic interactions. It therefore captures the broad range of systems of interest in the many different fields mentioned in the introduction to this chapter. Starting from this general Hamiltonian  $H^{\text{tot}}$ , we can now set up a description for the open system dynamics.

## 2.2 The quantum state of the open system

In principle, the dynamics of the above described system are already determined by the basic rules of quantum mechanics. These rules dictate that the time-dependent physical state of the total closed many-body system, consisting of the open system and the reservoirs in the environment, is represented by a normalized Hilbert space state vector  $|\Psi^{\text{tot}}(t)\rangle$ . This state obeys the time-dependent Schrödinger equation governed by the total Hamiltonian  $H^{\text{tot}}$ . Moreover, the Born rule yields the probability for the system to be in a certain many-particle state  $|\phi\rangle$  at time  $t$  via  $|\langle\phi|\Psi^{\text{tot}}(t)\rangle|^2$ . The problem is, however, that for any realistic setup, it is not even numerically feasible to solve the Schrödinger equation, as the number of degrees of freedom described by the time-dependent state is simply too high.

To overcome this problem, one essentially needs to rephrase the question: instead of asking for the time-dependent state of the entire system, one only asks for the quantum state of open system, containing only the information on how the open system evolves *in the presence of the environment*. Unfortunately, unlike for the total closed system, there are no quantum mechanical principles that allow to make statements about the time evolution of this state; a priori, it is not even clear how the quantum state of the open subsystem should be defined, since the vector  $|\Psi^{\text{tot}}\rangle$  cannot in general be written as a tensor product of two vectors that individually correspond to the open system and the environment:  $|\Psi^{\text{tot}}\rangle \neq |\Psi\rangle \otimes |\Psi^{\text{R}}\rangle$ . One common way to solve this issue is to switch to a density operator description, and then to perform an operation referred to as the *partial trace* over the environment. This yields the *reduced density operator* as an equivalent of the quantum state for the open system, since it contains all the relevant information about its time evolution. What is, however, less commonly discussed is what this partial trace operation actually means for a many-body system with an anti-symmetric state of *indistinguishable* objects, such as for the model introduced in Sec. 2.1. Since the central object to study the time evolution of the systems presented in this work is exactly this reduced density operator, we first start by physically motivating and then explicitly defining this operator.

In our concrete case, environment and open subsystem are defined by the single-particle states which they encompass. Accounting for the fact that these states are occupied by indistinguishable fermionic (quasi-)particles, we can characterize how the open system evolves in time by considering the set of occupation numbers  $\{n_j\}$  for all its single-particle states  $|j\rangle$ . First, we need the time-dependent probability of finding a specific set of these occupation numbers. Starting from the probabilistic interpretation of state overlaps in the full closed system, one sees that the total probability  $P_{\{n_j\}}(t)$  to find the specific occupation numbers  $\{n_j\}$  in the open system is obtained by summing over all possible combinations

of occupation numbers  $\{n_{\mathbf{k}i}\}$  in the environment:

$$P_{\{n_j\}}(t) = \sum_{\{n_{\mathbf{k}i}\}} |\langle \{n_{\mathbf{k}i}\}; \{n_j\} | \Psi^{\text{tot}}(t) \rangle|^2. \quad (2.6)$$

Second, we require a measure for quantum superpositions between different sets of occupation numbers in the open system. We realize that within the total closed system, two types of quantum superpositions can emerge: non-local superpositions of at least two states,  $\alpha |\{n_{\mathbf{k}i}\}_1; \{n_j\}_1\rangle + \beta |\{n_{\mathbf{k}i}\}_2; \{n_j\}_2\rangle$ , for which the occupations in both the environment and in the open system differ, and purely local superpositions,  $\alpha |\{n_{\mathbf{k}i}\}_1; \{n_j\}_1\rangle + \beta |\{n_{\mathbf{k}i}\}_1; \{n_j\}_2\rangle$ , in which only the occupations of the open system differ. The purely local superpositions, referred to as local coherences, are quantified analogously to how one obtains the probabilities (2.6), namely, by summing over the occupations in the environment:

$$P_{\{n_j\}, \{n'_j\}}(t) = \sum_{\{n_{\mathbf{k}i}\}} \langle \{n_{\mathbf{k}i}\}; \{n_j\} | \Psi^{\text{tot}}(t) \rangle \langle \Psi^{\text{tot}}(t) | \{n_{\mathbf{k}i}\}; \{n'_j\} \rangle. \quad (2.7)$$

Crucially, we here sum over a set of reservoir occupation numbers which are the same in both scalar products. This means that if there are only non-local superpositions between the subsystems, in the sense described above, the local coherences vanish. In other words, (2.7), and in fact also all probabilities (2.6), *implicitly* also contain information about the presence of non-locally entangled superpositions between the environment and the open system. This motivates to *define* the quantum state of the open system by combining the probabilities and local coherences into what is commonly referred to as the reduced density operator:

$$\begin{aligned} \rho(t) &= \sum_{\{n_{\mathbf{k}i}\}, \{n_j\}, \{n'_j\}} [\langle \{n_{\mathbf{k}i}\}; \{n_j\} | \Psi^{\text{tot}}(t) \rangle \langle \Psi^{\text{tot}}(t) | \{n_{\mathbf{k}i}\}; \{n'_j\} \rangle] \times |\{n_j\}\rangle \langle \{n'_j\}| \\ &\equiv \text{Tr}_R [|\Psi^{\text{tot}}(t)\rangle \langle \Psi^{\text{tot}}(t)|] \\ &= \text{Tr}_R [\rho^{\text{tot}}(t)]. \end{aligned} \quad (2.8)$$

Equation (2.8) introduces the partial *Fock-space* trace  $\text{Tr}_R [\rho^{\text{tot}}(t)]$  which yields the reduced density operator  $\rho(t)$  from the full operator  $\rho^{\text{tot}}(t) = |\Psi^{\text{tot}}(t)\rangle \langle \Psi^{\text{tot}}(t)|$  by summing over the single-particle state occupations in the environment. This definition implies that  $\rho(t)$  inherits all important properties for a state interpretation: hermiticity,  $\rho(t) = \rho^\dagger(t)$ , positive semi-definiteness, and a conserved total probability,  $\text{Tr} \rho(t) = 1$ .

We stress that whereas closed system time evolution can be equally well represented by the wave function  $|\Psi^{\text{tot}}(t)\rangle$  or the operator  $\rho^{\text{tot}}(t) = |\Psi^{\text{tot}}(t)\rangle \langle \Psi^{\text{tot}}(t)|$ , only the density operator approach straightforwardly extends the concept of time-dependent quantum states<sup>1</sup> to open many-body systems with indistinguishable

<sup>1</sup>To calculate observables, one can also employ non-equilibrium Green's functions [113] or stochastic Schrödinger equations [114, 115].

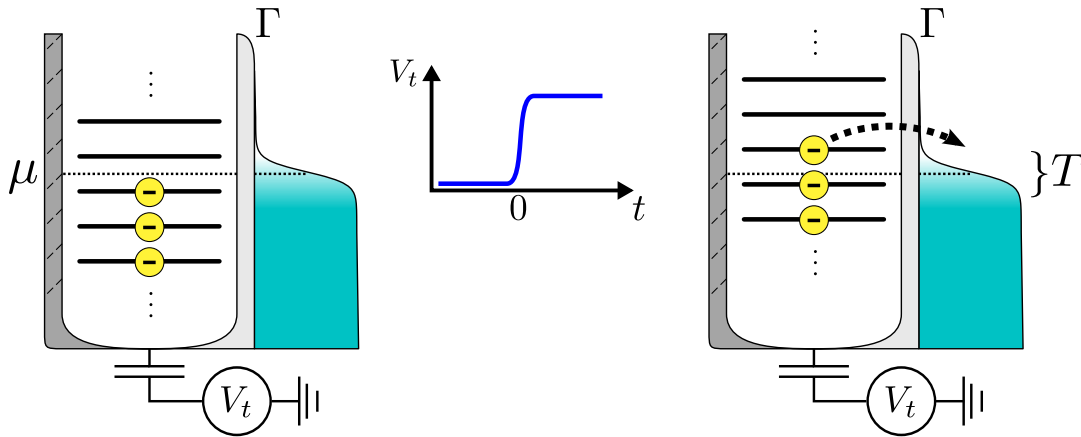


**Figure 2.2:** Example of a voltage switch applied to an open quantum system with  $n$  discrete (many-particle) eigenenergies, tunnel-coupled with tunneling strength  $\Gamma$  to an electronic reservoir at chemical potential  $\mu$  and temperature  $T$ . Initially, the system is filled up to the Fermi edge  $\mu$ . The voltage switch described by  $V(t)$  then leads to an approximately instantaneous shift of the open system energies, thereby driving the system out of stationarity. This induces tunneling process(es) which let the system relax to a new stationary state.

fermions. This work studies the time evolution of observables such as charge and energy currents by starting from the dynamics of the entire reduced density operator  $\rho(t)$ . As it will become apparent in Sec. 2.6.2, our reason to not instead start by evaluating a particular correlation function, as commonly done in Green's function approaches [113], is that by first understanding all physical processes that influence the time-dependent state  $\rho(t)$ , one can more systematically identify how all these effects reflect in the respective observables of interest. In the following, we explain this in more detail by first formulating the underlying equations that dictate the time evolution of  $\rho(t)$ .

## 2.3 Transient open system dynamics after an instantaneous switch

Our main interest is the *transient* behavior of the reduced density operator  $\rho(t)$  in response to an initial non-stationarity, induced, e.g., by a switch of some externally applied field at a fixed time  $t_0 \equiv 0$  as sketched in Fig. 2.2. Hence, the first step to set up a theoretical description for the dynamics of  $\rho(t)$  after the switch is to precisely define the initial state from which the system evolves. Subsequently, we can formulate the kinetic equations that dictate *how* this initial state evolves.

First, we assume the open subsystem to be in a stationary state  $\rho(t < t_0) = \rho_0$  for any time before the switch,  $t < t_0$ . Furthermore, we make the common

assumption that the initial state of the open system is uncorrelated with the environment. This means that the initial density operator of the total closed system factorizes in the many-body sense:

$$\mathrm{Tr}_R [A^R B \rho_0^{\mathrm{tot}}] = \mathrm{Tr}_R [A^R \rho_0^R] \cdot \mathrm{Tr}_R [B] \rho_0 \quad (2.9)$$

for any operation  $A^R$  that only depends on the occupations in the environment, and any operation  $B$  that only depends on the open system occupations. In this expression, the initial environment state, obtained by the partial trace over the *open system occupations*  $\rho_0^R = \mathrm{Tr} \rho_0^{\mathrm{tot}}$ , forms a local equilibrium in which each reservoir  $r$  is described by a grand-canonical ensemble, characterized by its temperature  $T_r$  ( $k_B$  is set to 1) and chemical potential  $\mu_r$ :

$$\rho_0^R = \exp\left(-\sum_r (H^r - \mu^r N^r) / T_r\right) / \mathrm{Tr}_R \left[\exp\left(-\sum_r (H^r - \mu^r N^r) / T_r\right)\right]. \quad (2.10)$$

The particle number operator for each reservoir  $r$  is labeled  $N^r$ . The trace  $\mathrm{Tr}_R$  here does not denote the partial trace, but instead the full Fock-space trace over the environment.

With the initial state characterized, we continue by setting up the dynamical equations for the time-dependent reduced density operator  $\rho(t) = \mathrm{Tr}_R [\rho^{\mathrm{tot}}(t)]$ . The effect of the switch at  $t_0 = 0$  is that a number of parameters in the Hamiltonian  $H^{\mathrm{tot}}$  of the full system changes. This induces a time evolution of the quantum state  $\rho^{\mathrm{tot}}(t) = |\Psi^{\mathrm{tot}}(t)\rangle\langle\Psi^{\mathrm{tot}}(t)|$  for the full system which follows the solution to the Liouville von-Neumann equation:

$$\begin{aligned} \partial_t \rho^{\mathrm{tot}}(t) &= -i [H^{\mathrm{tot}} |\Psi^{\mathrm{tot}}(t)\rangle\langle\Psi^{\mathrm{tot}}(t)| - |\Psi^{\mathrm{tot}}(t)\rangle\langle\Psi^{\mathrm{tot}}(t)| H^{\mathrm{tot}}] = -i L^{\mathrm{tot}} \rho^{\mathrm{tot}}(t) \\ \Rightarrow \rho^{\mathrm{tot}}(t) &= \exp(-i L^{\mathrm{tot}} t) \rho_0^{\mathrm{tot}} \quad \forall t > 0, \end{aligned} \quad (2.11)$$

where we have introduced the Liouvillian  $L^{\mathrm{tot}\bullet} = [H^{\mathrm{tot}}, \bullet]$  as the commutator with the Hamiltonian. Importantly, Eq. (2.11) assumes the parameter switch to be instantaneous, meaning that it is fast compared to any other frequency scale in the full Hamiltonian (2.1). This implies that *during the switch*, the state  $\rho^{\mathrm{tot}}(t)$  can be well approximated by the constant initial state  $\rho_0^{\mathrm{tot}}$ . Accordingly, we solve the Liouville von-Neumann equation with  $\rho_0^{\mathrm{tot}}$  as the initial condition  $\rho^{\mathrm{tot}}(t = 0_+)$ , and with a time-independent total Liouvillian  $L^{\mathrm{tot}}$  defined in terms of all system parameters *after* the switch. This then leads to the simple exponential solution shown in Eq. (2.11).

Finally, we use Eq. (2.8) to obtain the reduced density operator  $\rho(t)$ :

$$\begin{aligned} \rho(t) &= \mathrm{Tr}_R [\rho^{\mathrm{tot}}(t)] = \mathrm{Tr}_R [\exp(-i L^{\mathrm{tot}} t) \rho_0^{\mathrm{tot}}] \\ &= \mathrm{Tr}_R [\exp(-i L^{\mathrm{tot}} t) \rho_0^R] \rho_0 \\ &= \Pi(t) \rho_0 \quad \forall t > 0, \end{aligned} \quad (2.12)$$

where we have used that the initial state factorizes according to Eq. (2.9) in order to introduce the time propagator

$$\Pi(t) = \text{Tr}_R \left[ \exp(-iL^{\text{tot}}t) \rho_0^R \right]. \quad (2.13)$$

This formally solves the problem of determining the time evolution of the open system. Yet, Eq. (2.12) hardly allows for any explicit results, since the tunnel coupling  $L^T \bullet = [H^T, \bullet]$  in the total Liouvillian  $L^{\text{tot}} = L + L^R + L^T$  makes it very difficult to carry out the partial reservoir trace  $\text{Tr}_R$ . For weakly tunnel-coupled systems such as the ones at focus in paper I and II, this is typically solved by treating the expression on the right hand side of Eq. (2.13) perturbatively in orders in the coupling Liouvillian  $L^T$ . Using diagrammatic techniques as shown in [116, 117], or more recently, in [62, 76], this leads to what is known as the *generalized master equation*, or quantum kinetic equation, see Sec. 2.5. To discuss this equation and its solution in an accessible way, we first need a notation that better suits the Liouvillian approach used in Eq. (2.13).

## 2.4 The Liouville space of the open system

The time evolution propagator  $\Pi(t)$  given in Eq. (2.13) formally represents a linear *superoperator* that acts on linear operators  $x$ , which in turn live in the *Liouville space* of all linear operators that act on the Hilbert space of the reduced system. Since we study the open system dynamics with its density operator  $\rho(t)$ , and not with some Hilbert space vector  $|\Psi^{\text{tot}}(t)\rangle$ , it is very useful to clearly distinguish between superoperators and operators already in the notation. Here, we adopt the approach used, e.g, in Refs. [26, 62, 76]: any operator  $x$  acting on the Hilbert subspace of the open system is denoted as a superket vector  $|x\rangle$ , living in the Liouville space of all operators  $\{x_n\}_n$  acting on the open system. Adjoint superbra vectors  $(x|\bullet = (|x\rangle)^\dagger \bullet$  spanning the dual Liouville space are defined through the Fock space trace over the open system. More precisely, denoting any orthonormal basis of the *Hilbert* Fock space for the local system as  $(|\phi\rangle)$ , we write

$$|x\rangle = x \quad , \quad (x|\bullet = \text{Tr}[x^\dagger \bullet] = \sum_{\phi} \langle \phi | x^\dagger \bullet | \phi \rangle. \quad (2.14)$$

The second term in this equation defines the Hilbert-Schmidt trace scalar product of  $x^\dagger$  with any other operator  $\bullet$ , and introduces  $(x|\bullet$  or simply  $(x|$  as a short-hand notation for this scalar product. The reduced density operator  $\rho(t)$  and its basis elements are expressed as superkets  $|\rho\rangle$ , traces containing observable operators  $A = A^\dagger$ , probability projectors  $P_\phi = |\phi\rangle\langle\phi|$  and general matrix element extractors  $P_{\phi\phi'} = |\phi\rangle\langle\phi'|$  acting on an operator  $\bullet$  (e.g., a density operator) as superbras  $(A|$ ,  $(P_\phi|$  and  $(P_{\phi\phi'}|$ .

Using the above defined objects, dot observable averages  $\langle A \rangle$  and state matrix elements  $\rho_{\phi\phi'}$  can be conveniently written as

$$\langle A \rangle = (A|\rho) = \text{Tr}[A\rho] \quad , \quad \rho_{\phi\phi'} = (P_{\phi\phi'}|\rho) = \text{Tr}[(|\phi\rangle\langle\phi'|)^\dagger\rho] = \langle\phi|\rho|\phi'\rangle. \quad (2.15)$$

The idea of introducing this notation is to express the action of *superoperators*  $\mathcal{A}$ , such as the time propagator  $\Pi(t)$  [Eq. (2.13)], on the reduced density operator  $|\rho\rangle$ . To achieve this, we first notice that since the Liouville space and its dual space are also vector spaces, we can express superkets  $|x\rangle$  and superbras  $\langle x|$  in terms of basis vectors  $|v_n\rangle$  and  $\langle v'_n|$ :  $|x\rangle = \sum_n \alpha_n(x)|v_n\rangle$ ,  $\langle x| = \sum_n \alpha'_n(x)\langle v'_n|$ . Note that the basis vectors are not necessarily adjoint to each other, meaning  $\langle v'_n| \neq [|\!|v_n\rangle]^\dagger$ . In fact, the basis can be built from *any* two sequences  $(|v_n\rangle)_n$ ,  $(\langle v'_n|)_n$  of linearly independent operators that span the Liouville space of the reduced system and the dual space of scalar products. However, here we only use operators that are bi-orthogonal to each other with respect to the scalar product defined in Eq. (2.14). This means

$$\langle v'_n|v_m\rangle = \text{Tr}[(v'_n)^\dagger v_m] \propto \delta_{nm} \quad , \quad I\bullet = \sum_n \frac{1}{\langle v'_n|v_n\rangle} |v_n\rangle \langle v'_n| \bullet = \bullet, \quad (2.16)$$

where  $I$  is the superidentity which is a superoperator that acts trivially on any  $|x\rangle$  or  $\langle x|$ . For such orthogonal and complete bases, one finds

$$|x\rangle = \sum_n \underbrace{\frac{\langle v'_n|x\rangle}{\langle v'_n|v_n\rangle}}_{=\alpha_n(x)} |v_n\rangle \quad , \quad \langle x| = \sum_n \underbrace{\frac{\langle x|v_n\rangle}{\langle v'_n|v_n\rangle}}_{=\alpha'_n(x)} \langle v'_n|, \quad (2.17)$$

meaning that the basis expansion coefficients  $\alpha$  can be determined by Hilbert-Schmidt scalar products  $\langle a|b\rangle$ .

With the operator expansion given in Eq. (2.17), it is now possible to systematically describe the effect of superoperators  $\mathcal{A}$  acting on the (time-dependent) reduced density operator  $|\rho\rangle$ . Using the superoperator identity  $I$ , we obtain

$$\mathcal{A}|\rho\rangle = I\mathcal{A}I|\rho\rangle = \sum_{nm} \alpha_{nm} \langle v'_m|\rho\rangle |v_n\rangle \quad , \quad \alpha_{nm} = \frac{\langle v'_n|\mathcal{A}|v_m\rangle}{\langle v'_n|v_n\rangle \langle v'_m|v_m\rangle}. \quad (2.18)$$

If the basis of the Liouville space is constructed by physical state density operators  $\{|v_n\rangle\}$ , the coefficients  $\alpha_{nm}$  describe rates for transitions from the state  $|v_m\rangle$  to  $|v_n\rangle$  due to the effect that is represented by the action of the superoperator  $\mathcal{A}$ .

## 2.5 Master equation and transport quantities

As concluded in Sec. 2.3, we determine the time evolution of the reduced density operator  $|\rho(t)\rangle$  by evaluating Eq. (2.12) perturbatively in the coupling  $L^T$ , with the help of the diagrammatic techniques shown, e.g., in [27, 62, 76, 116–118]. This yields the *generalized master equation*, also known as quantum kinetic equation:

$$\partial_t |\rho(t)\rangle = -iL|\rho(t)\rangle + \int_0^t dt' \mathcal{W}(t-t') |\rho(t')\rangle. \quad (2.19)$$

This equation forms the *basic starting point* for the following analysis of the reduced system dynamics, and has been used in many other older [116, 117, 119] and more recent works [120–123]. The first term on the right hand side of Eq. (2.19) describes the purely local, coherent dynamics of the open system, governed by its local Liouvillian  $L\bullet = [H, \bullet]$ . The integral and its kernel  $\mathcal{W}(t-t')$  are due to the coupling to the environment, and hence depend on the parameters in the local Liouvillian  $L$  as well as in the tunneling  $L^T$ , and furthermore on the reservoir density of states as well as the temperatures  $T_r$  and chemical potentials  $\mu_r$  of the initial reservoir state  $\rho_0^R$  [Eq. (2.10)]. This coupling leads to non-Markovian dynamics with memory effects, relating  $\partial_t |\rho(t)\rangle$  to the state  $|\rho(t')\rangle$  at an earlier time  $t' < t$ . The kernel  $\mathcal{W}$  here only depends on the time difference  $t-t'$ , since the system does not have any explicitly time-dependent parameter after the switch. Importantly, as a consequence of the fundamental requirement of probability conservation ( $\mathbb{1}|\rho(t)\rangle = 1$ ), the kernel must obey  $\text{Tr}[\mathcal{W}(t-t')\bullet] = (\mathbb{1}|\mathcal{W}(t-t') = 0$  for any operator  $\bullet$  in the Liouville space of the open system, and for any two times  $t, t'$  after the time of the initial switch,  $t_0 = 0$ . Finally, for dissipative open systems as studied in this work, the coupling  $\mathcal{W}$  to the environment eventually causes  $|\rho(t)\rangle$  to decay to a stationary state  $|\rho_\infty\rangle = \lim_{t \rightarrow \infty} |\rho(t)\rangle$ .

Together with the initial state  $|\rho_0\rangle$ , the generalized master equation (2.19) in principle allows us to theoretically predict the time-dependent decay of the entire reduced density operator  $|\rho(t)\rangle$ . In experiments, it is, however, seldom feasible to measure the complete state. Instead, one aims to measure physical observables of the open system which yield the parts of the full information contained in  $|\rho(t)\rangle$  which one is most interested in. In our concrete case of tunnel-coupled systems with electrons or fermionic quasi-particles, the experimentally most natural and relevant quantities to characterize how  $|\rho(t)\rangle$  decays as a function of time are the average particle- ( $I_N(t)$ ) and heat current ( $I_Q(t)$ ) into the reservoirs<sup>1</sup>, due to tunneling induced by the non-stationarity of the initial state  $\rho_0$ . For each reservoir  $r$ , these tunnel currents can be defined by the time derivative of the respective

<sup>1</sup>For systems with Zeeman splitting, one can also consider spin resolved currents.

average particle number and energy<sup>1</sup>:

$$I_N^r(t) = \partial_t \langle N^r \rangle (t) = \partial_t \text{Tr} \text{Tr}_R [N^r \rho^{\text{tot}}(t)] \quad (2.20)$$

$$I_Q^r(t) = \partial_t \langle H^r - \mu_r N^r \rangle (t) = \partial_t \text{Tr} \text{Tr}_R [(H^r - \mu_r N^r) \rho^{\text{tot}}(t)]. \quad (2.21)$$

Since the particle number is conserved, meaning that each particle leaving the reservoir enters the open system, one can easily show [App. B.1] that the particle current can be rewritten in terms of the total charge number operator for the open system,  $N$ , and only a part of the full coupling kernel  $\mathcal{W}$ :

$$I_N^r(t) = - \int_0^t dt' (N | \mathcal{W}^r(t-t') | \rho(t')) \quad , \quad \mathcal{W}(t-t') = \sum_r \mathcal{W}^r(t-t'), \quad (2.22)$$

where  $\mathcal{W}^r(t-t')$  represents a coupling to the reservoir  $r$  that is renormalized by the presence of all other reservoirs.

By contrast, the energy current  $I_E^r(t) = \partial_t \langle H^r \rangle (t)$  is generally not conserved, since the tunnel barrier itself can store energy. To rewrite the heat current definition Eq. (2.21), one therefore has to introduce the energy current kernel  $\mathcal{W}_E^r$  to write [118]

$$I_Q^r(t) = \int_0^t (\mathbb{1} | \mathcal{W}_E^r(t-t') | \rho(t')) - \mu_r I_N^r(t). \quad (2.23)$$

This transient heat current has one important feature: unlike the average particle current  $I_N^r(t)$ , which is a single-particle quantity, the heat current is directly influenced by two-particle effects, as it contains the energy due to particle-particle interactions in the open system. This means that, much like the particle current *noise*, the heat current contains more information about the evolution of the full quantum state  $|\rho(t)\rangle$  than the average particle current. In case of a single spin-degenerate orbital with a maximum occupation of two electrons – the system discussed in chapter 4 and paper II – the heat current allows, in combination with the particle current, to determine *all* probabilities in the density operator  $|\rho(t)\rangle$ .

Let us now continue by showing how to extract the time-dependent decay behavior of the open system from the generalized master equation (2.19), given a non-stationary initial state  $|\rho_0\rangle \neq |\rho_\infty\rangle$  and a weakly tunnel-coupled environment.

## 2.6 Time-dependent decay for weakly coupled systems

Starting from the generalized master equation (2.19), we aim to physically interpret how the systems we are interested in – dissipative open fermion systems that are weakly tunnel-coupled [ $\Gamma/T \ll 1$ , see Eq. (2.5)] to the environment – decay

<sup>1</sup>We acknowledge that the definition of the time-dependent heat current used here is only consistent with thermodynamic laws in the weak coupling limit, see [105, 106].

to their stationary state as a function of time. In this weak coupling regime, a justified and insightful approximation of the exact solution to Eq. (2.19) that captures the essence of time-dependent decay is the Markovian, lowest order coupling approximation, commonly referred to as Born-Markov approximation. In the following, we first briefly sketch this approximate solution for the master equation, and then investigate in detail its physical implications for the time-dependent reduced density operator  $|\rho(t)\rangle$ .

### 2.6.1 Born-Markov approximation

As its name suggests, the Born-Markov approximation consists in fact of two approximations. On the one hand, the Born approximation involves calculating the kernel  $\mathcal{W}(t-t')$  only up to the leading, linear order in the coupling constants  $\Gamma$  [Eq. (2.5)]:  $\mathcal{W}(t-t') \rightarrow \mathcal{W}_1(t-t')$ , where the 1 in the index indicates the first order in the coupling. The Markov approximation, on the other hand, neglects all memory effects due to the tunnel coupling to the environment, and thus transforms the generalized master equation into a fully time local equation. Combined with the Born approximation, we can write

$$\partial_t |\rho(t)\rangle \approx \left[ -iL + \int_0^t dt' \mathcal{W}_1(t-t') \right] |\rho(t)\rangle \approx \left[ -iL + \int_{-\infty}^t dt' \mathcal{W}_1(t-t') \right] |\rho(t)\rangle. \quad (2.24)$$

Both the Born and the Markov approximation can be justified when realizing that  $\mathcal{W}(t-t')$  is peaked around  $t' = t$  with a typical broadening given by the memory time of the environment. For non-interacting reservoirs as studied here, this memory time is on the order of the inverse temperature  $1/T$ . Therefore, we can approximate the kernel as  $\propto \delta(t' - t)$  if we assume that the memory time is much smaller than the typical tunneling time  $1/\Gamma$ , meaning  $1/T \ll 1/\Gamma$  or  $\Gamma \ll T$ . This then allows us to approximate the integral in the last step of Eq. (2.24) by taking its lower bound to  $-\infty$ . Furthermore, it justifies the Born expansion of the kernel  $\mathcal{W}$  in the linear order in the couplings  $\Gamma$ , since any higher-order effect is suppressed by the factor  $\Gamma/T$ . This factor occurs because it describes the time ratio that determines whether two or more tunneling events are seen by the environment as simultaneous, coherent events (e.g., co-tunneling with virtual intermediate states), or as sequential events in between which the environment loses any memory of the respective previous tunneling event.

Here, we always work in the *weak coupling regime*,  $\Gamma \ll T$ , meaning that the influence of any second order contribution becomes negligible. In this regime,  $|\rho(t)\rangle$  follows from the Born-Markov master equation

$$\partial_t |\rho(t)\rangle = [-iL + W_1] |\rho(t)\rangle \quad , \quad W_1 = \lim_{\omega \rightarrow i0} \int_0^\infty dt \mathcal{W}_1(t) e^{i\omega t}. \quad (2.25)$$

The kernel  $W_1$  is the Fourier-Laplace transform  $W_1(\omega)$  of the first-order  $\Gamma$  kernel evaluated in the limit of zero imaginary frequency  $\omega \rightarrow i0$ . Physically, the matrix

elements of this kernel with respect to some basis states  $|ij\rangle = |i\rangle\langle j|$  of the open system Liouville space,

$$W_{1,ijkl} = (ij|W_1|kl), \quad (2.26)$$

constitute state transition rates ( $i = j, k = l$ ) as well as couplings to coherences ( $i \neq j$  and/or  $k \neq l$ ).

With a more rigorous justification for Eq. (2.25) given in Sec. 2.7, we here continue by stating its solution. Defining the combined kernel  $A_1 = -iL + W_1$ , one finds

$$\boxed{|\rho(t)\rangle = \exp(A_1 t)|\rho_0\rangle}. \quad (2.27)$$

This general result shows that the time evolution of the open system in the Born-Markov limit behaves purely exponential. Due to its importance for our work, we devote the next subsection to a detailed discussion of this formula. Before we come to this discussion, we point out that in the Born-Markov limit, one also obtains formulas for the particle- and heat current into the reservoirs which are simpler compared to their general expressions given in Eq. (2.22) and Eq. (2.23). Namely, applying the scheme outlined from Eq. (2.24) to Eq. (2.27) to the general expressions for the currents, Eq. (2.22) and Eq. (2.23), one finds

$$I_N^r(t) \rightarrow -(N|W_1^r|\rho(t)) \quad , \quad I_Q^r(t) \rightarrow (\mathbf{1}|W_{1,E}^r|\rho(t)) - \mu_r I_N(t). \quad (2.28)$$

The kernels  $W_1^r$  and  $W_{1,E}^r$  are the leading order  $\Gamma$ , zero frequency Laplace transforms of the reservoir resolved kernels introduced in equations (2.22) and (2.23). Note that for the systems considered in this work, the energy current is in fact conserved in the Born-Markov limit, as shown in App. B.2. This means that the heat current into the reservoir is the heat current *out of* the open system:

$$I_Q^r(t) \approx -(H - \mu_r N|W_1^r|\rho(t)) \quad (2.29)$$

Equations (2.27), (2.28) and (2.29) together form the basic tool set for all explicit calculations carried out in paper I and II. To understand the physics these equations involve, it is particularly important to precisely interpret the exponential form of  $|\rho(t)\rangle$  according to Eq. (2.27). As we show below, this can be achieved in the eigenmode expansion of the time evolution kernel  $A_1$ .

## 2.6.2 Time scales, modes and amplitudes

To further analyze the reduced system dynamics in the Born-Markov limit, we continue by expanding  $A_1$  entering the time evolution (2.27) in the biorthonormal basis of its left- and right eigenvectors, ( $|x'\rangle$ ) and ( $|x\rangle$ ), corresponding to the eigenvalues labeled as  $-\gamma_x$ . This yields

$$|\rho(t)\rangle = \sum_x (x'|\rho_0\rangle) e^{-\gamma_x t} |x\rangle. \quad (2.30)$$

Since the kernel  $A_1$  conserves probability for any physical system,  $(z'| = (\mathbb{1}|$  is always a left eigenvector of  $A_1$  to the eigenvalue  $\gamma_z = 0$ :  $(\mathbb{1}|A\bullet = \text{tr}[A\bullet] = 0$ . This also implies the existence of at least one right eigenvector  $|z\rangle$  to the eigenvalue 0, and suggests to split the expression for  $|\rho(t)\rangle$  according to

$$|\rho(t)\rangle = (\mathbb{1}|\rho_0)|z\rangle + \sum_{x \neq z} (x'|\rho_0)e^{-\gamma_x t}|x\rangle. \quad (2.31)$$

For the models of interest here, in particular in the appended papers, the zero eigenvector  $|z\rangle$  is the *unique trace normalized stationary state*<sup>1</sup>:

$$\lim_{t \rightarrow \infty} |\rho(t)\rangle = |z\rangle \quad , \quad A_1|z\rangle = 0 \quad , \quad (\mathbb{1}|z\rangle = 1. \quad (2.32)$$

Its prefactor in Eq. (2.31) equals  $(\mathbb{1}|\rho_0) = 1$ , since the initial state is also trace normalized by assumption. This yields the important final result

$$\boxed{|\rho(t)\rangle = |z\rangle + \sum_{x \neq z} (x'|\rho_0) \exp(-\gamma_x t) \cdot |x\rangle.} \quad (2.33)$$

This relation generally describes the voltage-switch induced transient behavior of the open quantum system in the Markovian, weak tunnel-coupling limit. Let us in the following develop a detailed understanding of Eq. (2.33).

The reciprocal values of all the  $\gamma_x$  appearing in Eq. (2.30) yield the typical time scales on which the system evolves. For the systems and observables of interest in paper I and II, these rates  $\gamma_x$  can be considered as real positive numbers,  $\gamma_x > 0$ , meaning that they represent decay rates governing the *exponential relaxation* of  $|\rho(t)\rangle$  to the stationary state  $|z\rangle$  due to dissipation into the environment<sup>2</sup>.

For any rate  $\gamma_x$ , the corresponding left and right eigenvectors  $(x'|$  and  $|x\rangle$  in the expansion (2.33) determine *how exactly* the rate enters the relaxation dynamics. The right eigenvectors are the decay modes  $|x\rangle$ . The basis elements of these modes specify how a certain probability or coherence evolves in relation to all other probabilities and/or coherences *on the same specific time scale* determined by  $\gamma_x$ . The corresponding left eigenvectors  $(x'|$  are called *amplitude covectors*, as the overlap  $(x'|\rho_0)$  of these vectors  $(x'|$  with the initial state  $|\rho_0\rangle$  determines how strongly the given time scale influences the entire time evolution  $|\rho(t)\rangle$  of the reduced system *in comparison to all other time scales*. In particular, the amplitude vectors yield quantities that evolve *exclusively* on the corresponding

<sup>1</sup>More generally, the zero eigenvalue can be degenerate, meaning that the stationary state is a linear combination of several eigenvectors. Furthermore, it is not strictly guaranteed that the state is reached.

<sup>2</sup>The scales  $\gamma_x$  can in general have finite imaginary parts,  $\text{Im}(\gamma_x) \neq 0$ , that correspond to oscillations of the state  $|\rho(t)\rangle$ . However, the real parts must in any case be non-negative, as  $\text{Re}(\gamma_x) < 0$  would imply an unphysical divergence of  $|\rho(t)\rangle$  for  $t \rightarrow \infty$ .

time scale  $\gamma_x$ , since biorthonormality dictates that

$$\langle x' \rangle (t) = (x' | \rho(t)) = (x' | \rho_0) e^{-\gamma_x t}. \quad (2.34)$$

These quantities and the corresponding modes  $|x\rangle$  are vital<sup>1</sup> in understanding which physical decay process is represented by which decay rate  $\gamma_x$ . The knowledge and proper analysis of modes and amplitudes is thus very important, and in fact the main motivation behind chapter 3.

### 2.6.3 Statistical interpretation of the reduced dynamics

To conclude this section, we now finish with a short discussion on the statistical interpretation of the reduced system dynamics as predicted by the central relation (2.33). Equation (2.34) shows that in order to experimentally access an individual rate  $\gamma_x$  entering the reduced density operator, one has to measure the quantity defined by the amplitude covector  $\langle x'|$ . However, apart from the question whether it is technically feasible to measure this quantity, it is important to understand how the predicted exponential behavior actually reflects in experimental data. Let us consider the simple example of the experiment by Fève et al., previously introduced in Fig. 1.2 in Sec. 1.2, and also in Fig. 2.2. In this experiment, the level-spectrum of a quantum dot is gate-pulsed such that only one singly-occupied level is lifted above the Fermi edge of a weakly coupled electronic reservoir. Under the assumption that the dynamics of the dot are well approximated by the dynamics of the occupation of only this single level, it was shown in [61, 75] that the deviation of the particle number  $N$  from its stationary average  $N_z = \langle N | z \rangle$  is represented by a left eigenvector of the Born-Markov coupling kernel  $W_1$ ,  $\langle c'| = \langle N | - N_z \langle \mathbf{1} |$ . It thus decays exponentially at a single rate  $\gamma_c$ :

$$\langle c' | \rho(t) \rangle = N(t) - N_z = (N_0 - N_z) e^{-\gamma_c t}. \quad (2.35)$$

Importantly, since the reduced density operator set up in Sec. 2.2 yields a probabilistic description of the open system state, Eq. (2.35) is a *statistical average* of the time-dependent particle number. As illustrated in Fig. 2.3(a) and experimentally demonstrated in charge counting experiments [19, 20, 22, 24], a realtime trace of the dot charge after a voltage switch does not show an exponential behavior. Rather, one notices discrete steps of the charge number at variable times  $\Delta t$  after the switch, indicating electron tunneling events. Only the time-dependent average over many such realtime traces exhibits the exponential behavior that is predicted by the theory, as shown, e.g., by the ensemble averages determined in the experiment by Fève et al. [Fig. 1.2].

<sup>1</sup>Unless there is only a single rate and only two states, for which the mode is trivially fixed by its vanishing trace, and the amplitude is mostly irrelevant since there is no other mode to which the influence on  $|\rho(t)\rangle$  can be compared.

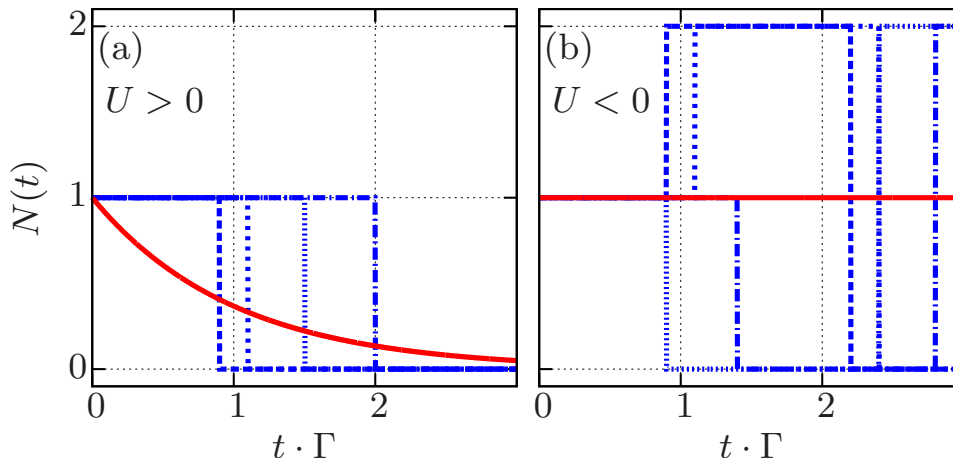


**Figure 2.3:** (a) Time resolved excess occupation number  $N(t)$  of a quantum dot that is weakly tunnel-coupled to its environment, and whose levels are rapidly shifted by a voltage-switch as shown, e.g., in Fig. 1.2 or Fig. 2.2. Assuming that the switch lifts only one singly-occupied level  $\epsilon$  above the Fermi edge of the reservoir, a tunneling process from this level into the environment is induced after a typical time  $1/\Gamma$  given by the coupling strength. The blue curves show, in a simplified way, typical time traces of  $N(t)$  that would be obtained in charge counting experiments, such as the ones shown in [17–20, 22, 24]. The red curve represents the time-dependent ensemble average as predicted by the Born-Markov master equation (2.25). We assume repulsive Coulomb interactions ( $U > 0$ ) on the dot. (b) Time-dependent excess charge number  $N(t)$  of a single, spin-degenerate level with (hypothetical) strong attractive interactions ( $U < 0$ ). The system is initially prepared in a highly unstable singly occupied state, and the level is tuned to the point where it is equally probable for the dot to be empty or doubly occupied, referred to as particle-hole symmetric point. At this level-position, the system decays with equal probability to an empty or doubly occupied stable state, and then continues to oscillate between zero and double occupation due to thermal excitations (if  $T/U \sim 1$ ).

It might appear almost as an irrelevant side remark for the simple situation reflected by Fig. 2.3(a), but this insight is in general important for the correct interpretation of time evolution as predicted by the generalized master equation (2.19). An example that seems unrealistic at first, but nevertheless turns out to be relevant for this work, is a single-level spin-degenerate quantum dot with strong local electron-electron *attraction*. For this so-called attractive Anderson model, it is known [124] that the singly occupied state is highly unstable, and thus always decays. However, if the dot level is set to the point where the system is equally likely in the empty or doubly occupied state – the particle-hole symmetric point – the time-dependent state constantly oscillates between zero and double occupation due to thermal fluctuations. In particular, since both states are assumed with equal probability, the *ensemble average* of the charge number as obtained from the theory presented above would not decay at all in this case, even though the measured occupation would change in every single instance, see Fig. 2.3(b).

## 2.7 Time evolution beyond the Born-Markov approximation

In chapter 3, the problem of physically interpreting the rates, modes and amplitudes determining the time evolution of open systems is approached by a theory that holds also for non-Markovian dynamics and strong tunnel couplings. An understanding of this theory therefore requires a basic overview of the formal, yet exact solution to the generalized master equation (2.19). Consequently, we finish this chapter by discussing time evolution in this general case.

The generalized master equation is, mathematically speaking, an integro differential equation with an integral constituting a convolution in time on finite support. Such equations can be solved exactly in the Fourier-Laplace space. Defining the Fourier-Laplace transform  $|\rho(\omega)\rangle = \int_0^\infty dt e^{i\omega t} |\rho(t)\rangle$ , and assuming  $\text{Im}(\omega) \geq 0$  for this transform to converge, the master equation yields

$$-i\omega|\rho(\omega)\rangle - |\rho_0\rangle = [-iL + W(\omega)]|\rho(\omega)\rangle \quad , \quad W(\omega) = \int_0^\infty dt e^{i\omega t} \mathcal{W}(t), \quad (2.36)$$

with the initial state written as  $|\rho_0\rangle = |\rho(t=0)\rangle$ . From this immediately follows

$$|\rho(\omega)\rangle = \Pi(\omega)|\rho_0\rangle \quad , \quad \Pi(\omega) = \frac{i}{\omega - iA(\omega)} \quad , \quad A(\omega) = -iL + W(\omega), \quad (2.37)$$

where we have again defined the now frequency-dependent combined kernel  $A(\omega)$ , in analogy to how the Born-Markov kernel is defined in Eq. (2.27). The inverse transform of the Fourier-Laplace transform yields the solution to  $|\rho(t)\rangle$  for  $t > 0$ . Formally, we obtain

$$\begin{aligned} |\rho(t)\rangle = \Pi(t)|\rho_0\rangle \quad , \quad \Pi(t) &= \frac{1}{2\pi} \int_{-\infty}^{\infty} d\omega e^{-i(\omega+i\eta)t} \Pi(\omega + i\eta) \\ &= \frac{-1}{2\pi i} \int_{-\infty}^{\infty} d\omega e^{-i(\omega+i\eta)t} \frac{1}{\omega + i\eta - iA(\omega + i\eta)} \quad , \quad \eta > 0, \end{aligned} \quad (2.38)$$

where  $\eta > 0$  is a real positive, but otherwise freely selectable constant that ensures that the integral path lies in the region of convergence for the Fourier-Laplace transform of the density operator,  $|\rho(\omega)\rangle$ , see Fig. 2.4. To carry out the integral in Eq. (2.38), we first set  $\eta = 0_+$  and then expand the kernel superoperator  $A(\omega)$  in terms of its frequency-dependent eigenvalues  $-\gamma_x(\omega)$  and corresponding left- and right eigenvectors,  $(x'(\omega)|$  and  $|x(\omega)\rangle$ ). This leads to

$$|\rho(t)\rangle = \frac{-1}{2\pi i} \sum_x \int_{-\infty}^{\infty} d\omega (x'(\omega + i0_+)|\rho_0\rangle) e^{-i\omega t} \frac{1}{\omega + i\gamma_x(\omega) + i0_+} |x(\omega + i0_+)\rangle. \quad (2.39)$$

Importantly, Eq. (2.39) clarifies the difference between the Born-Markov ap-

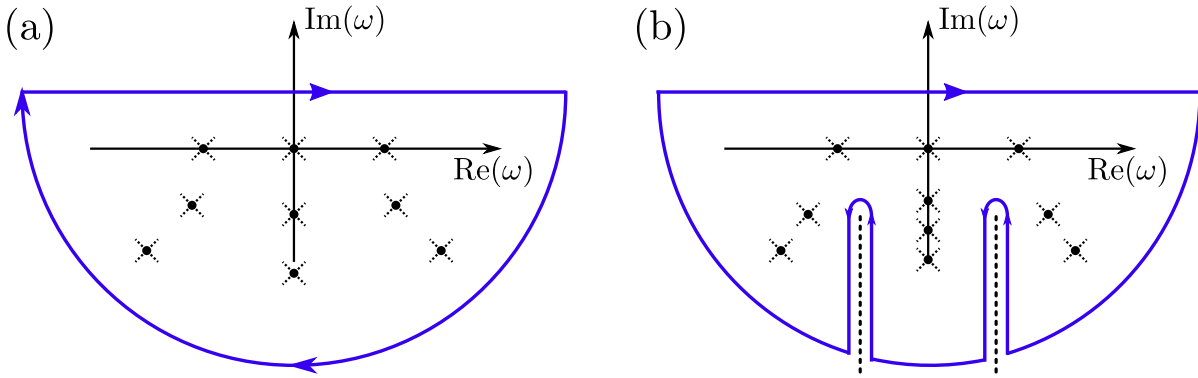


**Figure 2.4:** Carrying out the frequency integral in Eq. (2.38) by closing the integral contour (blue) in the lower half of the complex plane, both in the Born-Markov approximation (a) in which the combined kernel  $A(\omega) = -iL + W(\omega)$  is taken at zero imaginary frequency,  $A(\omega = i0_+)$ , as well for the exact case (b). The crosses mark the poles of the resolvent in both cases. Compared to the Born-Markov case, the poles are modified in the exact case, and additional poles may appear. Additionally, the exact kernel  $A(\omega)$  might have branch cuts around which one has to integrate, as illustrated by the black dashed lines in (b).

proximation and the exact solution to the generalized master equation (2.19), thereby further justifying the Markovian treatment, and consequently the Born approximation, if the coupling is weak:  $\Gamma \ll T$ . Namely, we notice that the time broadening of  $A(t)$  by the memory time  $\Delta t \sim \beta = 1/T$  corresponds to a frequency distribution  $A(\omega)$  with typical broadening on the order of  $\Delta\omega \sim T \gg \Gamma$ . In other words,  $A(\omega)$  deviates from its zero frequency value only for frequencies and rates much higher than the ones given by the tunnel couplings. Therefore, as long as we do not probe  $|\rho(t)\rangle$  for times on the order of the memory time  $\Delta t$  after the initial switch at time  $t_0$ , we can approximate  $A(\omega)$  by its value at zero imaginary frequency,  $A(i0_+)$ , and expand it only up to the first order in the couplings  $\Gamma$ . This then yields the Born-Markov result  $|\rho(t)\rangle = e^{A_1 t} |\rho_0\rangle$ : since all frequency dependence of the eigenvectors and eigenvalues is neglected, and the poles of the resolvents in Eq. (2.39) are hence simply given by  $-i\gamma_x$ , the integral can easily be carried out by closing the contour in the lower complex plane, and by using the Cauchy residue theorem [Fig. 2.4(a)].

However, if we study a regime in which we need to account for the frequency dependence of the eigenvalues  $-\gamma_x(\omega)$ , the poles of the resolvents do not anymore equal  $-i\gamma_x$ , but are instead given by the *frequency roots* of  $\omega + i\gamma_x(\omega)$ . Since there can be multiple roots for each  $\gamma_x(\omega)$ , this not only means that the reciprocal time scales  $\gamma_x$  that are captured by the Born-Markov approximation are modified. In fact, it also implies that there are further decay rates as well as oscillation frequencies which do not even appear at all in the Born-Markov description. This purely non-Markovian behavior is related to memory effects in the environment, and can thus play an important role for  $|\rho(t)\rangle$  for times after the switch which

are small compared to the memory time  $\sim 1/T$  [26]. Furthermore,  $\gamma_x(\omega)$  and the corresponding eigenvectors do not necessarily have to be analytic functions of  $\omega$  except for isolated poles; additionally, they could also have branch cuts [27]. As illustrated in Fig. 2.4(b), using the residue theorem to evaluate the frequency integral in Eq. (2.39) then requires to modify the closed integral contour such that none of these non-analytic regions is encircled by the integral contour. This modification typically leads to algebraically decaying pre-exponential factors as well as completely non-exponential behavior [27–29, 32–34], both also not predicted by the Born-Markov solution Eq. (2.33).

Nevertheless, it is important to note that despite the frequency dependence, the general result Eq. (2.39) is in many respects still very similar to what we have obtained in Eq. (2.33) within the Born-Markov limit. In particular, the right eigenvectors  $|x\rangle$  still represent modes of the time evolution which determine how the different probabilities and coherences in  $|\rho(t)\rangle\rangle$  evolve relatively to each other; and the overlaps  $\langle x'|\rho_0\rangle$  of the left eigenvectors with the initial state still determine how the different modes contribute relatively to each other. This emphasizes that a proper physical interpretation of modes and amplitudes is not only vital in understanding  $|\rho(t)\rangle\rangle$  for the systems of interest here – weakly tunnel-coupled systems in the Born-Markov limit. In fact, it is also important for much more general cases, including non-Markovian dynamics in the strong coupling regime.



## 3 The fermion-parity duality

We have concluded in the previous chapter that a proper physical understanding of transient open system dynamics requires knowledge and physical interpretations for the modes and amplitudes in the eigenmode expansion of the time propagator  $\Pi(t)$ , both in the Born-Markov limit [Eq. (2.33)] as well as in the general non-Markovian case. In this chapter, we present a theoretical approach to this problem which is motivated by a fundamental aspect of the time evolution in open quantum systems: its nonunitarity. To illustrate this point, we start by reviewing how unitarity facilitates the interpretation of the dynamics in *closed* quantum systems.

### 3.1 Time scales, modes and amplitudes in closed and open systems

Let us consider a *closed* system described by the Hamiltonian  $H$ . According to the principles of quantum mechanics, the density operator  $|\rho(t)\rangle\rangle$  of this system evolves from some initial state  $|\rho_0\rangle\rangle$  at time  $t_0 = 0$  according to the Liouville-von-Neumann equation:

$$|\rho(t)\rangle\rangle = e^{-iLt}|\rho_0\rangle\rangle. \quad (3.1)$$

In other words, the Liouvillian  $L\bullet = [H, \bullet]$  forms the time evolution kernel of the system. The right eigenvectors of this kernel – the modes – are constructed from the many-body energy eigenstates  $|E_i\rangle$  of  $H$  with energy  $E_i$ :

$$L|E_{ij}\rangle\rangle = [H, |E_i\rangle\rangle\langle E_j|] = (E_i - E_j)|E_{ij}\rangle\rangle \quad , \quad |E_{ij}\rangle\rangle = |E_i\rangle\rangle\langle E_j|. \quad (3.2)$$

Importantly, the time evolution in Eq. (3.1) must, again by the principles of quantum mechanics, be unitary. This is guaranteed by the hermiticity of the Liouvillian with respect to the *Hilbert Schmidt scalar product on the Liouville space*<sup>1</sup>:  $L^\dagger = L$ . This ensures that the energy differences  $E_i - E_j$  are real eigenvalues of the Liouvillian, and also dictates that the left eigenvectors of  $L$  – the amplitude covectors – are simply adjoint to the modes given by the right eigenvectors:

$$\langle E_{ij}|L\bullet = \text{Tr} \left[ (|E_i\rangle\rangle\langle E_j|)^\dagger [H, \bullet] \right] = \text{Tr} \left[ [|E_j\rangle\rangle\langle E_i|, H] \bullet \right] = (E_i - E_j)\langle E_{ij}| \bullet. \quad (3.3)$$

---

<sup>1</sup>With respect to the Hilbert space scalar product  $\langle x | \dots | y \rangle$ , the Liouvillian  $(L\bullet)^\dagger = -L(\bullet)^\dagger$  is in fact anti-hermitian.

The eigenmode expansion of the time evolution operator  $e^{-iLt}$  therefore simply yields

$$|\rho(t)\rangle = \sum_{ij} [ |E_{ij}\rangle e^{-i(E_i - E_j)t} \langle E_{ij}| ] |\rho_0\rangle = \sum_{ij} (E_{ij}|\rho_0) \exp(-i(E_i - E_j)t) \cdot |E_{ij}\rangle. \quad (3.4)$$

In this expression, every ingredient has a clear physical meaning. The mode  $|E_{ij}\rangle = |E_i\rangle\langle E_j|$  is the operator representation of either the energy eigenstate  $|E_i\rangle$  ( $i = j$ ), or of a coherent superposition between two eigenstates  $|E_i\rangle \neq |E_j\rangle$ . The energy differences  $E_i - E_j$  are the frequencies at which the system oscillates between the corresponding energy eigenstates if it is in a coherent superposition. Finally, the overlap of the amplitude covectors  $(E_{ij}|$  with the initial state simply equals a product of two many-particle wave function overlaps:  $(E_{ii}|\rho_0) = |\langle E_i|\rho_0\rangle|^2$  for the eigenstate probabilities, and  $(E_{ij}|\rho_0) = \langle E_i|\rho_0\rangle\langle\rho_0|E_j\rangle$  for the coherent superpositions. This means that the relative contribution of every energy eigenstate  $|E_i\rangle$  to the full time evolution is determined by how much the initial state  $\rho_0$  can be represented in terms of this specific eigenstate. In particular,  $|\rho(t)\rangle$  does not evolve further if the initial state is already an energy eigenstate,  $|\rho_0\rangle = |E_{ii}\rangle = |E_i\rangle\langle E_i|$ .

Let us contrast these results to the discussion for *open systems* in Sec. 2.6.2, where the local system  $H$  couples to the environment  $H^R$  via tunneling  $H^T$ . In this case, Eq. (3.4) generalizes to the Born-Markov result written in Eq. (2.33):

$$|\rho(t)\rangle = e^{A_1 t} |\rho_0\rangle = \sum_x (x'|\rho_0) \exp(-\gamma_x t) \cdot |x\rangle, \quad (3.5)$$

where  $A_1 = -iL + W_1(i0)$  is the previously introduced, combined time evolution kernel, sometimes referred to as effective Liouvillian. Since the open system dissipates energy into the environment, its time evolution is nonunitary, meaning in particular that the kernel  $A_1$  is nonhermitian. As a first consequence, the eigenvalues  $-\gamma_x$  can have both a non-zero imaginary and real part, where the latter constitutes a relaxation rate entering the exponential decay of  $|\rho(t)\rangle$  due to dissipation.

The second difference to closed systems is that the modes  $|x\rangle$  and the amplitudes  $(x'|$  which correspond to the rates  $\gamma_x$  are not anymore adjoint to each other with respect to the Hilbert Schmidt product:  $(x'| \neq [|x\rangle]^\dagger$ . Already as a mere consequence of orthogonality to the zero amplitude  $(\mathbb{1}|$ , no mode  $|x\rangle$  with  $\gamma_x \neq 0$  can have a simple physical state interpretation such as in closed systems, since the trace  $(\mathbb{1}|x) = 0$  is not normalized to 1. However, given that one is indeed able to physically interpret the form of the mode  $|x\rangle$ , this nevertheless does not tell much about the amplitude  $(x'|$  and the overlap  $(x'|\rho_0)$ , as there is no obvious physical<sup>1</sup> connection to the mode. Likewise, if a certain amplitude  $(y'|$  is understood, there

<sup>1</sup>By basic linear algebra, the basis expansion coefficient matrix of all amplitudes is *mathematically* related to the expansion coefficient matrix for the modes by matrix inversion.

is no systematic and physically insightful relation to interpret the corresponding mode  $|y\rangle$ . The aim of this chapter and the more general part of paper II is to shed a new light onto this problem. Namely, we discuss a non-trivial, yet insightful *duality relation* between modes and amplitudes that applies to a very large class of *open* fermionic many-body systems. This duality and its implications form the core of all subsequent analyses of the dynamics for the specific single-level quantum dot system treated in chapter 4 and paper II.

## 3.2 Mode-amplitude duality for open fermionic systems

The duality  $(E_{ij} | = [|E_{ij}\rangle]^\dagger$  between modes and amplitudes in closed systems via the adjoint is induced by the hermiticity of the time evolution kernel, given by the Liouvillian  $L$ . This suggests that in order to find a mode-amplitude duality for open systems, one has to find a generalization of hermiticity for the open system kernel  $A(\omega) = -iL + W(\omega)$  [Eq. (2.37)], and in particular, for the coupling  $W(\omega)$ . A detailed derivation given in paper II shows that this is indeed possible for *any* fermionic open system governed by the Hamiltonian set up in Sec. 2.1, given that the system can be described in the so-called *wide-band limit*. In this limit, the tunneling constant [Eq. (2.5)] can be approximated as energy independent,  $\Gamma_{ijj'}(E) \rightarrow \Gamma_{ijj'}$ , since the bandwidth is assumed to be much larger than the typical energy splitting in the open system. With this approximation, it follows as a mere consequence of the fermion-parity superselection principle<sup>1</sup> [77–80] that the frequency-dependent time evolution kernel  $A(\omega) = -iL + W(\omega)$  introduced in Sec. 2.7 obeys<sup>2</sup>

$$A(\omega; L, L^T, \{\mu_r\}) = -\Gamma + \mathcal{P}A^\dagger(\bar{\omega}; \bar{L}, \bar{L}^T, \{\bar{\mu}_r\})\mathcal{P}. \quad (3.6)$$

This relation generalizes hermiticity for closed systems,  $L^\dagger = L$ , to *any* open system that belongs to the large class of systems defined by the general model set up in Sec. 2.1, given energy independent but otherwise *arbitrarily strong* tunnel couplings. Next to the adjoint, Eq. (3.6) involves the following

---

<sup>1</sup>The fermion-parity superselection principle prohibits any physical quantum state to be in a quantum superposition of a many-body state with an even fermion number, and another many-body state with an odd fermion number.

<sup>2</sup>Paper II in fact shows this relation only for the coupling  $W$ , but since  $L^\dagger = L$ ,  $[\mathcal{P}, L] = 0$  and thus  $(-iL) = \mathcal{P}(-i(-L))^\dagger\mathcal{P}$ , the relation trivially extends to the combined kernel  $A = -iL + W$ .

three additional operations:

1. A shift by the real non-negative constant  $\Gamma$ , defined as the lumped sum over all assumingly energy independent coupling constants  $\Gamma_{ijj}$  with two equal multi-indices  $j$  for the single-particle states of the open system:

$$\Gamma = \sum_{ij} \Gamma_{ijj} = 2\pi \sum_{ijk} \delta(E - \epsilon_i(k)) \cdot |\tau_{kij}|^2 \geq 0. \quad (3.7)$$

2. Left multiplication by the fermion-parity operator of the open system,  $\mathcal{P}\bullet = (-\mathbf{1})^N \bullet = e^{i\pi N} \bullet$ . The total occupation number operator  $N = \sum_j N_j = \sum_j d_j^\dagger d_j$  is the sum of all occupation number operators  $N_j$  for the single-particle states  $|j\rangle$  defining the open system.

3. A transformation to a *dual model*, defined in terms of

$$\begin{aligned} &\text{inverted energy signs in the open system, } \bar{L} = -L, \\ &\text{inverted signs for the chemical potentials, } \bar{\mu}_r = -\mu_r, \\ &\text{“Wick rotated” couplings, } \bar{L}^T = iL^T, \\ &\text{the same reservoir dynamics and temperatures, } H^R \text{ and } T_r. \end{aligned} \quad (3.8)$$

In Eq. (3.6), the kernel  $A(\bar{\omega}; \bar{L}, \bar{L}^T, \{\bar{\mu}_r\})$  of this dual model is evaluated at the dual frequency  $\bar{\omega} = i\Gamma - \omega^*$ , with the complex-conjugated Laplace frequency  $\omega^*$ .

As we now explain, Eq. (3.6) elucidates the physical relation between modes and amplitudes for open systems. The kernel  $A(\omega; L, L^T, \{\mu_r\})$  contains, according to its perturbation expansion [27, 62, 76, 116, 117], only even orders in the tunneling Liouvillian  $L^T$ , and can thus be written as a function of the coupling constants  $\Gamma_{ijj'}$  [Eq. (2.5)]. Consequently, the imaginary unit in the dual coupling  $\bar{L}^T = iL^T$  effectively leads to an inversion of the signs of all these coupling constant:  $\Gamma_{ijj'} \rightarrow -\Gamma_{ijj'}$ . Altogether, this means that the dual kernel can be constructed entirely by applying a sequence of parameter substitutions to the kernel of interest  $A(\omega; L, L^T, \{\mu_r\})$  *before* evaluating it at the dual frequency  $\bar{\omega} = i\Gamma - \omega^*$ : an inversion of the signs of all energies entering the local dynamics  $L$  as well as all chemical potentials  $\mu_r$ , and a parameter substitution that inverts the signs of all couplings  $\Gamma_{ijj'}$ . Denoting these substitutions as the operator  $\mathcal{I}$ , we can rewrite the relation (3.6) as

$$A(\omega; L, L^T, \{\mu_r\}) = -\Gamma + \mathcal{P}\mathcal{I}A^\dagger(\bar{\omega}; L, L^T, \{\mu_r\})\mathcal{I}\mathcal{P}. \quad (3.9)$$

Note carefully that by definition,  $\mathcal{I}$  does not act on  $i\Gamma$  in the dual frequency argument  $\bar{\omega}$ . We furthermore stress that due to the overall shift by  $-\Gamma$  in Eq. (3.9),

the inversion of all signs of the couplings on the r.h.s. of (3.9) does not lead to an exponential divergence in the time domain.

Importantly, the relation (3.9) non-trivially *cross-links* modes and amplitudes for *different eigenvalues* via the fermion-parity  $(-1)^N$  and the dual model (3.8). Namely, let us assume that we know a frequency-dependent mode  $|x(\omega)\rangle$  with  $A|x(\omega)\rangle = -\gamma_x(\omega)|x(\omega)\rangle$  on a parameter and frequency space containing both the values of interest,  $\{\epsilon_j\}$ ,  $\{\mu_r\}$ ,  $\{\Gamma_{ijj'}\}$ ,  $\omega, \dots$ , as well as their dual counterparts  $\{-\epsilon_j\}$ ,  $\{-\mu_r\}$ ,  $\{-\Gamma_{ijj'}\}$ ,  $i\Gamma - \omega^*, \dots$ . Then, by applying  $(\bar{x}(\bar{\omega})|\mathcal{P}$  with  $\bar{x} = \mathcal{I}x$  from the left to Eq. (3.9), one obtains

$$\begin{aligned}
(\bar{x}(\bar{\omega})|\mathcal{P}A(\omega; L, L^T, \{\mu_r\}) &= -\Gamma(\bar{x}(\bar{\omega})|\mathcal{P} + (\bar{x}(\bar{\omega})|\mathcal{P}\mathcal{P}\mathcal{I}A^\dagger(\bar{\omega}; L, L^T, \{\mu_r\})\mathcal{I}\mathcal{P} \\
&= -\Gamma(\bar{x}(\bar{\omega})|\mathcal{P} + \mathcal{I}[(x(\bar{\omega})|A^\dagger(\bar{\omega}; L, L^T, \{\mu_r\})]\mathcal{I}\mathcal{P} \\
&= -\Gamma(\bar{x}(\bar{\omega})|\mathcal{P} + \mathcal{I}[A(\bar{\omega}; L, L^T, \{\mu_r\})|x(\bar{\omega})]^\dagger\mathcal{I}\mathcal{P} \\
&= -\Gamma(\bar{x}(\bar{\omega})|\mathcal{P} - \mathcal{I}[\gamma_x(\bar{\omega})|x(\bar{\omega})]^\dagger\mathcal{I}\mathcal{P} \\
&= -[\Gamma + (\bar{\gamma}_x(\bar{\omega}))^*](\bar{x}(\bar{\omega})|\mathcal{P}, \tag{3.10}
\end{aligned}$$

where  $\bar{\gamma} = \mathcal{I}\gamma$ . We can proceed analogously if we know an amplitude  $(x'(\omega)|$ . Together, this leads to the frequency-dependent *mode-amplitude duality*

$$\boxed{
\begin{aligned}
A(\omega)|x(\omega)\rangle = -\gamma_x(\omega)|x(\omega)\rangle &\Rightarrow (y'(\omega)|A(\omega) = -\gamma_y(\omega)(y'(\omega)| \\
(x'(\omega)|A(\omega) = -\gamma_x(\omega)(x'(\omega)| &\Rightarrow A(\omega)|y(\omega)\rangle = -\gamma_y(\omega)|y(\omega)\rangle \\
(y'(\omega)| = (\bar{x}(i\Gamma - \omega^*)|\mathcal{P} &\quad |y(\omega)\rangle = \mathcal{P}|\bar{x}'(i\Gamma - \omega^*) \\
\gamma_y(\omega) = \Gamma + (\bar{\gamma}_x(i\Gamma - \omega^*))^* & \tag{3.11}
\end{aligned}$$

Once a frequency-dependent eigenvalue and its mode or its amplitude are known and physically understood, the relations (3.11) provide a systematic starting point to calculate and interpret another eigenvalue and its amplitude or mode. In particular, (3.11) imposes restrictions on the degrees of freedom in the time evolution  $|\rho(t)\rangle$ , and these restrictions have, as we show and explain in detail in the following sections, at least the following two general consequences:

1. The inverted sign of all energies in the local Liouvillian  $L$  in the dual model in particular leads to an inversion of the Liouvillian describing local interactions,  $L^{\text{int}\bullet} = [H^{\text{int}}, \bullet] \rightarrow -L^{\text{int}\bullet}$  [Eq. (2.1)]. This dictates, on very general grounds via the duality (3.11), that the time evolution  $|\rho(t)\rangle$  of open systems with repulsive local fermionic interactions exhibits signatures of *fermion attraction*, either via the mode or the amplitude corresponding to any eigenvalue  $-\gamma_x$ .
2. As a mere consequence of the fundamental requirement of probability conservation and Eq. (3.11), the fermion-parity operator  $|(-1)^N\rangle$  is always a

mode of both  $W(\omega)$  and  $A(\omega)$ . Its eigenvalue is solely determined by the lumped sum of couplings  $-\Gamma$  [Eq. (3.7)]. If the open system consists of  $m \in \mathbb{N}$  single-particle states, this mode only influences the time evolution of  $m$ -particle observables ( $O_m^\dagger|\rho(t)$ ), therefore reflecting non-trivial *many-particle* effects.

For weakly tunnel-coupled systems in the Born-Markov limit, which includes the quantum dot systems of interest in paper I and II, the duality (3.11) becomes particularly insightful. Namely, expanding both sides of Eq. (3.9) up to the linear order in the coupling constants  $\Gamma_{ijj'}$  and evaluating the result at zero frequency<sup>1</sup>, we obtain a duality for the modes  $|x\rangle$  and amplitude covectors  $\langle x'|$  that directly enter the Born-Markov expression for  $|\rho(t)\rangle$  written in the time domain in Eq. (2.33):

$$\boxed{\begin{aligned} \langle x'|A_1 = -\gamma_x \langle x'| &\Rightarrow A_1|y\rangle = -\gamma_y|y\rangle & , & |y\rangle = \mathcal{P}|\bar{x}'\rangle, \\ A_1|x\rangle = -\gamma_x|x\rangle &\Rightarrow \langle y'|A_1 = -\gamma_y \langle y'| & , & \langle y'| = \langle \bar{x}|\mathcal{P} \\ & \gamma_y = \Gamma + \bar{\gamma}_x^* \end{aligned}} \quad (3.12)$$

where  $A_1 = -iL + W_1$  is the zero-frequency Born-Markov kernel introduced in Sec. 2.6.1 Eq. (2.27). The important additional implications of the duality (3.12) are that

- the decay rate  $\Gamma$  corresponding to the fermion-parity mode  $|(-1)^N\rangle$  is the largest decay rate of the system of interest, namely,  $\Gamma \geq \text{Re}(\gamma_x) \geq 0$  for all decay modes  $|x\rangle$ , as argued in the supplementary material to paper II,
- the physical properties of the dual model with *inverted interactions* can possibly be directly visible in the time-dependent quantity that is determined by the amplitude covector [Eq. (2.34)],  $\langle x'|\rho(t)\rangle$ , and that decays at the single rate  $\gamma_x$ .

The general duality relation (3.11) in the frequency domain and the Born-Markov mode-amplitude duality (3.12) are the central relations of this thesis. Their above stated main consequences – the general existence of the fermion-parity mode and the influence of inverted interactions – are to be explained in more detail in the following. In chapter 4 and paper II, these consequences are furthermore illustrated in a concrete physical context for a single-level spin-degenerate quantum dot in the weak coupling regime.

---

<sup>1</sup>More precisely, we expand both sides of Eq. (3.9) in the two dimensionless variables  $\Gamma_{ijj'}/T$  and  $\omega/T$  around  $\Gamma_{ijj'}/T = 0, \omega/T = i0$ , and only consider the constant part which still scales linearly in the couplings  $\Gamma_{ijj'}$ !

### 3.3 The fermion-parity mode

As already mentioned in the discussion of the generalized master equation (2.19), the conservation of total probability in  $|\rho(t)\rangle$  implies that the integral kernel  $\mathcal{W}(t)$  entering Eq. (2.19) is traceless. In other words,  $(\mathbb{1}|$  always constitutes the zero left eigenvector of the kernel, both in the time domain but in particular also in the frequency domain:  $(\mathbb{1}|\mathcal{W}(\omega) = 0$  for arbitrary frequencies  $\omega$  and for any model parameter choice. Together with  $(\mathbb{1}|L\bullet = 0$ , this also implies the vanishing trace of the combined kernel,  $(\mathbb{1}|A(\omega) = -i(\mathbb{1}|L + (\mathbb{1}|\mathcal{W}(\omega) = 0$ . Using the duality as written in Eq. (3.11), this immediately gives the important result

$$\boxed{W(\omega)|(-\mathbb{1})^N) = A(\omega)|(-\mathbb{1})^N) = -\Gamma|(-\mathbb{1})^N)}. \quad (3.13)$$

For a weakly tunnel-coupled single-level quantum dot, this mode and its corresponding rate  $\Gamma$  given by the lumped sum of couplings (3.7) was first noted in [61]; its general existence even for non-Markovian dynamics was shown in [62, 76]. Here and in paper II, it is revealed that both the mode  $|(-\mathbb{1})^N\rangle$  and the parameter-independent rate  $\Gamma$  are in fact completely determined by *probability conservation*, via the duality relation (3.6) based on the fermion-parity superselection principle and the wide-band limit.

To get a first impression of how this affects the time evolution  $|\rho(t)\rangle$ , we apply Eq. (3.13) to the general frequency-dependent eigenmode expansion of  $|\rho(t)\rangle$  given in Eq. (2.39), and obtain

$$|\rho(t)\rangle = a_p \cdot e^{-\Gamma t}|(-\mathbb{1})^N\rangle + |\rho^{\text{rest}}(t)\rangle, \quad (3.14)$$

where  $a_p$  is the amplitude of the parity mode which we discuss in more detail in Sec. 3.4, and  $|\rho^{\text{rest}}(t)\rangle$  is the part of the density operator that does not depend on the parity mode. In other words, the fermion-parity yields a completely Markovian contribution that is characterized by a simple exponential decay at the parity rate  $\Gamma > 0$  – a surprising result given the general complexity of  $|\rho(t)\rangle$ .

To understand which time-dependent physical observable *can in principle be influenced* by the parity rate  $\Gamma$ , we realize from Eq. (3.14) that the parity mode enters an expectation value  $\langle O \rangle(t) = (O^\dagger|\rho(t)\rangle$  whenever the observable operator  $O$  obeys  $(O^\dagger|(-\mathbb{1})^N) \neq 0$ . As shown in App. C, this requires that  $O$  must be *linearly dependent* on the product of all occupation number operators  $N_j$  of single-particle states  $|j\rangle$  defining the open system:

$$O \stackrel{!}{=} \alpha \cdot \prod_j N_j + O^{\text{rest}} \quad , \quad \alpha \in \mathbb{R}^{\neq 0}, \quad (3.15)$$

with the remaining part  $O^{\text{rest}}$  defined to be linear independent of  $\prod_j N_j$ . Equation (3.15) has two main implications:

- In an open system comprised of  $m \in \mathbb{N}$  single-particle states  $|j\rangle$ , the  $m$ -particle fermion-parity mode  $|(-\mathbb{1})^N\rangle$  and its rate  $\Gamma$  only influence  $m$ -particle observables, namely those which are linearly dependent on the product  $\prod_j N_j$  measuring full occupation by  $m$  particles. This implies that the time-dependent expectation value of any observable for a *subsystem* of the open system, such as the occupation  $N_j$  of a *specific* single-particle state  $|j\rangle$ , is not influenced by the fermion-parity mode. A typical example is the setup discussed in paper I, in which a quantum dot and another sensor quantum dot form two subsystems of one big open system. In this case, the fermion-parity mode associated with the full open system combining the two subsystems does not affect any observables localized on the dot to be measured or on the sensor dot.
- The fermion-parity mode  $|(-\mathbb{1})^N\rangle$  does not affect off-diagonal elements of  $|\rho(t)\rangle$  written in the occupation number basis for the single-particle states of the open system  $|j\rangle$ . Hence, if the occupation number states are eigenstates of the local many-body Hamiltonian  $H$ , which is the case for the specific setups studied in paper I and II, the parity mode is not at all seen in the decay of the coherences.

For the nanoscale capacitors of interest here [8, 51–59, 61, 75, 107, 108], the typical level splitting  $\Delta\epsilon$  is at least on the order of the typical potential bias  $\Delta\mu = \mu_r - \mu_{r'}$  in the environment,  $\Delta\epsilon \gtrsim \Delta\mu$ . Hence, the open system and its dynamics  $|\rho(t)\rangle$  can effectively be described by the occupations of only a small number of single-particle states with energies close to the Fermi edge, and the parity mode consequently becomes important already for few-particle observables. This is in particular true for the time-resolved heat current out of the spin-degenerate single-level quantum dot discussed in paper II and chapter 4. For this system, the parity mode is even the *dominant* relaxation mode for the dissipation of the two-particle Coulomb interaction energy. Moreover, as discussed in paper I and chapter 5, the parity rate  $\Gamma$  can in principle even be measured by single-particle observables if the corresponding open system is capacitively coupled to another open system acting as a measurement device.

Interestingly, paper I also shows that the influence of capacitive measurement backaction on the parity rate associated only with the measured single-level dot is relatively weak compared to the effect on all the other decay rates governing the dynamics of the probed system. This observation can be better explained once we clarify *which decay process* is represented by the parity mode, and which is so little influenced by the measurement. To understand this in more detail, we now end this chapter by analyzing the *amplitude covector* of the parity mode. As we will see, this closely connects to the influence of inverted interactions as the above mentioned, second main consequence of the duality relation (3.11) next to the general existence of the parity mode  $|(-\mathbb{1})^N\rangle$ .

## 3.4 The amplitude of the fermion-parity mode

In Sec. 2.6 and, more generally, in Sec. 2.7, we have shown that the amplitudes to the given decay modes entering  $|\rho(t)\rangle$  determine how strongly the modes contribute to the time evolution for a given initial state  $|\rho_0\rangle$ . Thereby, the amplitudes directly relate to the actual *physical decay processes* that are reflected by the respective modes. In particular, for weakly tunnel-coupled systems which are at focus here, we have pointed out in Sec. 2.6.2 that the amplitude covectors  $\langle x'|$  yield quantities that evolve exponentially on a single time scale [Eq. (2.34)]. The following section analyzes the amplitude corresponding to the fermion-parity mode  $|(-\mathbb{1})^N\rangle$  in order to reveal more about the decay process which is represented by this mode and its rate  $\Gamma$ .

### 3.4.1 The parity amplitude covector

We start by deriving the parity amplitude covector from the duality relation (3.11). Since  $\langle \mathbb{1}|$  is a left zero eigenvector of the frequency-dependent kernel  $A(\omega)$ , there exists a single, possibly frequency-dependent, corresponding right zero eigenvector  $|z(\omega)\rangle$  that is trace normalized<sup>1</sup>,  $\langle \mathbb{1}|z(\omega)\rangle = 1$ . Applying the mode-amplitude duality (3.11) to this mode, we obtain an amplitude covector to the rate  $\Gamma$ :

$$\langle p'(\omega)|A(\omega) = -\Gamma\langle p'(\omega)| \quad , \quad \langle p'(\omega)| = \langle \bar{z}(i\Gamma - \omega^*)(-\mathbb{1})^N| \quad , \quad \bar{z} = \mathcal{I}z. \quad (3.16)$$

This vector is, by construction, the single covector normalized to the fermion-parity operator<sup>2</sup>,  $\langle p'(\omega)|(-\mathbb{1})^N\rangle = 1$ , and hence the frequency-dependent amplitude covector corresponding to the parity mode  $|(-\mathbb{1})^N\rangle$ . With this insight, we can use the general frequency-dependent eigenmode expansion (2.39) of  $|\rho(t)\rangle$  and the Cauchy residue theorem to rewrite the contribution of the parity decay

<sup>1</sup>In general, there can be several left and right eigenvectors of  $A(\omega)$  to the eigenvalue 0, but the subspace of right zero eigenvectors can always be spanned by a single vector  $|z(\omega)\rangle$  with  $\langle \mathbb{1}|z(\omega)\rangle = 1$  and other eigenvectors obeying  $\langle \mathbb{1}|z_j(\omega)\rangle = 0$ . The corresponding subspace of left eigenvectors is then analogously spanned by  $\langle \mathbb{1}|$  and further left zero eigenvectors with  $\langle z'_j(\omega)|z(\omega)\rangle = 0$ .

<sup>2</sup>We use that  $|z(\omega)\rangle$  is, by construction (see previous footnote), the *only* trace normalized zero right eigenvector for *any* value of the system parameters and the frequency  $\omega$ , including the ones for the dual model obtained from the parameter substitution  $\mathcal{I}$ :  $1 = \langle \mathbb{1}|\bar{z}(i\Gamma - \omega^*)\rangle^* = \langle \bar{z}(i\Gamma - \omega^*)|\mathbb{1}\rangle = \langle p'(\omega)|(-\mathbb{1})^N\rangle$ . In particular, since any other right zero eigenvector obeys  $\langle \mathbb{1}|z_j(\omega)\rangle = 0 = \langle z_j(\omega)|\mathbb{1}\rangle$  for any parameter and frequency value, the corresponding covector obtained from the duality is orthogonal to the parity mode:  $\langle \bar{z}_j(i\Gamma - \omega^*)(-\mathbb{1})^N|(-\mathbb{1})^N\rangle = \langle \bar{z}_j(i\Gamma - \omega^*)|\mathbb{1}\rangle = 0$ .

mode to the reduced density operator shown in Eq. (3.14):

$$\begin{aligned}
|\rho(t)\rangle &= \frac{-1}{2\pi i} \int_{-\infty}^{\infty} d\omega \underbrace{(\mathbf{1}|\rho_0)}_{=1} e^{-i\omega t} \frac{1}{\omega + i0_+} |z(\omega + i0_+)\rangle \\
&\quad + \frac{-1}{2\pi i} \int_{-\infty}^{\infty} d\omega (p'(\omega + i0_+)|\rho_0) e^{-i\omega t} \frac{1}{\omega + i\Gamma + i0_+} |(-\mathbf{1})^N\rangle \\
&\quad + \dots
\end{aligned} \tag{3.17}$$

$$\begin{aligned}
&= |z(\omega = -i0_+ + i0_+)\rangle + (\bar{z}(\omega = i\Gamma - (-i\Gamma)^*)|\rho_0) \cdot e^{-\Gamma t} |(-\mathbf{1})^N\rangle + |\rho^{\text{rest}}(t)\rangle \\
&= |z(i0)\rangle + (\bar{z}(i0)(-\mathbf{1})^N|\rho_0) \cdot e^{-\Gamma t} |(-\mathbf{1})^N\rangle + |\rho^{\text{rest}}(t)\rangle,
\end{aligned} \tag{3.18}$$

where  $|\rho^{\text{rest}}(t)\rangle$  here includes the contributions from all other modes, that is,  $|x(\omega)\rangle \neq |z(\omega)\rangle$  and  $|x(\omega)\rangle \neq |(-\mathbf{1})^N\rangle$ , and also any algebraically decaying term that could possibly emerge from the frequency integrals in Eq. (3.17). This means that we have identified the amplitude  $a_p$  of the parity mode introduced in Eq. (3.14) as the overlap of the following two vectors: the trace normalized zero right eigenvector of the zero-frequency kernel  $\bar{A}(i0)$  for the *dual model* (3.8), and the initial state  $\rho_0$  multiplied by the fermion-parity operator  $(-\mathbf{1})^N$ :

$$\boxed{a_p = (z_i|(-\mathbf{1})^N|\rho_0) \quad , \quad |z_i\rangle = |\bar{z}(i0)\rangle \quad , \quad \bar{z} = \mathcal{I}z}. \tag{3.19}$$

This expression for  $a_p$  generally holds for any fermionic system belonging to the class of models set up in Sec. 2.1, even without any approximation except for energy-independent couplings  $\Gamma_{ijj'}$ . However, its physical meaning is particularly clear for the weakly tunnel-coupled ( $\Gamma \ll T$ ), dissipative quantum dot systems with strong local Coulomb repulsion ( $U \gg T$ ) we are interested in, most importantly the ones studied in the two appended papers. In these cases,  $|z\rangle = |z(i0)\rangle$  represents the unique stationary state  $|z\rangle = \lim_{t \rightarrow \infty} |\rho(t)\rangle$  in the Born-Markov limit, and  $|z_i\rangle$  consequently becomes the stationary state<sup>1</sup> of the respective *dual model*. This state is also denoted as the *inverted stationary state*, since it is determined with respect to inverted local energies  $L \rightarrow -L$  and inverted chemical potentials  $\{\mu_r\} \rightarrow \{-\mu_r\}$ , see Fig. 3.1. As we now discuss, the key to a physical interpretation of the parity mode for weakly coupled open systems lies in the properties of this inverted stationary state  $|z_i\rangle$ .

---

<sup>1</sup>We assume that the parameter substitution  $\mathcal{I}$  generating the dual model does not map  $|z\rangle$  into any unphysical regime. This particularly relies on the shift by the lumped sum of couplings  $\Gamma$  in the mode-amplitude duality (3.12).

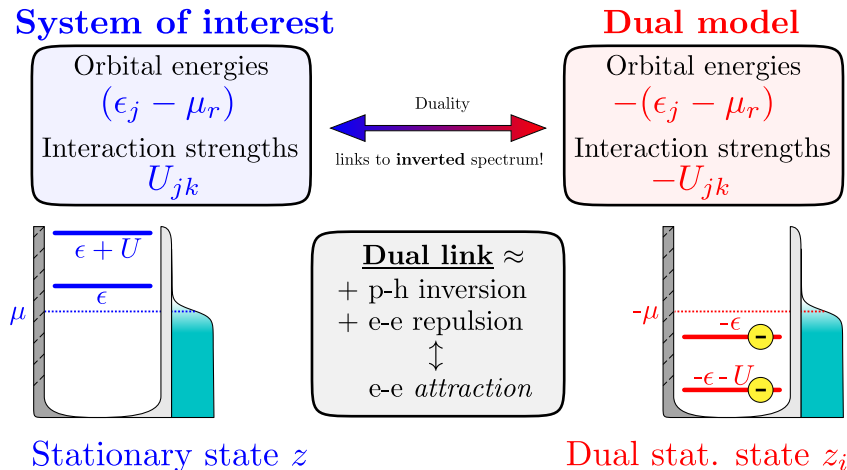


**Figure 3.1:** Illustration of how the duality relation (3.12) links the system of interest (blue) to the dual model with an inverted spectrum (red), resulting in a particle-hole transformed and interaction inverted dual stationary state. The shown example system is a spin-degenerate single-level quantum dot, characterized by the level position  $\epsilon$  and local interaction strength  $U$ , which is tunnel-coupled to a reservoir with chemical potential  $\mu$ .

### 3.4.2 The stationary state of the dual model

The first step to a better understanding of the parity mode for weakly tunnel-coupled systems is, as we see further below, to realize that in the Born-Markov limit,  $|z_i\rangle$  is a valid physical density operator. Thus, we start this subsection by summarizing the formal properties of the vector  $|z_i\rangle = |\bar{z}\rangle = |\mathcal{I}z\rangle$  which verify this. We find: (1)  $z_i = z_i^\dagger$  is hermitian because the stationary state operator  $z$  is hermitian by assumption, and because the parameter substitution  $\mathcal{I}$  does not involve any complex conjugation. (2)  $|z_i\rangle$  is trace normalized by biorthonormality of the parity amplitude covector  $(z_i(-\mathbb{1})^N | (-\mathbb{1})^N)$  [Eq. (3.16)] to the fermion-parity mode, dictating that  $1 \stackrel{!}{=} (z_i(-\mathbb{1})^N | (-\mathbb{1})^N) = (z_i | \mathbb{1}) = (\mathbb{1} | z_i) = \text{Tr}[z_i]$ . (3) Finally, as argued in the supplementary material to paper II for an open system with a finite amount of single-particle states and reservoirs in the wide-band limit, the mere parameter substitution  $\mathcal{I}$  does not map the assumingly positive stationary state  $|z\rangle$  into an unphysical regime with negative probabilities. Consequently,  $z_i = \mathcal{I}z$  also has positive probabilities, and is thus a valid density operator. Together with  $\bar{A}_1|z_i\rangle = 0$  for the dual Born-Markov kernel  $\bar{A}_1$ , this confirms that  $|z_i\rangle$  is indeed the density operator that represents the stationary state of the dual model.

Next, let us explain the *physical properties* of the inverted stationary state  $|z_i\rangle$ . As illustrated by Fig. 3.1, this state is obtained from the stationary state  $|z\rangle$  of the open system of interest by inverting all single-particle potentials,  $(\epsilon_j - \mu_r) \rightarrow -(\epsilon_j - \mu_r)$ , and all interaction energies,  $U \rightarrow -U$ , after the initial switch which induces the time evolution  $|\rho(t)\rangle$ , see Sec. 2.3. The inversion of the single-particle

energies in  $|z_i\rangle$ ) has the simple effect of particle-hole transforming the occupations in the stationary state  $|z\rangle$ , since the reservoir occupations are antisymmetric with respect to the chemical potentials  $\mu_r$ . The inverted sign of the interactions generally leads to additional, and less straightforwardly interpretable effects. Nevertheless, for *spinful* fermions and strong local Coulomb repulsion, we can already identify one important consequence of the interaction inversion. Namely, for typical Coulomb energies  $U$  much larger than the typical temperature  $T$  and the Zeeman splitting due to any external magnetic field  $B$ , it is clear that the strong attraction in the *dual model* generally forces the dual fermionic (quasi-)particle occupation number to be an even number. The reason is that fermionic levels for non-zero spin always have an even number of Zeeman splittings or degeneracies, and an occupation of one such level immediately attracts more fermions that fill the remaining levels if the interaction is strongly attractive. This means that the inverted stationary state becomes, up to corrections  $\sim \max(B, T)/U$ , a mixed state in the even parity sector:  $(-1)^N |z_i\rangle \approx |z_i\rangle$ . This is, as we now show, a second key insight for a better understanding of the parity mode.

### 3.4.3 The decay process represented by the parity mode

With the main properties of the inverted stationary state  $|z_i\rangle$  pointed out, we can finally discuss the relevance of the parity mode and its rate  $\Gamma$  for the dynamics of the class of open systems considered in paper I and II: weakly tunnel-coupled ( $\Gamma \ll T$ ) spinful<sup>1</sup> multi-level sites with strong local repulsive Coulomb interactions ( $U \gg T$ ). First of all, the fact that  $|z_i\rangle$  is a physical state density operator implies that the parity amplitude  $a_p = (z_i(-1)^N |\rho_0\rangle)$  at which the mode  $|(-1)^N\rangle$  contributes to  $|\rho(t)\rangle$  [Eq. (2.33)] for a given initial state  $|\rho_0\rangle$  lies in the interval

$$-1 \leq a_p = (z_i(-1)^N |\rho_0\rangle) \leq 1. \quad (3.20)$$

Using  $z_i = z_i^\dagger$ , from which follows  $(z_i(-1)^N |\rho\rangle) \in \mathbb{R}$ , and the mixed state property  $0 < (z_i|z_i), (\rho_0|\rho_0) \leq 1$ , the relation (3.20) readily follows from the Cauchy-Schwartz inequality applied to  $|(z_i(-1)^N |\rho_0\rangle)|^2$ . This relation is important whenever one is interested in the *relative influence* of the parity mode on a certain observable, as Eq. (3.20) imposes a restriction on this influence. We use this result in paper II when evaluating the relevance of the parity mode for the time-dependent heat current out a single-level quantum dot.

Next, to explain exactly which decay process is reflected by the parity mode  $|(-1)^N\rangle$  and its rate, we consider the time-dependent average  $(z_i(-1)^N |\rho(t)\rangle)$  of the quantity defined by the parity amplitude covector  $(z_i(-1)^N |)$ , as this average

---

<sup>1</sup>For the analytical treatment, paper I assumes a spinless detector level. However, we also show numerical results for the more realistic case of a spin-degenerate detector with strong local repulsion.

decays exclusively at the parity rate  $\Gamma$  [Eq. (2.34)]. Using the dual state property  $(-\mathbb{1})^N |z_i\rangle \approx |z_i\rangle$  previously deduced for open systems with strongly repulsive Coulomb interactions, we see that the parity amplitude  $a_p = (z_i(-\mathbb{1})^N |\rho_0\rangle)$  becomes a mixed state overlap between the inverted stationary state and the initial state; the quantity that decays exclusively at the parity rate  $\Gamma$  likewise becomes the overlap between  $|z_i\rangle$  and the *time-dependent* system state  $|\rho(t)\rangle$ :

$$a_p \approx (z_i|\rho_0) \quad , \quad (z_i(-\mathbb{1})^N |\rho(t)\rangle) \approx (z_i|\rho(t)) \approx (z_i|\rho_0)e^{-\Gamma t} \quad \forall U \gg T, B. \quad (3.21)$$

From a fundamental point of view, this relation is interesting because the interpretation of an amplitude as a state overlap is completely analogous to *closed system dynamics*, see Sec. 3.1. More practically, Eq. (3.21) provides a more concrete understanding of the fermion-parity mode:

Given that  $|\rho_0\rangle$  has a finite overlap with  $|z_i\rangle$  in the even parity sector – such that  $a_p > 0$  and the mode is excited – the fermion-parity mode and the rate  $\Gamma$  essentially represent the time-dependent effect of the *first* of several tunneling processes induced by the initial switch, as this process drives  $|\rho(t)\rangle$  to the odd parity sector in which  $(z_i|\rho_0)e^{-\Gamma t} = (z_i|\rho(t)) \rightarrow 0$  must have decayed.

The crucial point is that for the systems discussed here, the parity mode *cannot* in general be associated with any specific physical observable with a straightforward physical interpretation, such as charge or spin. Rather, the mode reflects a *specific tunneling process* that can, however, be clearly identified within the sequential tunneling picture in the lowest order  $\Gamma$  approximation. Namely, each physical observable of which the time-dependent average is dominated by the first of several sequential tunneling events is strongly affected by the parity mode. Furthermore, in order to see a sizable effect of this mode, the initial state  $|\rho_0\rangle$  and the final parameters after the switch specifying  $|z_i\rangle$  have to be chosen to achieve a large initial overlap  $(z_i|\rho_0)$ , meaning that one has to induce, on average, more than one tunneling event. In the following chapters 4 and 5, which review the appended papers I and II, this interpretation of equation (3.21) is put into a concrete physical context for the interacting single-level quantum dot.

### 3.5 Summary

Let us summarize the main insights of this chapter.

1. We have discussed a general duality relation [Eq. (3.11)] between the frequency-dependent modes and amplitudes governing the time evolution of the reduced density operator for open fermionic quantum systems. This duality was first identified in paper II. It applies to all systems that can be described by
  - an *arbitrary* fermionic local Hamiltonian  $H$ ,
  - an environment  $H^R$  consisting of a number of effectively non-interacting fermionic reservoirs at arbitrary temperature and electrochemical potential,
  - and a bilinear (tunnel) coupling between the local system and the environment that is characterized by assumingly energy-independent, but otherwise arbitrarily strong couplings.
2. This duality generally dictates the fermion-parity of the open system to be a decay eigenmode  $|(-\mathbf{1})^N\rangle$  whose decay rate equals the lumped sum  $\Gamma$  of coupling constants (3.7). The rate is thus independent of any reservoir or open system parameter. In an open system consisting of  $m \in \mathbb{N}$  single-particle states, this mode only affects the time evolution of  $m$ -particle observables. For the concrete models discussed in the appended papers, the parity mode governs the transient open system behavior which reflects the first of several sequential tunneling events.
3. Finally, the duality links the decay behavior of the open system to the physical properties of a *dual model* with inverted energies. This predicts, on very general grounds, that the time-dependent decay of open systems with repulsive local interactions exhibits signatures of *fermion attraction*. This becomes most explicit for systems with spinful fermions and strong repulsive Coulomb interaction,  $U \gg T$ , described in the Born-Markov limit. In those cases, the parity mode and its rate  $\Gamma$  govern the decay of the time-dependent overlap between the system state  $|\rho(t)\rangle$  and the *stationary state of the dual model*,  $|z_i\rangle$ . This inverted stationary state derives from the stationary state of interest,  $|z\rangle$ , via a particle-hole transform combined with an inversion of the interaction, and the latter leads to signatures of attraction in the time evolution of the system. The properties of the inverted state allow to identify the parity mode as the mode reflecting the effect of the first tunneling process after the initial switch whenever more than one tunneling event is induced by this switch.

# 4 Time-dependent energy relaxation of an interacting quantum dot

While one key result of paper II is the general duality relation Eq. (3.6) discussed in the previous chapter 3, the actual aim of this paper is to study a very concrete and recent, yet up to now only little discussed issue in the field of electronic heat transport through nanoscale systems [50–59, 81–84, 108, 125]: the *transient* electronic energy dissipation of a small open electron system, characterized by a large level splitting and *strong local Coulomb repulsion*, into a weakly tunnel-coupled reservoir. One main aim of this chapter is to summarize the findings of paper II which relate specifically to this topic. However, since this paper is very brief in providing the more basic, yet necessary background knowledge, we first expand on a few aspects concerning the description of the time-dependent density operator  $|\rho(t)\rangle$ . Let us start by setting up the model Hamiltonian.

## 4.1 Model

We study the system depicted in Fig. 4.1. It consists of a single-level spin-degenerate quantum dot – the open system – that is tunnel-coupled to a single electronic reservoir. Accordingly, the full Hamiltonian  $H^{\text{tot}} = H + H^{\text{R}} + H^{\text{T}}$  set up in Sec. 2.1 Eq. (2.2) - Eq. (2.4) simplifies to a local part  $H$  governing only the quantum dot, an environment part  $H^{\text{R}}$  with only one reservoir, and the tunnel coupling  $H^{\text{T}}$  between reservoir and dot. The dot part  $H$  describes a single spin-degenerate electronic level of which the level position  $\epsilon$  can be controlled time-dependently by an external gate potential  $V_{\text{t}}$ . If the dot is doubly occupied, we also take into account the on-site Coulomb interaction giving rise to the additional charging energy  $U$ . The Hamiltonian reads

$$H = \sum_{\sigma=\uparrow,\downarrow} \epsilon d_{\sigma}^{\dagger} d_{\sigma} + U N_{\uparrow} N_{\downarrow} = \epsilon N + U N_{\uparrow} N_{\downarrow}. \quad (4.1)$$

The first term is the single-particle contribution, which is proportional to the dot occupation number operator  $N = \sum_{\sigma=\uparrow,\downarrow} d_{\sigma}^{\dagger} d_{\sigma}$  and thus quadratic in creation (annihilation) operators  $d_{\sigma}^{\dagger}$  ( $d_{\sigma}$ ) for dot electrons with spin  $\sigma \in \{\uparrow, \downarrow\}$ . The second

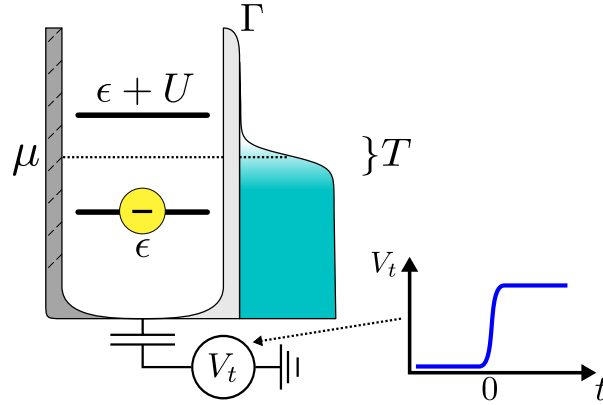


**Figure 4.1:** Sketch of the spin-degenerate single-level quantum dot tunnel-coupled to an electronic reservoir. The level-position of the dot is denoted by  $\epsilon$ . It can be tuned time-dependently via the applied gate potential  $V_t$ . The Coulomb interaction strength on the quantum dot is given by  $U$ , the spin-independent tunneling strength by  $\Gamma_{\uparrow} = \Gamma_{\downarrow} = \Gamma/2$ . The reservoir is described by a non-interacting Fermi sea which is characterized by its chemical potential  $\mu$  and its temperature  $T$ . Our main interest is the time-dependent response of the system to a sudden shift of the level-position at some initial time  $t = 0$ , as indicated in the sketch. We work in the weak tunnel-coupling regime,  $\Gamma/T \ll 1$ , but assume strong Coulomb interaction,  $U/T \gg 1$ .

contribution is the quartic 2-particle interaction term, given by the product of the two occupation number operators  $N_{\sigma} = d_{\sigma}^{\dagger}d_{\sigma}$  for the individual spins times the interaction strength  $U$ .

The Hamiltonian of the single non-interacting reservoir is, apart from the absence of the reservoir quantum number  $r$ , equal to the general Hamiltonian of the environment  $H^R$  discussed in Sec. 2.1 [Eq. (2.3)]:

$$H^R = \sum_{\mathbf{k}i} \epsilon_i(\mathbf{k}) c_{\mathbf{k}i}^{\dagger} c_{\mathbf{k}i}, \quad (4.2)$$

with the Bloch vector  $\mathbf{k}$  and the multi-index  $i = n_i, \sigma_i, \dots$  for electrons with spin  $\sigma$ , band index  $n$ , and any further quantum number required to fully characterize the single-particle states.

The dot shall couple to the environment via spin-conserving and spin-symmetric electron tunneling. The corresponding general coupling Hamiltonian  $H^T$  [Eq. (2.4)] therefore simplifies to

$$H^T = \sum_{\mathbf{k}i} [\tau_{\mathbf{k}i} c_{\mathbf{k}i}^{\dagger} d_{\sigma_i} + \text{H.c.}], \quad (4.3)$$

where the tunneling amplitudes shall obey  $\tau_{\mathbf{k},\uparrow,\dots} = \tau_{\mathbf{k},\downarrow,\dots}$ . This Hamiltonian yields the spin-symmetric tunneling frequencies according to the general expression Eq. (2.5):

$$\Gamma(E)/2 = \Gamma_{\uparrow}(E) = \Gamma_{\downarrow}(E) = 2\pi \sum_{\mathbf{k}i} \delta_{\sigma_i\uparrow} \delta(E - \epsilon_i(\mathbf{k})) |\tau_{\mathbf{k}i}|^2. \quad (4.4)$$

The crucial assumption to exploit the insights of the duality relation (3.11) given in Sec. 3.2 is the wide-band limit, in which the tunneling strength can be regarded as *effectively* energy independent:

$$\Gamma(E)/2 \rightarrow \Gamma/2 = \Gamma_{\uparrow} = \Gamma_{\downarrow}, \quad (4.5)$$

where  $\Gamma = \Gamma_{\uparrow} + \Gamma_{\downarrow}$  is the lumped sum of coupling constants [Eq. (3.7)]. Importantly, we are interested in the experimentally relevant [50, 89] regime of weak coupling,  $\Gamma \ll T$ , which in the following allows us to treat the transient dynamics of the quantum dot in the Born-Markov limit [Sec. 2.6].

More precisely, we are interested in how the above described open quantum dot system dissipates its stored energy *in time* via electron tunneling due to an initial non-equilibrium, induced by a fast level shift  $\epsilon_0 \rightarrow \epsilon$  at a fixed initial time  $t_0 \equiv 0$ , see Fig. 4.1. Our aim is to study the transient transport using the general Born-Markov expressions for the charge and heat current into the reservoir, Eq. (2.28), and in particular the simplified heat current formula Eq. (2.29) which is valid for the spin-degenerate single-level quantum dot [App. B]:

$$I_N(t) = -(N|W_1|\rho(t)) \quad , \quad I_Q(t) = -(H|W_1|\rho(t)) - \mu I_N(t), \quad (4.6)$$

where  $W_1$  is the coupling kernel entering the Born-Markov master equation (2.25). To understand these expressions, paper II first establishes the time-dependent reduced density operator  $|\rho(t)\rangle$ . However, due to length restrictions, the paper focuses mainly on the new aspect, which is to illustrate the implications of the Born-Markov duality relation (3.12) for the heat current  $I_Q(t)$ ; some more basic intermediate steps are only briefly discussed or omitted entirely. In the following section 4.2 and in the appendices referenced therein, we intend to fill these gaps. Readers which are already familiar with the Born-Markov treatment of the given quantum dot system may, however, continue directly with Sec. 4.3. This section discusses a concrete illustration of the inverted stationary state for the studied single-level dot.

## 4.2 Reduced density operator of the quantum dot

The system described in the previous section belongs to the general class of open fermionic quantum systems discussed in Sec. 2.1. Hence, we can follow the procedure outlined in Sec. 2.3 and Sec. 2.6 to arrive at the Born-Markov limit solution [Eq. (2.33)] to the generalized master equation governing the quantum dot dynamics  $|\rho(t)\rangle$  due to an initial non-stationarity:

$$|\rho(t)\rangle = |z\rangle + \sum_{x \neq z} (x'|\rho_0) e^{-\gamma_x t} |x\rangle, \quad (4.7)$$

with the initially prepared dot state  $|\rho_0\rangle$  before the switch at  $t = 0$ , and the stationary state  $|z\rangle = \lim_{t \rightarrow \infty} |\rho(t)\rangle$ , which for a single reservoir is simply given

by the thermal equilibrium state  $|z\rangle = e^{-(H-\mu N)/T} / \text{Tr} [e^{-(H-\mu N)/T}]$ . Importantly, as shown explicitly in App. A.2, the kernel  $A_1$  governing the Born-Markov time evolution  $|\rho(t)\rangle = e^{A_1 t} |\rho_0\rangle$  [Eq. (2.27)] for a single-level quantum dot with spin conserving tunneling does not couple the coherences in  $|\rho(t)\rangle$  to the eigenstate probabilities. This implies that we can reduce the description of  $|\rho(t)\rangle$  to the Liouville space spanned solely by the projectors for the energy eigenstates of the quantum dot many-body Hamiltonian  $H$ . These are constructed from the occupation number states representing zero occupation, single spin-up or spin-down occupation, and double occupation of the dot orbital:

$$\begin{aligned} |0\rangle &= |0\rangle\langle 0| = |n_\uparrow = 0; n_\downarrow = 0\rangle\langle n_\uparrow = 0; n_\downarrow = 0| \\ |\uparrow\rangle &= |\uparrow\rangle\langle\uparrow| = |n_\uparrow = 1; n_\downarrow = 0\rangle\langle n_\uparrow = 1; n_\downarrow = 0| \\ |\downarrow\rangle &= |\downarrow\rangle\langle\downarrow| = |n_\uparrow = 0; n_\downarrow = 1\rangle\langle n_\uparrow = 0; n_\downarrow = 1| \\ |2\rangle &= |2\rangle\langle 2| = |n_\uparrow = 1; n_\downarrow = 1\rangle\langle n_\uparrow = 1; n_\downarrow = 1|. \end{aligned} \quad (4.8)$$

In this subspace, only the reservoir coupling  $W_1$  of the time evolution kernel  $A_1 = -iL + W_1$  is relevant for the dynamics<sup>1</sup>. As explained in App. A.2, this coupling describes dot eigenstate transitions via the well known Fermi's Golden rule transition rates [74], implying positive relaxation rates  $\gamma_x > 0$  as well as the uniqueness of the stationary state  $|z\rangle$  [App. A.3]. Moreover, since the coupling is fully spin-symmetric and since we are not interested in any spin resolved observables, we can use the mixed state  $|1\rangle = \frac{1}{2} [|\uparrow\rangle + |\downarrow\rangle]$  to further reduce the dimension of the relevant Liouville space to 3. The basis vectors are then simply  $|0\rangle, |1\rangle$  and  $|2\rangle$ , and the dual space of scalar products is analogously spanned by  $\langle 0|, \langle 1|, \langle 2|$ . In paper II, we determine the reduced density operator  $|\rho(t)\rangle$  within this subspace, using the general insights provided by the Born-Markov duality relation (3.12) introduced in chapter 3:

$$\boxed{|\rho(t)\rangle = |z\rangle + (z_i(-\mathbf{1})^N |\rho_0\rangle \cdot e^{-\Gamma t} |(-\mathbf{1})^N\rangle + \frac{N_0 - N_z}{2} e^{-\gamma_c t} (-\mathbf{1})^N [|N\rangle - N_i |1\rangle])}. \quad (4.9)$$

The state  $|z_i(\epsilon, U, \mu, T)\rangle = |\mathcal{I}z\rangle = |z(-\epsilon, -U, -\mu, T)\rangle$  is the inverted stationary state of the dual model [Eq. (3.8)] for the single-level quantum dot in the weak coupling limit; it enters directly in the amplitude covector  $(z_i(-\mathbf{1})^N |$  to the parity mode  $|(-\mathbf{1})^N\rangle$  [Eq. (3.13)], corresponding to the parity rate  $\Gamma = \Gamma_\uparrow + \Gamma_\downarrow$ , but also through its average occupation  $N_i = (N|z_i)$ . Furthermore,  $N_0 = (N|\rho_0)$  and  $N_z = (N|z)$  are the initial and stationary occupation number of the dot. The only decay rate in Eq. (4.9) next to the parity rate is given by  $\gamma_c = \frac{\Gamma}{2} [f^+(\epsilon) + f^-(\epsilon + U)]$ , written in terms of the Fermi functions  $f^\pm(\epsilon) = [\exp(\pm(\epsilon - \mu)/T) + 1]^{-1}$ . This rate exclusively governs the time-dependent decay of the charge number  $N(t) =$

<sup>1</sup>Note that the energy eigenstate projectors  $|E\rangle$  are zero eigenmodes of the dot Liouvillian,  $L|E\rangle = 0$ , and thus not influenced by the coherent dynamics governed by  $L$ .

$(N|\rho(t))$  as the only relevant single-particle observable for the system [61, 75], and is therefore called charge rate.

Importantly, Eq. (4.9) clearly shows that the inverted stationary state of the dual model is crucial for the understanding of  $|\rho(t)\rangle$ , as it enters both through the parity amplitude covector  $(z_i(-\mathbb{1})^N|$  and through its occupation number  $N_i$  in the mode decaying at the charge rate  $\gamma_c$ . In paper II, we focus on how this peculiar dependence on  $|z_i\rangle$  influences the transient heat current  $I_Q(t)$ , but only provide a short discussion on the inverted stationary state itself. Given its importance for  $|\rho(t)\rangle$ , let us therefore in the following first describe  $|z_i\rangle$  in more detail before we summarize the results for the transient heat current  $I_Q(t)$ .

## 4.3 The inverted stationary state

We have pointed out in Sec. 3.4.2 that  $|z_i\rangle$  is derived from the stationary state  $|z\rangle$  by inverting the sign of all interaction energies, and by applying a particle-hole transform. For the concrete case of a spin-degenerate single-level quantum dot, this yields the particle-hole transformed stationary state of an *attractive Anderson model* [124] with switched stationary probabilities for the empty and doubly occupied state, as explicitly shown in the supplementary material to paper II. To illustrate how such a system behaves, Fig. 4.2 graphically compares  $|z\rangle$  and  $|z_i\rangle$ , as well as their average occupations  $N_z$  and  $N_i$ , for different level positions  $\epsilon - \mu$  and a strong interaction,  $U \gg T$ . Let us state the main insights that emerge from this comparison:

1. The attractive interaction prohibits a stable single occupation *in the dual model*,  $|z_i\rangle \neq |1\rangle$  (up to corrections  $\sim T/U$ ), even at the particle-hole symmetry point<sup>1</sup>,  $\epsilon - \mu = -U/2$ , where the *average* dual occupation number equals  $N_i(\epsilon - \mu, U) = N_z(-\epsilon + \mu, -U) = N_z(U/2, -U) = 1$  because of the *even* mixture between zero and double occupation. This explicitly confirms  $(-\mathbb{1})^N|z_i\rangle \approx |z_i\rangle$  and hence Eq. (3.21), predicting that the fermion-parity rate governs the decay of the overlap between the inverted stationary state and the time-dependent dot state,  $(z_i|\rho(t)) \propto e^{-\Gamma t}$ . For a doubly occupied stationary state  $|z\rangle \rightarrow |2\rangle$ , this overlap describes the decay of an initially empty state  $|0\rangle$  [Fig. 4.2(a)]; for a stationary zero occupation,  $|z\rangle \rightarrow |0\rangle$ , it represents the relaxation of the doubly occupied state  $|2\rangle$  [Fig. 4.2(b)]. At the particle-hole symmetric point, the decay of *both*  $|0\rangle$  and  $|2\rangle$  to the stable singly occupied state  $|z\rangle \rightarrow |1\rangle$  of the quantum dot (not the dual model) is governed by the parity rate  $\Gamma = \Gamma_\uparrow + \Gamma_\downarrow$  [Fig. 4.2(c)]. In agreement with the interpretation of the parity mode given in Sec. 3.4.3, the rate  $\Gamma$  in any case yields the temperature-, level-, and interaction-independent

<sup>1</sup>Note that the charging energy  $U$  is always defined positive.

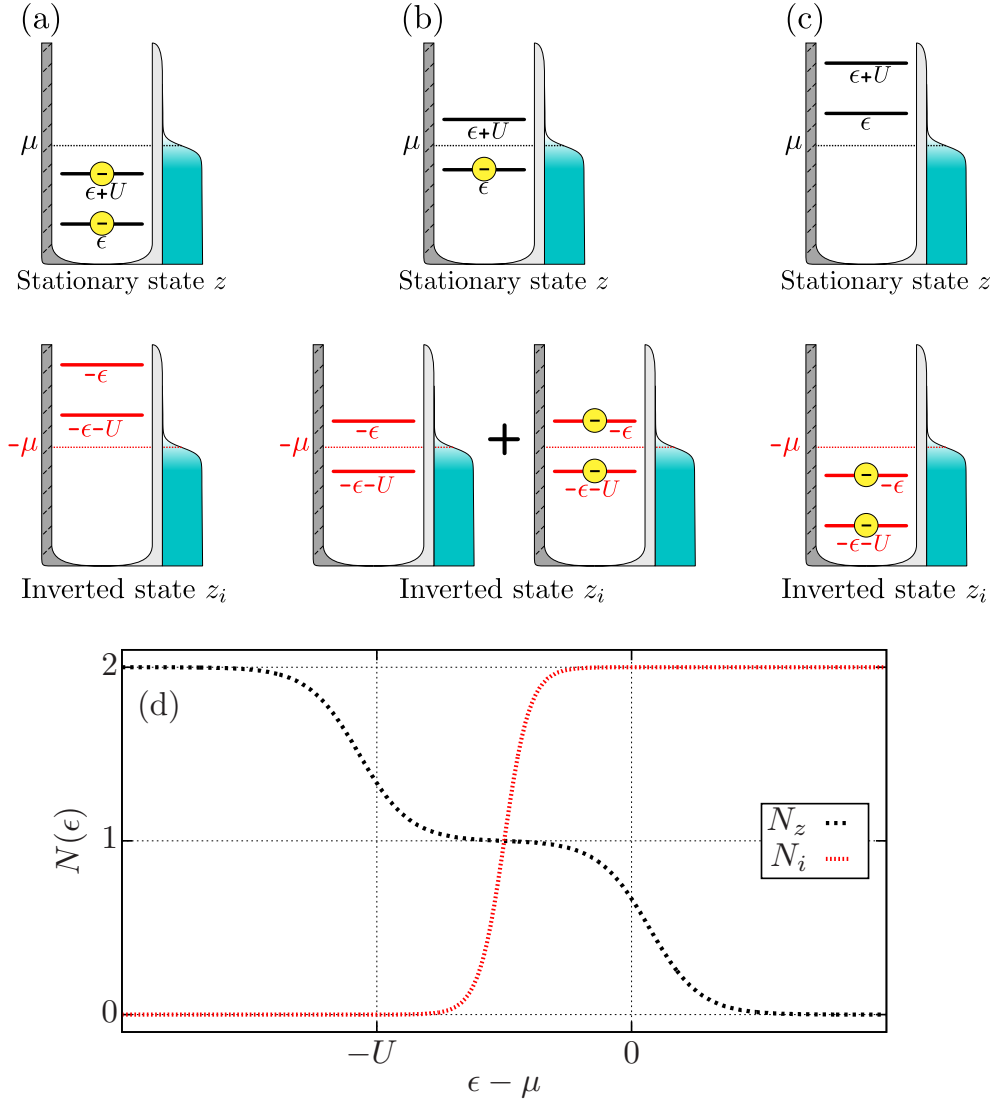


**Figure 4.2:** (a,b,c) Comparison between the stationary state  $|z\rangle$  and the inverted stationary state  $|z_i\rangle$  of the quantum dot for several level positions  $\epsilon$  relative to the chemical potential  $\mu$  of the environment. The + sign in (b) indicates that  $|z_i\rangle$  is a statistical mixture between the zero and doubly occupied state. (d) The average particle number in the stationary state,  $N_z = \langle N|z\rangle$ , and in the inverted stationary state,  $N_i = \langle N|z_i\rangle$ , as a function of the level position. In each plot, we assume a weak tunnel coupling,  $\Gamma \ll T$ , and a strong local Coulomb interaction strength,  $U \gg T$ , where  $T$  is the temperature of the reservoir.

typical time scale for the *first* tunneling event whenever more than one such event is induced by the level-shift.

2. A related consequence of the unstable single occupation in the dual model is that its stationary occupation number  $N_i$  takes a rapid transition between 0 and 2 when sweeping the level position through the particle-hole symmetry point  $\epsilon - \mu = -U/2$  [Fig. 4.2(d)]. Since  $N_i$  influences the charge mode and

the overlap  $(z_i(-\mathbb{1})^N|\rho_0)$ , see Eq. (4.9), this jump is expected to be visible in the parameter dependence of the quantum dot decay behavior.

The results of paper II which are summarized in the following show that the two above mentioned points are directly reflected in the behavior of the time-dependent heat current  $I_Q(t)$  into the environment.

## 4.4 Transient heat transport

In this final section, we summarize the main findings of paper II for the time-dependent electronic heat current  $I_Q(t)$  out of the dot into the reservoir due to an instant dot level shift  $\epsilon_0 \rightarrow \epsilon$  [Fig. 4.3(a, b)]. Assuming a constant interaction strength and temperature,  $U \gg T$ , these results follow by evaluating the formulas Eq. (4.6) for the transient electronic particle current  $I_N(t)$  and heat current  $I_Q(t)$  with a time-dependent state  $|\rho(t)\rangle$  described by Eq. (4.9). We choose the stationary state with respect to the *initial* level  $\epsilon_0$  as the initially prepared state:  $|\rho_0\rangle = |z(\epsilon_0, U, \mu, T)\rangle$ . The final result, which is derived and directly linked to the duality relation (3.12) in paper II, can be summarized by the following set of expressions<sup>1</sup>:

$$\begin{aligned}
 I_N(t) &= \gamma_c (N_0 - N_z) e^{-\gamma_c t} \\
 I_Q(t) &= \left[ \epsilon - \mu + \frac{2 - N_i}{2} U \right] I_N(t) + U\Gamma (z_i(-\mathbb{1})^N |\rho_0) e^{-\Gamma t} \\
 &= a_c e^{-\gamma_c t} + a_p e^{-\Gamma t} \\
 a_c &= \gamma_c \cdot \left[ \epsilon - \mu + \frac{2 - N_i}{2} U \right] \cdot (N_0 - N_z) \\
 a_p &= U\Gamma (z_i(-\mathbb{1})^N |\rho_0) = \frac{U\Gamma}{2} \left\{ (N_i - 1)(N_0 - 1) + \frac{1}{2} (p_i + p_0) \right\}. \quad (4.10)
 \end{aligned}$$

The main insights that paper II extracts from these equations, and in particular from the amplitudes  $a_c$  and  $a_p$  that are shown in Fig. 4.3(c,d) as a function of the initial ( $\epsilon_0$ ) and final ( $\epsilon$ ) level of the switch, are:

1. The electronic heat current consists of two contributions: (I) a “tight-coupling”-part [50] that is proportional to the charge current  $I_N(t)$ , and hence describes the average energy that is carried by each tunneling electron, and (II) a particle-particle correlation term that arises solely as consequence of the Coulomb energy dissipation in the heat current, and is thus not visible in the charge current which constitutes only a single-particle observable.

<sup>1</sup>In contrast to chapter 3, the parity amplitude  $a_p$  is here defined to include the factor  $U\Gamma$ .

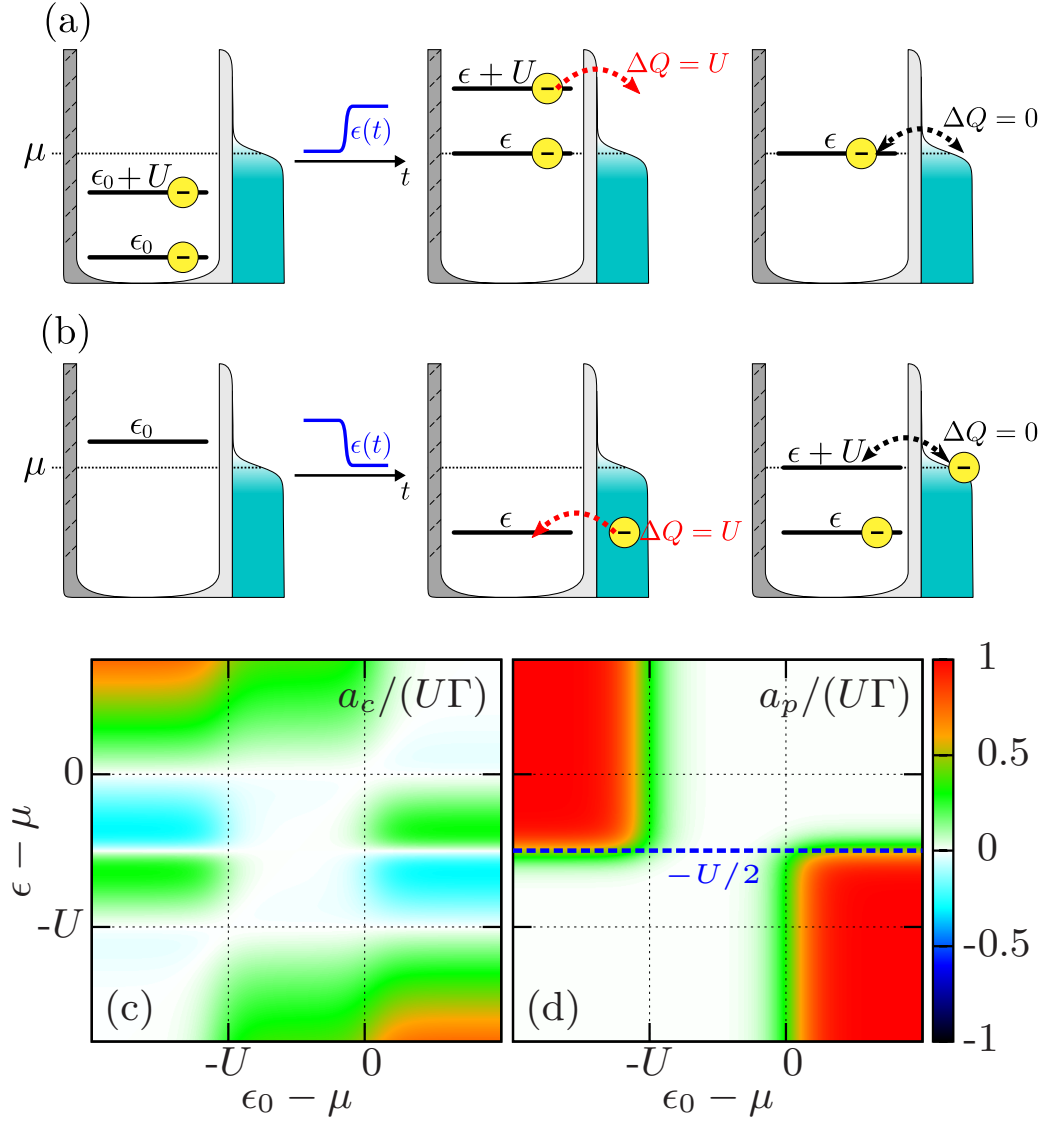


**Figure 4.3:** (a,b) Illustration of the time-dependent heat dissipation from the quantum dot after a shift of the initial level position  $\epsilon_0$  from the regime of stable double occupation,  $\epsilon_0 - \mu < -U$ , to the Coulomb resonance  $\epsilon - \mu = 0$  (a), and from an empty dot,  $\epsilon_0 - \mu > 0$ , to the resonance  $\epsilon - \mu = -U$  (b). In each case, only the first tunneling event leads to heat dissipation, since the following charge fluctuations occur at resonance with the chemical potential  $\mu$  of the reservoir. (c,d) Amplitudes  $a_c$  and  $a_p$  entering the time-dependent heat current  $I_Q(t)$  [Eq. (4.10)] as a function of the initial and final level,  $\epsilon_0$  and  $\epsilon$ . The blue dashed line at  $\epsilon - \mu = -U/2$  marks the characteristic energy of the attractive dual model, see Sec. 4.3. We set  $T/U = 0.1$  and assume  $\Gamma/T \ll 1$ .

2. The time dependence of the two-particle interaction term is described by the fermion-parity mode, exponentially decaying at the rate  $\Gamma = \Gamma_\uparrow + \Gamma_\downarrow$ . In Sec. 3.3, we have shown that, as a consequence of the duality relation (3.11) and the fundamental requirement of probability conservation, this

rate is protected against changes of any parameter except for the couplings  $\Gamma$  themselves. This explains the, a priori, surprising observation that the rate  $\Gamma$  is independent of the interaction strength  $U$ , even though entering the heat current  $I_Q(t)$  only because of the interaction.

3. To excite the parity mode and observe it in the heat current, the switch needs to start either in the zero occupation  $[(\epsilon_0 - \mu)/T \gg 1]$  or in the double occupation  $[-(\epsilon - \mu + U)/T \gg 1]$  regime. This is directly related to the fact that the inverted stationary state  $|z_i\rangle$  is always a mixture between the zero and double occupation, as illustrated in Sec. 4.3. Namely, the parity amplitude  $a_p \approx U\Gamma(z_i|\rho_0)$  [Eq. (3.21)] can only assume a sizable value if  $|\rho_0\rangle$  is either the empty or doubly occupied state.
4. Both excitation amplitudes,  $a_c$  and  $a_p$ , exhibit a sharp transition when sweeping the *final* level  $\epsilon$  through  $\epsilon - \mu = -U/2$ , as marked by the blue dashed line in Fig. 4.3(d). The origin of this jump is the dependence of both amplitudes on the stationary occupation number of the *attractive dual model*,  $N_i = (N|z_i\rangle)$ , which abruptly changes between 0 and 2 at the characteristic energy  $\epsilon - \mu = -U/2$ , see Fig. 4.2(d).
5. Finally, we notice that for switches  $\epsilon_0 \rightarrow \epsilon$  within the Coulomb window  $-U < \epsilon - \mu + \frac{U}{2} < U$ , the parity mode yields the *dominant* contribution to the heat current whenever it is excited: as indicated by Fig. 4.3(c,d), the parity amplitude  $a_p$  then assumes its constant maximal value  $U\Gamma$  [Eq. (3.20)], whereas the tight-coupling contribution  $\propto I_N(t)$  enters at an amplitude  $|a_c| \lesssim U\Gamma/2$ . This difference is particularly pronounced at the Coulomb resonances  $\epsilon - \mu = 0, -U$ , where the tight-coupling contribution vanishes almost completely. The reason for this is, as illustrated by Fig. 4.3(a,b), that the heat transfer at these level positions is entirely due to the *first* tunneling event, and that it is, according to Sec. 3.4.3, precisely this first event which happens on the typical time scale given by the parity rate.

We furthermore argue in paper II, based on the above stated results, that by measuring the time resolved heat current  $I_Q(t)$  into the environment, one should be able to experimentally expose both the constant fermion-parity rate  $\Gamma$  as well as the signatures of the dual attractive model in the excitation amplitudes. This then even allows to fully characterize the time evolution of *all* probabilities in the quantum dot density operator  $|\rho(t)\rangle$  [Eq. (4.9)]. However, it is already interesting to only measure the constancy of the parity rate, and to achieve this, one can also exploit the core result of paper I, stating that the parity rate is in fact also visible in the *particle current* through a properly tuned, capacitively coupled sensor quantum dot. Hence, the now following chapter 5 gives an overview over paper I, focusing in particular on the procedure used to extract the parity rate.



# 5 Detecting the fermion-parity rate

The main motivation behind paper I comes from an earlier publication from Contreras-Pulido et al. [61]. This publication has noted the parity rate as an additional rate next to the charge relaxation rate in the exponential decay of the previously discussed single-level quantum dot. Importantly, the paper has also predicted that, despite the fact that this rate is not visible in the transient charge current out of the dot, it should be possible to measure this rate with a nearby charge detector. In paper I, we discuss a concrete model of such a detector – a sensor quantum dot (SQD) that is capacitively coupled to the quantum dot (QD) to be measured [21] – and devise a protocol that extracts the parity rate by applying the same type of sudden level switch to the QD that is considered in the previous chapter 4. We show in particular that this protocol is not susceptible to any *backaction effects* on the dynamics of the QD that can emerge due to the capacitive coupling to the SQD.

This chapter reviews the basic working principle behind the SQD detector and the detection scheme that is theoretically suitable to measure the parity rate. Since paper I already provides a detailed theoretical formulation of this working principle within the master equation framework, we refer to this paper for any further reading on the more technical or formal aspects of this work. Here, we instead focus on the important physical explanations and interpretations. We start by describing the detector setup.

## 5.1 Sensor quantum dot detector

The dot-detector setup we consider in this chapter is displayed in Fig. 5.1. The top part of the figure shows the single-level spin-degenerate quantum dot (QD) that has been discussed in detail in Sec. 4.1. We here denote its externally tunable level position as  $\epsilon_d$ , and the on-site Coulomb interaction strength as  $U_d$ ; the wide-band limit tunnel coupling is labeled  $\Gamma_C$ , and the electrochemical potential of the coupled reservoir defines the energy reference  $\mu = 0$ . The decay dynamics of this dot due to a sudden shift of the level-position  $\epsilon_d$ , induced by a switch of the gate-potential  $V_{g,d}$ , shall be observed by a *sensor quantum dot* (SQD). As shown in the lower part of Fig. 5.1, this sensor dot is in principle another single-level quantum dot with a level position  $\epsilon_{\text{SQD}}$ , tunable by the gate voltage  $V_{g,s}$ , that is capacitively coupled to the QD with coupling strength  $U$ . However, the SQD

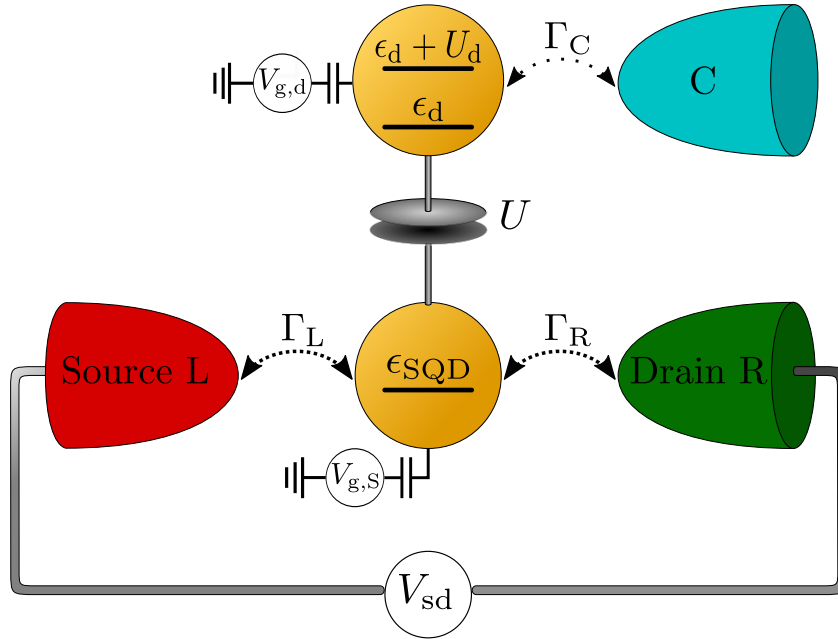


**Figure 5.1:** Model of a single-level quantum dot (QD) capacitively coupled to an effectively spinless sensor quantum dot (SQD). We denote the level-position of the dot by  $\epsilon_d$ , and of the SQD by  $\epsilon_{\text{SQD}}$ . Both levels are time-dependently tunable via the applied gate potentials  $V_{g,d}$  (QD) and  $V_{g,S}$  (SQD). The Coulomb interaction strength on the quantum dot is given by  $U_d$ , the capacitive interaction between QD and SQD is quantified by a coupling energy  $U$  which is smaller than the local dot interaction,  $U < U_d$ , but still strong compared to the common temperature  $T$  of the environment,  $U \gg T$ . The dot is tunnel coupled to a single reservoir with chemical potential  $\mu \equiv 0$ , and the SQD to two leads L and R whose chemical potentials  $\mu_L$  and  $\mu_R$  are biased by the source-drain voltage  $V_{\text{sd}}$ . We assume  $\Gamma_C \ll \Gamma_{L,R}$  for the generally weak and spin-independent tunnel couplings,  $\Gamma_{L,R,C} \ll T$ .

differs from the QD in two crucial aspects which distinguish it as a measurement device.

First of all, the SQD is tunnel coupled to *two biased* leads L and R at chemical potentials  $\mu_L \neq \mu_R$ , where  $eV_{\text{sd}} = \mu_L - \mu_R$  is the applied bias voltage. This reflects that in an actual experiment, electronic external readout of the SQD necessarily requires it to be integrated into an electrical circuit that is either current biased or, as in our case, voltage biased [7, 126]. Second, the coupling constants  $\Gamma_L$  and  $\Gamma_R$  of the detector must be much larger<sup>1</sup> than the coupling between the QD and its reservoir,  $\Gamma_{L/R} \gg \Gamma_C$ . This is crucial for a *time-resolved* readout of the transient dot behavior. Namely, the latter is only possible if the SQD reacts quickly enough to changes of the QD state, requiring the tunneling between the SQD and its coupled leads to be much faster than the tunneling between the dot and its reservoir.

<sup>1</sup>We are, however, still in the weak coupling regime, implying:  $T \gg \Gamma_{L,R} \gg \Gamma_C$ .

Finally, note that we consider an SQD with a very large on-site interaction that can only be either zero or singly occupied. For simplicity, we describe the SQD as a single *spinless* level, and explicitly justify this simplification in paper I. Namely, the paper shows no significant difference between the results for a truly spinless SQD, and the results for the experimentally more realistic situation of a spin-degenerate sensor dot that prohibits double occupation by a large on-site interaction.

## 5.2 Time-resolved readout of the quantum dot dynamics

Let us now consider a concrete example that shows how to use the sensor quantum dot as a detector for the *dynamics* of the quantum dot. The basic principle is shown in Fig. 5.2. In the given example, we assume that the dot is initially doubly occupied and then level-shifted into the regime of stable zero occupation,  $\epsilon_d - \mu \gg T$ . The electrochemical potential of the SQD is tuned into the bias window between  $\mu_L$  and  $\mu_R$ , such that initially, a finite particle current  $I_{\text{SQD}}$  flows from the left to the right lead via the SQD [Fig. 5.2(a)]. The important point is now that the SQD potential  $\epsilon_{\text{SQD}} + 2U$  is initially given by the *sum* of the orbital energy  $\epsilon_{\text{SQD}}$  and the charging energy  $2U$  due to the capacitive coupling to the *two* electrons occupying the QD. After the first QD electron has tunneled out, that is, after a typical time  $1/\Gamma_C$ , the SQD potential has decreased to  $\epsilon_{\text{SQD}} + U$  and does not lie in the bias window anymore. It therefore does not any longer allow for a current, regardless of whether and when the second electron tunnels out of the QD [Fig. 5.2(b,c)]. In other words, the SQD can be tuned such that the time dependence of its particle current  $I_{\text{SQD}}(t)$  [Fig. 5.2(d)] reflects the time-dependent probability for the dot to be in a particular state – here given by the doubly occupied initial state. An average over many such measurements with different SQD configurations then allows to characterize all time-dependent QD probabilities for a given level switch  $\epsilon_{d,0} \rightarrow \epsilon_d$ .

To experimentally determine the current  $I_{\text{SQD}}(t)$ , one can measure the current through the lead either on the left (L) or right (R) side of the SQD:  $I_{L,R}(t)$ . Importantly, due to the fact that the average occupation of the SQD changes in the measuring procedure, the sum of these *transient* currents into the left and right lead – the displacement current – does not vanish:  $I_L(t) + I_R(t) = -\partial_t N_{\text{SQD}}(t) = -\partial_t (N_{\text{SQD}}|\rho(t)) \neq 0$ , where  $N_{\text{SQD}}$  is the occupation number operator for the SQD, and  $|\rho(t)\rangle$  is the time-dependent state of the QD-SQD system. To eliminate the influence of this displacement current from the measured data,  $I_{L/R}(t)$ , one inverts the bias voltage,  $\mu_L \leftrightarrow \mu_R$ , and performs a second measurement, yielding  $\bar{I}_{L/R}(t)$ . As argued in paper I, the difference between the two time traces,  $I_{\text{SQD}}(t) = I_{L/R}(t) - \bar{I}_{L/R}(t)$ , then yields only the part of the current through the detector

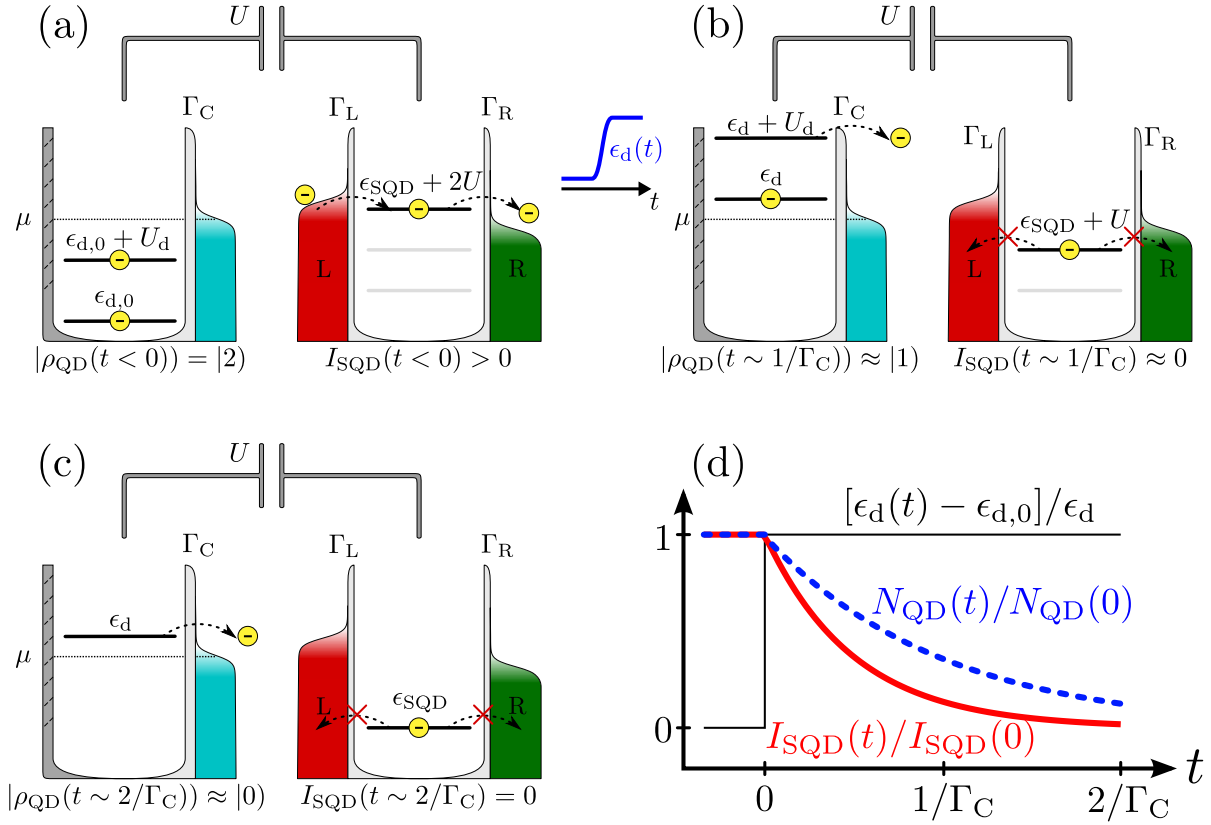


**Figure 5.2:** Time resolved readout of the quantum dot (QD) state  $|\rho_{\text{QD}}(t)\rangle = \text{Tr}_{\text{SQD}} |\rho(t)\rangle$  using the time-dependent current through the sensor quantum dot,  $I_{\text{SQD}}(t)$ . (a) The dot is initially ( $t < 0$ ) in the doubly occupied state, and the SQD level  $\epsilon_{\text{SQD}}$  is tuned such that the SQD potential  $\epsilon_{\text{SQD}} + 2U$  is initially in the bias window between the electrochemical potentials of the left and right lead connecting to the SQD, thus supporting a particle current. (b,c) The voltage-switch induced dot potential shift  $\epsilon_{d,0} \rightarrow \epsilon_d$  at time  $t = 0$  drives the dot into the regime of stable zero occupation, causing two electrons to sequentially tunnel out of the QD (weak coupling,  $\Gamma_C/T \ll 1$ ). (d) Comparison of the average dot occupation  $N_{\text{QD}}(t)$  and the sensor particle current  $I_{\text{SQD}}(t)$  as a function of time after the dot level shift at  $t = 0$ . The current has mostly vanished already after the first tunneling event, when the time-dependent average dot charge  $N_{\text{QD}}(t) \lesssim 1$  and the SQD potential  $\epsilon_{\text{SQD}} + U$  has fallen below the bias window, see (b).

dot that is exclusively due to the bias. This current decays mainly on the typical time scale of the dot,  $1/\Gamma_C$ , determining how long the SQD potential remains within the bias window after the switch, see Fig. 5.2(b).

In paper I, we detail protocols on how to use  $I_{\text{SQD}}(t)$  to extract the dot charge relaxation rate  $\gamma_c$ , and, in particular, the so far not experimentally detected dot parity rate  $\Gamma_C$ . However, based on the insights from all previous chapters and paper II, it is clear that we need to apply a switch that drives the dot between zero and double occupation, and then tune the SQD level to support only a

current until the first of possibly two tunneling processes has happened. This is *exactly* the process that Fig. 5.2 illustrates, and which according to paper I indeed yields  $I_{\text{SQD}}(t) \sim e^{-\Gamma_C t}$ , thereby allowing to extract the parity rate. The paper also explicitly verifies that by eliminating the displacement current as described above, the remaining contributions from the internal SQD dynamics in the data  $I_{\text{SQD}}(t)$  are at least two orders of magnitude smaller than the terms due to the QD relaxation. Moreover, by setting  $1/\Gamma_{L,R} \ll 1/\Gamma_C$ , we make sure that these terms decay on a much smaller timescale, and can thus be neglected in practice.

Yet, there is one fundamental aspect of this measurement scheme that in principle poses a problem and that we have not addressed so far. Namely, we have only argued that the capacitive effect of the QD on the SQD allows the latter to detect the dynamics of the former, but we have not shown how strongly the capacitive effect of the *SQD onto the QD* affects the quantum dot dynamics. In particular, the general theory behind the parity rate shown in Sec. 3.3 holds exactly only for the *combined* QD-SQD system but not for any subsystem. We can thus only be sure to measure the parity rate  $\Gamma_C = \Gamma_{C,\uparrow} + \Gamma_{C,\downarrow}$  of the quantum dot<sup>1</sup> once we have verified that the rate is sufficiently well protected against capacitive backaction. Let us therefore finish by briefly pointing out the effects of this detector backaction on the relaxation rates – in particular on the dot parity rate.

### 5.3 Capacitive detector backaction

In general, the relaxation rates which govern the reduced density operator  $|\rho(t)\rangle$  are a combination of rates describing the decay of the quantum dot and of the sensor dot respectively. More precisely, for vanishing capacitive coupling,  $|\rho(t)\rangle$  factorizes into a QD and SQD part, and the combined decay rates are simply given by a sum of rates for the subsystems. For the spinless detector dot, there exists only the zero eigenvalue and the charge<sup>2</sup> relaxation rate  $\Gamma_{\text{SQD}}$ ; for the dot, we find, according to Sec. 4.2, the zero eigenvalue, the charge relaxation rate  $\gamma_c$  and the parity rate  $\Gamma_C = \Gamma_{C,\uparrow} + \Gamma_{C,\downarrow}$ . This leads to  $2 \times 3 = 6$  combined rates<sup>3</sup>:

$$0, \gamma_c, \Gamma_C, \Gamma_{\text{SQD}}, \Gamma_{\text{SQD}} + \gamma_c, \Gamma_{\text{SQD}} + \Gamma_C. \quad (5.1)$$

When accounting for the capacitive coupling between QD and SQD, the general theory presented in Sec. 3.3 only guarantees that the zero eigenvalue and the *combined parity rate*  $\Gamma_{\text{SQD}} + \Gamma_C$  stay unaffected; the remaining rates can be influenced by the capacitive coupling, see Eq. (26)-(28) from the paper. More precisely, paper I elucidates that the QD-SQD interaction manifests itself in the rates in the following different ways:

<sup>1</sup>Note that in paper I, we define the dot parity rate to be  $2\Gamma_C$ , where  $\Gamma_C = \Gamma_{C,\uparrow} = \Gamma_{C,\downarrow}$ .

<sup>2</sup>For only one single-particle state, the charge relaxation rate *is* in fact the parity rate.

<sup>3</sup>In paper I, we in fact also consider the spin rate for the dot, leading to 8 rates for the combined system.

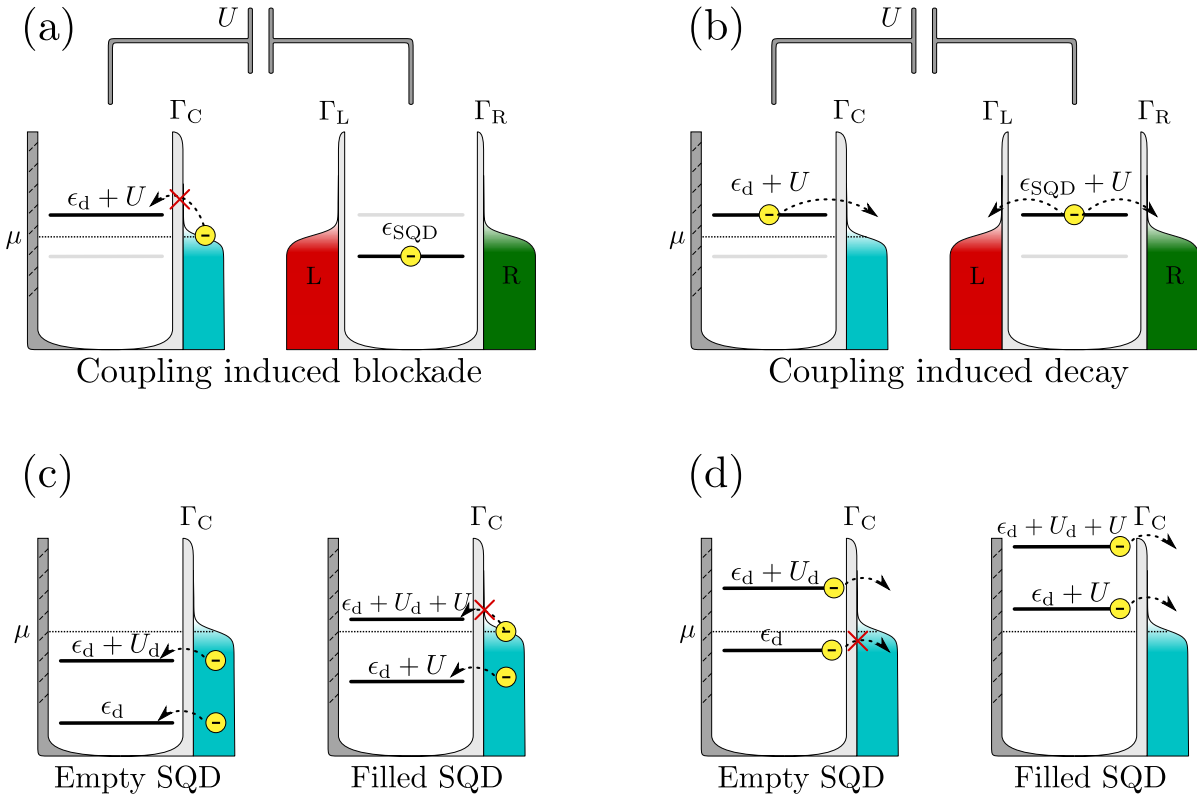


**Figure 5.3:** Illustrations of the possible effects of the capacitive coupling between the quantum dot (QD) and sensor quantum dot (SQD) on the decay rates of the system. (a) The capacitive coupling of the dot to an already occupied SQD prevents electrons from tunneling into the QD. As the grayed out dot level  $\epsilon_d$  is below the Fermi edge of the reservoir, such tunneling events would be possible without the coupling. (b) Both the QD and the SQD are initially occupied, but due to the coupling, simultaneous occupation of both the QD and SQD is not stable, forcing an electron to tunnel out of one of the two dots. Note that in (a) and (b), we neglect, for simplicity, the bias which is applied to the SQD. (c,d) Effect of the SQD on the tunneling events for dot-level switches between the regimes which support either stable double occupation without capacitive coupling to the SQD (c), or stable zero occupation with capacitive coupling (d). Since  $U < U_d$ , at least one electron tunnels to or from the QD regardless of whether the SQD is occupied or not, and this tunneling event happens on a typical time scale given by the dot parity rate, thereby explaining the robustness of the latter.

1. **Capacitive shift:** In case the SQD is occupied regardless of how many electrons are in the dot, the only difference in the description of the QD dynamics is that the potential of the dot is effectively shifted by the charging energy:  $\epsilon_d \rightarrow \epsilon_d + U$ . This implies in particular  $\gamma_c(\epsilon_d) \rightarrow \gamma_c(\epsilon_d + U)$  for the charge rate of the dot.
2. **Coupling induced blockade:** Fig. 5.3(a) illustrates a situation in which a tunneling process into/out of the QD or SQD would be possible without interaction between the systems, but is blocked due to the shift of the ef-

fective potentials by the capacitive coupling  $U$ . In this case, the relaxation rate which is related to the corresponding decay process that is blocked is reduced, depending on the respective level-positions and the ratio of the temperature and the coupling strength,  $T/U$ . Since this effect is completely analogous to the effect of Coulomb blockade due to the on-site interaction in the quantum dot, we also refer to this rate reduction as *externally induced* Coulomb blockade.

3. **Coupling induced decay:** The complementary effect to the externally induced blockade is that a certain occupation of the dot and the SQD would be stable without the interaction, but becomes unstable in the presence of the capacitive coupling [Fig. 5.3(b)]. This leads to an *enhancement* of the corresponding decay rate.

Paper I furthermore shows that the capacitive interaction leads to a coupling of decay modes for the individual systems. For example, there exists one *exact* eigenmode of the combined QD-SQD system which in most cases takes the role of the quantum dot charge relaxation mode with rate  $\gamma_c$ , but for some level switches also couples to the dot parity mode.

By contrast, we find the QD parity mode and its rate  $\Gamma_C$  to remain relatively uninfluenced by the above mentioned effects as long as  $(U_d - U)/T \gg 1$ , that is, as long as the on-site interaction strength in the QD is larger than the capacitive coupling. The reason for this can be understood using the insights from Sec. 3.4.3. It follows from this section that whenever the decay process of the QD involves on average more than one tunneling process to or from the QD, the parity mode and its rate  $\Gamma_C$  is excited and reflects the time-dependence of the dot state due to the *first of possibly two* tunneling events. Hence, the parity rate can only be affected by the capacitive coupling if this first tunneling event is blocked as a consequence of the coupling. Carefully contemplating Fig. 5.3(c,d), one realizes that this is only possible for level-positions  $-U_d < \epsilon_d - \mu < -U$ , under the physically hard to realize<sup>1</sup> condition  $U > U_d$ . This explains the robustness of  $\Gamma_C$ .

In conclusion, the paper I therefore shows that it is theoretically possible to operate a sensor quantum dot as described in Sec. 5.2 in order to perform time-resolved measurements of the dot dynamics which *expose the dot parity rate*  $\Gamma_C$ .

---

<sup>1</sup>Due to the  $1/r$  dependence of the Coulomb interaction and the geometry of the setup,  $U > U_d$  is very unlikely.



# 6 Conclusion

## 6.1 Summary

Based on the appended papers I and II, this thesis has studied the time-dependent charge and energy relaxation for a driven single-level quantum dot with strong local Coulomb interaction and a weak tunnel coupling to an electronic bath. Paper I has investigated the detection of the typical decay time scales in the transient dynamics of the quantum dot; paper II has identified and discussed a general duality relation dictating the dynamics of a large class of fermionic open systems with a tunnel-coupled fermionic environment. This duality and its implications for the quantum dot dynamics has been the central topic of this thesis.

We have started with an introduction to the scientific context and relevance of the appended papers in chapter 1, followed by a review of the necessary theoretical background knowledge of time-dependent decay in open fermionic quantum systems in chapter 2. Chapter 3 has discussed general implications of the central mode-amplitude duality relation Eq. (3.11) identified in paper II. We have shown that this duality generally dictates the existence of the fermion-parity decay mode [Eq. (3.13)], with a decay rate which only depends on the properties of the tunnel coupling between the open system and the environment. Furthermore, we have demonstrated that the duality links the entire decay behavior of the open system to the physical properties of a *dual model* with inverted energy signs, implying in particular inverted signs for the *interactions*.

In chapter 4, we have summarized the results of paper II which relate to the time-dependent heat current out of the quantum dot. These results show how the duality relation and the parity mode influence the level-switch induced, transient heat current emitted from a single-level spin-degenerate quantum dot with strong local interaction and a weakly coupled bath. Most importantly, we have found that the parity mode is the *dominant* decay mode for the dissipation of the Coulomb interaction energy. Moreover, the level-position dependence of the excitation amplitudes of each decay mode present in the time-dependent heat current has been shown to reflect the physics of electron-electron attraction emerging in the effective *dual model* for the quantum dot.

Finally, chapter 5 has reviewed paper I, which theoretically studies the working principle of a sensor quantum dot as a detector for the transient decay behavior of the single-level quantum dot discussed in paper II. We have addressed the effect of capacitive backaction on the quantum dot due to the coupling to the sensor

quantum dot, which generally leads to both a suppression or an enhancement of the dot rates compared to the situation in the absence of the detector. Most importantly however, we have demonstrated that the dot parity rate  $\Gamma_C$  can be extracted from time resolved measurements of the current through a properly tuned sensor dot. Furthermore, we have shown that the parity rate remains mostly unaffected by capacitive backaction effects.

## 6.2 Open questions

Many open questions of this work are raised by the generality of the duality relation Eq. (3.11). Most importantly, we need to investigate if and how far the relation can be extended to bosonic systems or systems with couplings between fermions and bosons (electron-phonon coupling). Moreover, an extension of the duality beyond the wide-band limit is desirable, since many devices of potential interest here rely on energy-dependent couplings [50, 85–89, 127].

While we have shown a proof of the general duality relation Eq. (3.11), we have not yet fully established which fundamental physics and symmetries are behind this relation, and which are responsible for it to hold for almost arbitrary fermionic open systems, and even for strong couplings leading to highly non-trivial non-Markovian physics. The inverted sign of the energies in the dual model (3.8) clearly suggests a relation to time reversal. This in return leads to the question whether the duality can be formulated as a fluctuation relation that, similarly to the quantum Crooks and Jarzynski relations [128–132], allows to make fundamental statements about thermodynamic quantities. It would, e.g., be of interest if and how the parity rate  $\Gamma$  is generally related to heat or entropy.

Since the duality has so far only been used either in its exact form (3.11) or in the Born-Markov limit, see Eq. (3.12), it is also interesting to investigate how the second and higher orders in the coupling, and also real time renormalization group schemes beyond the standard perturbative treatment, are restricted by the duality. In particular, one needs to check how the parity rate and the inverted stationary state enter.

Finally, what requires further attention is the problem of measuring the parity rate and, more generally, possible signatures of the dual model. One possibility is to re-examine the sensor quantum dot system studied in paper I with the duality taken into account from the start. In paper II, we also propose a way to experimentally study the parity mode with the time-dependent heat current, but so far, the development of time-resolved measurements of single energy quanta is still in its infancy, and has not yet reached the precision necessary to study the energy scales to which our theory applies, that is, interaction energies on the order of a few meV. One can alternatively check whether signatures of the dual model are already visible in *stationary* quantities or in time averages of observables in periodically driven systems, as such quantities are experimentally more accessible.

# Appendices



# Appendix A

## Coupling kernel in the Born-Markov approximation

In Sec. 2.6.1, we introduce the coupling kernel  $W_1$  as the Fourier-Laplace transform of the time evolution kernel  $\mathcal{W}(t-t')$  [Eq. (2.19)], expanded up to the lowest order in the coupling Liouvillian  $L^\bullet = [H^\bullet, \bullet]$  [Eq. (2.4)] and evaluated at zero imaginary frequency,  $\omega = i0$ . Here, we derive an explicit expression for this kernel. We focus on systems in the *single channel limit*, implying that each *spin resolved* reservoir only couples to one single-particle state in the open system<sup>1</sup>. Furthermore, we only consider Hubbard type interaction terms, meaning that the particle number states are the many-body energy eigenstates of the open system Hamiltonian. The environment shall be described by an effectively non-interacting Fermi gas or liquid. We do not consider Bogoliubov quasi-particles used to describe, e.g., superconductors or superfluids. Importantly, all the mentioned restrictions are fulfilled by the two quantum dot models studied in paper I and II.

Note that in this appendix, we assume that the reader is familiar with the diagrammatic perturbation theory based on the causal superfermion approach, developed in [62, 76] and also briefly introduced in the supplementary material to paper II.

### A.1 Superfermions and tunneling Liouvillian

We first write the tunneling Hamiltonian Eq. (2.4) for fermionic (quasi-)particles in a more compact notation:

$$H^\bullet = \sum_{j,i} T_{j;i} d_j c_i. \quad (\text{A.1})$$

Creation and annihilation operators of orthonormal single particle states in the open system are labeled as  $d$ ; for the environment, we use  $c$ . The multi-indices

$$j = \eta_j l_j \sigma_j, \quad i = \eta_i r_i \mathbf{k}_i \nu_i \sigma_i. \quad (\text{A.2})$$

---

<sup>1</sup>This is, for example, not the case for an open system with two spinless quantum dots that also tunnel couple to each other to a double dot system [Fig. 1.1(b)], therefore exhibiting two states – the bonding- and anti-bonding state – to which each reservoir can couple.

attached to the open system operators  $d$  and to the reservoir operators  $c$  here mean the following: the particle-hole indices  $\eta_j, \eta_i \in \{+1, -1\}$  define whether the operator is a creation ( $\eta = +1$ ) or annihilation operator ( $\eta = -1$ ). The orbital indices  $\mathbf{k}_i \nu_i$ , including the Bloch vector  $\mathbf{k}_i$  and any further quantum numbers  $\nu_i$ , as well as the spin projection  $\sigma_i \in \{\uparrow, \downarrow\}$  onto a fixed quantization axis (preferably parallel to a homogeneous magnetic field  $\vec{B}$ ) comprise all quantum numbers describing the single particle orbitals with energy  $\epsilon_i = \epsilon_{r_i \mathbf{k}_i \nu_i \sigma_i}$  in the reservoirs  $r_i$ . Analogously,  $l_j \sigma_j$  represent the states in the reduced system with spin  $\sigma_j$  and any other quantum number  $l_j$  necessary to describe the orbitals. A barred multi-index  $\bar{i} = \bar{\eta}_i \dots$  is equal to the unbarred multi-index  $i$  apart from a negated charge index  $\bar{\eta} = -\eta$ . Finally, the tunneling amplitude  $T_{j;\bar{i}}$  is given by

$$T_{j;\bar{i}} = (\text{Re}\tau_{j;\bar{i}} - \eta_j \cdot i \cdot \text{Im}\tau_{j;\bar{i}}) \cdot \delta_{\eta_j \bar{\eta}_i} \delta_{\sigma_j \sigma_i} \delta_{l_j l_{r_i}} \quad (\text{A.3})$$

with Kronecker deltas  $\delta_{\dots}$ , and with the tunneling matrix element  $\tau_{j;\bar{i}}$  between single-particle state  $l_j \sigma_j$  in the open system, and the state  $r_i \mathbf{k}_i \nu_i \sigma_i$  in the environment. Notably, the tunneling conserves the spin, as expressed by  $\delta_{\sigma_j \sigma_i}$ , and furthermore connects each reservoir  $r_i$  only to a single orbital in the open system. We denote this particular orbital as  $l_{r_i}$ , where the index here simply signifies that this is the only single-particle state to which the reservoir  $r_i$  couples.

With this more compact notation, we now continue by writing the tunneling *Liouvillian*  $L^{\mathbf{T}\bullet} = [H^{\mathbf{T}}, \bullet]$  in terms of fermionic superoperators [62, 76]. Let us first state their definition:

$$\begin{aligned} G_j^{q_j \bullet} &= \frac{1}{\sqrt{2}} [d_j \bullet + q(-\mathbf{1})^N \bullet (-\mathbf{1})^N d_j] \\ J_i^{q_i \bullet} &= \frac{1}{\sqrt{2}} [c_i \bullet + q(-\mathbf{1})^{N^{\text{R}}} \bullet (-\mathbf{1})^{N^{\text{R}}} c_i], \end{aligned} \quad (\text{A.4})$$

with the Keldysh<sup>1</sup> index  $q = \pm 1$ . Next, let us express the left and right action of field operators for the open system and for the reservoirs in terms of these superoperators:

$$\begin{aligned} d_j \bullet &= \frac{1}{\sqrt{2}} \sum_{q_j=\pm 1} G_j^{q_j \bullet} \bullet, & c_i \bullet &= \frac{1}{\sqrt{2}} \sum_{q_i=\pm 1} J_i^{q_i \bullet} \bullet \\ \bullet d_j &= \frac{1}{\sqrt{2}} \sum_{q_j=\pm 1} q_j G_j^{q_j} (-\mathbf{1})^{L_N} \bullet, & \bullet c_i &= \frac{1}{\sqrt{2}} \sum_{q_i=\pm 1} q_i J_i^{q_i} (-\mathbf{1})^{L_{N^{\text{R}}}} \bullet. \end{aligned} \quad (\text{A.5})$$

with  $L_N \bullet = [N, \bullet]$  being the commutator with the total open system number operator  $N = \sum_j \delta_{\eta_j} d_j d_j$ , with the fermion-parity *superoperator*  $(-\mathbf{1})^{L_N} \bullet = (-\mathbf{1})^N \bullet (-\mathbf{1})^N$ , and with the analogous superoperators  $L_{N^{\text{R}}}$  and  $(-\mathbf{1})^{L_{N^{\text{R}}}}$  for the reservoir number operator  $N^{\text{R}} = \sum_i \delta_{\eta_i} c_i c_i$ .

<sup>1</sup>The name Keldysh index stems from the analogy to Keldysh rotated Greens functions.

Using Eq. (A.5), we can rewrite the tunneling Liouvillian  $L^{\mathbf{T}\bullet} = [H^{\mathbf{T}}, \bullet]$ :

$$\begin{aligned}
L^{\mathbf{T}\bullet} &= \sum_{j,i} T_{j;i} [d_j c_i \bullet - \bullet d_j c_i] \\
&= \sum_{\substack{q_j, q_i \\ j, i}} \frac{T_{j;i}}{2} [G_j^{q_j} J_i^{q_i} + q_i J_i^{q_i} (-\mathbf{1})^{L_{N^{\text{R}}}} q_j G_j^{q_j} (-\mathbf{1})^{L_N}] \bullet \\
&= \sum_{\substack{q_j, q_i \\ j, i}} \frac{T_{j;i}}{2} [G_j^{q_j} J_i^{q_i} + q_i q_j J_i^{q_i} G_j^{q_j} (-\mathbf{1})^{L_{N^{\text{tot}}}}] \bullet \\
&= \sum_{\substack{q_j, q_i \\ j, i}} T_{j;i}^{q_j; q_i} G_j^{q_j} J_i^{q_i} \bullet,
\end{aligned} \tag{A.6}$$

where we have defined the total particle number  $N^{\text{tot}} = N + N^{\text{R}}$  as well as the coefficient

$$T_{j;i}^{q_j; q_i} = T_{j;i} \cdot \delta_{q_j q_i} = (\text{Re}\tau_{j;i} - \eta_j \cdot i \cdot \text{Im}\tau_{j;i}) \cdot \delta_{\eta_j \bar{\eta}_i} \delta_{\sigma_j \sigma_i} \delta_{l_j l_{r_i}} \delta_{q_j q_i}. \tag{A.7}$$

To derive Eq. (A.6), we have used  $[G_j^{q_j}, J_i^{q_i}] = 0$ ,<sup>1</sup> and we have furthermore exploited that due to the fermion-parity superselection principle,  $(-\mathbf{1})^{L_{N^{\text{tot}}}} \bullet = \bullet$  for any relevant physical object  $\bullet$  on which the tunneling Liouvillian acts.

The form of the coupling Liouvillian given in equation (A.6) is a central ingredient in the proof of the duality relation Eq. (3.9) shown in the supplementary material to paper II. Here, it is used to calculate the Born-Markov coupling kernel  $W_1$  using the diagram rules established in [62, 76].

## A.2 Lowest order coupling kernel in the time and frequency domain

In the following calculations, we use the particle hole occupation functions  $f_r^\eta(\epsilon) = [\exp(\eta(\epsilon - \mu_r)/T_r) + 1]^{-1}$  for the reservoirs  $r$  at chemical potential  $\mu_r$  and temperature  $T_r$  ( $k_B = 1$ ). With the local Liouvillian of the open system defined as  $L\bullet = [H, \bullet]$ , we now write down the lowest order contribution to the kernel  $\mathcal{W}_1(t-t') = \mathcal{W}_1(\Delta t)$  [Eq. (2.24)] as obtained from the diagrammatic perturbation theory ( $\hbar = 1$ ) [62, 76]:

<sup>1</sup>This is based on the fact that one is free to choose  $[d_j, c_i] = 0$  for field operators of single-particle states on orthogonal subspaces of the single-particle Hilbert space.

$$\begin{aligned}
\mathcal{W}_1(\Delta t) &= - \sum_{\substack{\eta, r, \mathbf{k}, \nu \\ \sigma, q}} (\text{Re}(\tau_{l_r \sigma; r \mathbf{k} \nu \sigma}) + i\eta \text{Im}(\tau_{l_r \sigma; r \mathbf{k} \nu \sigma})) (\text{Re}(\tau_{l_r \sigma; r \mathbf{k} \nu \sigma}) - i\eta \text{Im}(\tau_{l_r \sigma; r \mathbf{k} \nu \sigma})) \\
&\quad \times e^{i\eta \epsilon_{r \mathbf{k} \nu \sigma} \Delta t} \left[ f_r^\eta(\epsilon_{r \mathbf{k} \nu \sigma}) - q f_r^{\bar{\eta}}(\epsilon_{r \mathbf{k} \nu \sigma}) \right] G_{\bar{\eta} l_r \sigma}^+ e^{-iL\Delta t} G_{\eta l_r \sigma}^q \\
&= \frac{-1}{2\pi} \sum_{\substack{\eta, \nu, r \\ \sigma, q}} \int_{-\infty}^{\infty} dE \Gamma_{r\nu\sigma}(E) \left[ f_r^\eta(E) - q f_r^{\bar{\eta}}(E) \right] G_{\bar{\eta} l_r \sigma}^+ e^{i[\eta E - L]\Delta t} G_{\eta l_r \sigma}^q. \quad (\text{A.8})
\end{aligned}$$

We have switched to a continuum limit description of the reservoirs by summing over the Bloch vector  $\mathbf{k}$  and by introducing a delta distribution, together defining the tunnel-coupling strength

$$\Gamma_{r\nu\sigma}(E) = 2\pi \sum_{\mathbf{k}} \delta(\epsilon_{r \mathbf{k} \nu \sigma} - E) \tau_{r \mathbf{k} \nu \sigma; l_r \sigma} (\tau_{r \mathbf{k} \nu \sigma; l_r \sigma})^* = (\Gamma_{r\nu\sigma}(E))^*. \quad (\text{A.9})$$

As the next intermediate step, we calculate the matrix elements of this kernel in the Liouville space basis spanned by the many-particle energy eigenstates  $|X\rangle$  for the open system Hamiltonian  $H$ , meaning  $H|X\rangle = E_X|X\rangle$ . We first introduce

$$\begin{aligned}
|X_\alpha X_\beta\rangle &= |X_\alpha\rangle \langle X_\beta| \\
|X_\alpha + \eta(l_r, \sigma) X_\beta\rangle &= |X_\alpha + \eta(l_r, \sigma)\rangle \langle X_\beta| = d_{\eta l_r \sigma} |X_\alpha\rangle \langle X_\beta| \\
|X_\alpha X_\beta + \eta(l_r, \sigma)\rangle &= |X_\alpha\rangle \langle X_\beta + \eta(l_r, \sigma)| = |X_\alpha\rangle \langle X_\beta| d_{\bar{\eta} l_r \sigma}, \quad (\text{A.10})
\end{aligned}$$

with  $|X_\alpha + \eta(l_r, \sigma)\rangle$  being the state that has one particle more ( $\eta = +1$ ) or less ( $\eta = -1$ ) compared to  $|X_\alpha\rangle$  in the single-particle state  $l_r \sigma$  ( $|X_\alpha + \eta(l_r, \sigma)\rangle$  vanishes if  $\eta = +1$  and  $l_r \sigma$  already occupied, or if  $\eta = -1$  and  $l_r \sigma$  unoccupied), and which is, by assumption (see above), an energy eigenstate as well. Next, we define

$$\begin{aligned}
\Delta E_{X_\alpha, X_\beta} &= E_{X_\alpha} - E_{X_\beta} \\
\Delta E_{X_\alpha}^{\eta(l_r, \sigma)} &= E_{X_\alpha + \eta(l_r, \sigma)} - E_{X_\alpha} \\
\Delta E_{\eta(l_r, \sigma)}^{X_\alpha} &= E_{X_\alpha} - E_{X_\alpha + \eta(l_r, \sigma)}. \quad (\text{A.11})
\end{aligned}$$

We furthermore write  $N_X^{\eta l_r \sigma}$  as the particle ( $\eta = +1$ ) or hole ( $\eta = -1$ ) number for the single-particle state  $l_r \sigma$  in the many particle state  $|X\rangle$ , and introduce<sup>1</sup> the state Kronecker delta  $\delta_{X_\alpha}^{X_\beta} = \langle X_\alpha | X_\beta \rangle$ . Using the definition for the fermionic superoperators  $G_{\eta l_r \sigma}^q$  given in Eq. (A.4), we now calculate the matrix element

<sup>1</sup>The notation  $\delta_{X_\alpha}^{X_\beta}$  instead of  $\delta_{X_\alpha, X_\beta}$  is only introduced to make the symbol shorter, and has no other meaning (such as covariant vs. contravariant, etc.) here!

$(XX|\bullet|X_\alpha X_\beta)$  of the dot superoperators appearing in Eq. (A.8):

$$\begin{aligned}
& (XX|G_{\bar{\eta}l_r\sigma}^+ e^{-iL\Delta t} G_{\eta l_r\sigma}^q |X_\alpha X_\beta) \\
&= \frac{1}{\sqrt{2}} \left[ (XX|G_{\bar{\eta}l_r\sigma}^+ e^{-iL\Delta t} |X_\alpha + \eta(l_r, \sigma)] X_\beta \right. \\
&\quad \left. + q(XX|G_{\bar{\eta}l_r\sigma}^+ e^{-iL\Delta t} |X_\alpha [X_\beta + \bar{\eta}(l_r, \sigma)]) \right] \\
&= \frac{1}{\sqrt{2}} \left[ e^{-i\Delta E_{X_\alpha + \eta(l_r, \sigma), X_\beta} \Delta t} (XX|G_{\bar{\eta}l_r\sigma}^+ |X_\alpha + \eta(l_r, \sigma)] X_\beta \right. \\
&\quad \left. + qe^{-i\Delta E_{X_\alpha, X_\beta + \bar{\eta}(l_r, \sigma)} \Delta t} (XX|G_{\bar{\eta}l_r\sigma}^+ |X_\alpha [X_\beta + \bar{\eta}(l_r, \sigma)]) \right] \\
&= \frac{1}{2} \left\{ e^{-i\Delta E_{X_\alpha + \eta(l_r, \sigma), X_\beta} \Delta t} \left[ N_{X_\alpha}^{\bar{\eta}l_r\sigma} (XX|X_\alpha X_\beta) - (XX|[X_\alpha + \eta(l_r, \sigma)] [X_\beta + \eta(l_r, \sigma)]) \right] \right. \\
&\quad \left. + qe^{-i\Delta E_{X_\alpha, X_\beta + \bar{\eta}(l_r, \sigma)} \Delta t} \left[ (XX|[X_\alpha + \bar{\eta}(l_r, \sigma)] [X_\beta + \bar{\eta}(l_r, \sigma)]) - N_{X_\beta}^{\eta l_r\sigma} (XX|X_\alpha X_\beta) \right] \right\} \\
&= \frac{\delta_{X_\beta}^{X_\alpha}}{2} \left\{ e^{-i\Delta E_{X_\alpha}^{\eta(l_r, \sigma)} \Delta t} \left[ N_{X_\alpha}^{\bar{\eta}l_r\sigma} \delta_{X_\alpha}^X - |\langle X|d_{\eta l_r\sigma}|X_\alpha\rangle|^2 \right] \right. \\
&\quad \left. - qe^{-i\Delta E_{\bar{\eta}(l_r, \sigma)}^{X_\alpha} \Delta t} \left[ N_{X_\alpha}^{\eta l_r\sigma} \delta_{X_\alpha}^X - |\langle X|d_{\bar{\eta}l_r\sigma}|X_\alpha\rangle|^2 \right] \right\} \\
&= \frac{\delta_{X_\beta}^{X_\alpha}}{2} \sum_{X_\gamma} \left\{ e^{-i\Delta E_{X_\alpha}^{\eta(l_r, \sigma)} \Delta t} \delta_{X_\alpha + \eta(l_r, \sigma)}^{X_\gamma} \left[ \delta_{X_\alpha}^X - \delta_{X_\gamma}^X \right] \right. \\
&\quad \left. - qe^{-i\Delta E_{\bar{\eta}(l_r, \sigma)}^{X_\alpha} \Delta t} \delta_{X_\alpha - \eta(l_r, \sigma)}^{X_\gamma} \left[ \delta_{X_\alpha}^X - \delta_{X_\gamma}^X \right] \right\}. \tag{A.12}
\end{aligned}$$

Using this relation, we can explicitly evaluate the matrix elements of the coupling kernel (A.8),  $(XX|\mathcal{W}_1|X_\alpha X_\beta)$ . Subsequently summing over  $q$ , we arrive at

$$\begin{aligned}
& (XX|\mathcal{W}_1(\Delta t)|X_\alpha X_\beta) \\
&= \frac{\delta_{X_\beta}^{X_\alpha}}{2\pi} \sum_{\substack{\eta, \nu, r \\ \sigma, X_\gamma}} \int_{-\infty}^{\infty} dE \Gamma_{r\nu\sigma}(E) \\
&\quad \times \left\{ f_r^\eta(E) e^{-i\Delta E_{X_\alpha}^{\eta(l_r, \sigma)} \Delta t} \delta_{X_\alpha + \eta(l_r, \sigma)}^{X_\gamma} \left[ \delta_{X_\gamma}^X - \delta_{X_\alpha}^X \right] \right. \\
&\quad \left. + f_r^{\bar{\eta}}(E) e^{-i\Delta E_{\bar{\eta}(l_r, \sigma)}^{X_\alpha} \Delta t} \delta_{X_\alpha - \eta(l_r, \sigma)}^{X_\gamma} \left[ \delta_{X_\gamma}^X - \delta_{X_\alpha}^X \right] \right\} \\
&\quad \times e^{i\eta E \Delta t} \\
&= \frac{\delta_{X_\beta}^{X_\alpha}}{\pi} \sum_{\substack{\nu, \sigma \\ r, X_\gamma}} \int_{-\infty}^{\infty} dE \Gamma_{r\nu\sigma}(E) \\
&\quad \left\{ f_r^+(E) \delta_{X_\alpha + (l_r, \sigma)}^{X_\gamma} \left( \delta_{X_\alpha + (l_r, \sigma)}^X - \delta_{X_\alpha}^X \right) \cos \left( (\Delta E_{X_\alpha}^{+(l_r, \sigma)} - E) \Delta t \right) \right. \\
&\quad \left. + f_r^-(E) \delta_{X_\alpha - (l_r, \sigma)}^{X_\gamma} \left( \delta_{X_\alpha - (l_r, \sigma)}^X - \delta_{X_\alpha}^X \right) \cos \left( (\Delta E_{X_\alpha}^{- (l_r, \sigma)} - E) \Delta t \right) \right\}. \tag{A.13}
\end{aligned}$$

Together with Eq. (A.8), the appearance of the Kronecker delta  $\delta_{X_\beta}^{X_\alpha}$  in Eq. (A.12) already proves that the, yet to be calculated, zero Laplace frequency Born-Markov coupling kernel  $W_1$  [Eq. (2.25)] for the systems of interest here does not couple the dynamics of the probabilities ( $XX|\rho(t)$ ) to the coherences ( $X_\alpha X_{\beta \neq \alpha}|\rho(t)$ ). This in particular implies that the combined kernel  $A_1 = -iL + W_1$  [Eq. (2.27)] does not couple probabilities to coherences, as claimed and used explicitly in Sec. 4.2. Since we are only interested in the probabilities, we continue by studying the matrix  $\mathbf{W}$  defined as

$$\mathbf{W}_{XX'}(t) = (XX| -iL + \mathcal{W}_1(t)|X'X') = (XX|\mathcal{W}_1(t)|X'X'). \quad (\text{A.14})$$

For this matrix, we now calculate the Fourier-Laplace transform  $\int_0^\infty dt \mathbf{W}(t) e^{i\omega t}$  for  $\text{Im}(\omega) > 0$ . First, we use that the unbounded energy integral  $\int_{-\infty}^\infty dE$  can in fact, due to the finite bandwidth, be replaced by the bounded integral  $\int_{\mu_r - D_r}^{\mu_r + D_r} dE$  for each individual reservoir  $r$ , where  $\mu_r$  is the electrochemical potential of the reservoir  $r$ , and the constant  $D_r$  is defined such that the interval  $(\mu_r - D_r, \mu_r + D_r)$  encloses the entire energy band for each reservoir. With this substitution, it is possible to first carry out the improper time integral of the Fourier-Laplace transform:

$$\begin{aligned} \mathbf{W}_{XX'}(\omega) &= \int_0^\infty dt \mathbf{W}_{XX'}(t) e^{i\omega t} \\ &\stackrel{(\text{A.13})}{=} \frac{1}{2\pi i} \sum_{\substack{\nu, \sigma \\ r, X_\gamma}} \int_{\mu_r - D_r}^{\mu_r + D_r} dE \Gamma_{r\nu\sigma}(E) \\ &\quad f_r^+(E) \left[ \delta_{X'+(l_r, \sigma)}^{X_\gamma} \left( \delta_{X'+(l_r, \sigma)}^X - \delta_X^{X'} \right) \right] \\ &\quad \times \left\{ \frac{1}{E - \left[ \Delta E_{X'}^{+(l_r, \sigma)} + \omega \right]} - \frac{1}{E - \left[ \Delta E_{X'}^{+(l_r, \sigma)} - \omega \right]} \right\} \\ &\quad + f_r^-(E) \left[ \delta_{X'-(l_r, \sigma)}^{X_\gamma} \left( \delta_{X'-(l_r, \sigma)}^X - \delta_X^{X'} \right) \right] \\ &\quad \times \left\{ \frac{1}{E - \left[ \Delta E_{X'}^{-}(l_r, \sigma) + \omega \right]} - \frac{1}{E - \left[ \Delta E_{X'}^{-}(l_r, \sigma) - \omega \right]} \right\}. \end{aligned} \quad (\text{A.15})$$

We can evaluate the bounded energy integral if we assume that on a simply connected subset  $\mathcal{U}$  in the upper half of the complex plane including the finite real interval  $(\mu_r - D_r, \mu_r + D_r)$ , the functions  $f_r^\pm(E) \Gamma_{r\nu\sigma}(E)$  are analytic functions in any point within  $\mathcal{U}$  except for a finite amount of isolated points  $\{z_i\}_i$  with  $\text{Im}(z_i) > 0$  and  $z_i \neq \epsilon + \eta\omega$  for any<sup>1</sup> real energy  $\epsilon$ . While this is true for the Fermi functions  $f^\pm$ , this assumption is in general not true for coupling  $\Gamma$ , as there

<sup>1</sup>Since we are interested in the limit  $\omega \rightarrow i0$ , we can always choose a reasonably small  $\omega$  such that  $z_i \neq \epsilon + \eta\omega$  is fulfilled.

can, e.g., be von-Hove singularities on the real axis. However, if one is interested only in energies which are close to the Fermi edge on the scale of the bandwidth, and if  $\Gamma$  is analytic in such a close environment around the Fermi edge (we do not consider a superconducting gap), our assumption is a justified approximation. This then allows us to carry out the energy integrals in Eq. (A.15) by closing the contour with a curve  $\mathcal{C}_{\mathcal{U}}$  in the above defined set  $\mathcal{U}$ , such that the area inside the closed contour contains the pole from the resolvent  $1/(E - \epsilon - \omega)$ , with  $\epsilon$  representing the respective energy differences  $\Delta E$  appearing in Eq. (A.15), and a finite amount of poles from the function  $f_r^{\pm}(E)\Gamma_{r\nu\sigma}(E)$ . The Cauchy residue theorem then gives rise to the following terms ( $\eta = \pm 1$ ):

$$\begin{aligned} \frac{1}{2\pi i} \int_{\mu_r - D_r}^{\mu_r + D_r} dE \frac{f_r^{\pm}(E)\Gamma_{r\nu\sigma}(E)}{E - \epsilon - \eta\omega} &= \delta_{\eta+} \Gamma_{r\nu\sigma}(\epsilon + \omega) f_r^{\pm}(\epsilon + \omega) \\ &+ \sum_i \text{Res} \left( \frac{f_r^{\pm}(z)\Gamma_{r\nu\sigma}(z)}{z - \epsilon - \eta\omega}, z = z_i, \text{Im}(z_i) > 0 \right) \\ &- \frac{1}{2\pi i} \int_{\mathcal{C}_{\mathcal{U}}} dz \frac{f_r^{\pm}(z)\Gamma_{r\nu\sigma}(z)}{z - \epsilon - \eta\omega}. \end{aligned} \quad (\text{A.16})$$

By assumption, the pole from the resolvent only contributes for  $\eta = +1$ , since  $\text{Im}(\omega) > 0$ , and the poles  $z_i$  from  $f_r^{\pm}(E)\Gamma_{r\nu\sigma}(E)$  are independent of, and unequal to  $\epsilon + \eta\omega$ . Substituting this result into Eq. (A.15) and taking the limit  $\omega \rightarrow i0_+$ , the secular terms in the Born-Markov time evolution kernel therefore simplify to

$$\begin{aligned} \mathbf{W}_{XX'} &= \sum_{r,\nu,\sigma} \left\{ \Gamma_{r\nu\sigma}(\Delta E_{X'}^{+(l,r,\sigma)}) f_r^+(\Delta E_{X'}^{+(l,r,\sigma)}) \sum_{X_\gamma} [\delta_{X'+(l,r,\sigma)}^{X_\gamma} (\delta_{X'+(l,r,\sigma)}^X - \delta_X^{X'})] \right. \\ &\quad \left. + \Gamma_{r\nu\sigma}(\Delta E_{X'}^{-}(l,r,\sigma)) f_r^-(\Delta E_{X'}^{-}(l,r,\sigma)) \sum_{X_\gamma} [\delta_{X'-(l,r,\sigma)}^{X_\gamma} (\delta_{X'-(l,r,\sigma)}^X - \delta_X^{X'})] \right\}. \end{aligned} \quad (\text{A.17})$$

These are the well-known Fermi's Golden rule transition rates for sequential tunneling events between the open system and its non-interacting fermionic environment [74], as claimed in Sec. 4.2 of the main thesis.

### A.3 The unique stationary state

In Sec. 4.2, we have used that the transition matrix representation  $\mathbf{W}$  of the Born-Markov kernel  $A_1$  [Eq. (2.27)] that we have found in Eq. (A.17) for the systems of interest here implies a unique stationary state of the dynamics. In this last section of App. A, we argue why this property holds.

First of all, it is immediately clear from the definition of the matrix via the Born-Markov kernel  $A_1$  that  $\text{Tr } \mathbf{W} = 0$ . This means that it has a left eigenvector to

the eigenvalue 0 which is given by the row vector  $\mathbf{e}^T = (1, 1, \dots, 1)$ . Furthermore, this guarantees the existence of a right eigenvector  $\mathbf{P}_z$  that obeys  $\mathbf{W} \cdot \mathbf{P}_z = 0$ , and that is trace-normalized,  $\mathbf{e}^T \cdot \mathbf{P}_z = 1$ .

Second, we notice that for *truly positive* temperatures  $T_r > 0$ , the off-diagonal elements are either given by 0 or by  $\Gamma_{r\nu\sigma}(E)f_r^\pm(E) > 0$  (assuming that  $\Gamma$  does not vanish on its support), and are thus non-negative:  $\mathbf{W}_{X \neq X'} \geq 0$ . Due to  $\mathbf{e}^T \cdot \mathbf{W} = 0$ , this means that the diagonal elements are *truly negative*. By the following argument, this implies that the right zero eigenvector  $\mathbf{P}_z$  is the unique stationary state for systems whose probabilities are given by the probability vector  $\mathbf{P}(t) = e^{\mathbf{W}t}\mathbf{P}_0$ , with the transition matrix  $\mathbf{W}$  determined by Eq. (A.17):

$$\mathbf{P}_z = \lim_{t \rightarrow \infty} \mathbf{P}(t) \quad , \quad \mathbf{e}^T \cdot \mathbf{P}_z = 1 \quad , \quad \mathbf{P}_{z,X} > 0, \quad (\text{A.18})$$

where we denote the vector components of  $\mathbf{P}_z$  as  $\mathbf{P}_{z,X}$ . To see this, we first define the matrix

$$\mathbf{V} = \mathbf{W} + \lambda_{\max} \mathbb{1} \quad , \quad \lambda_{\max} > \max_X (-\mathbf{W}_{XX}). \quad (\text{A.19})$$

The matrix  $\mathbf{V}$  is not only non-negative by definition, but in fact also primitive, meaning that there exists an  $m \in \mathbb{N}$  such that every matrix element of  $\mathbf{V}^m$  is truly positive. The primitiveness of the matrix  $\mathbf{V}$  can be seen as follows. The truly positive off-diagonal elements  $\mathbf{V}_{XX'} = \mathbf{W}_{XX'}$  together represent the rates for all possible transitions  $X \leftarrow X' \neq X$  between eigenstates differing by the occupation of a single fermion in the open system [Eq. (A.17)]. Since all energy eigenstates are occupation number states for the systems we consider, this means that every possible eigenstate transition can be decomposed into a sequence of such single occupation transitions with truly positive rates (e.g., a transition between zero and double occupation of a single spinful level is accomplished by a sequence of two transitions). Hence, there must be a maximum number of sequences  $m$  such any state transition  $X \leftarrow X'$  can be achieved in  $m$  or less steps. In other words, there exists an  $n_{X \leftarrow X'} \in \mathbb{N}^{\leq m}$  such that  $(\mathbf{V}^{n_{X \leftarrow X'}})_{XX'} > 0$ . The crucial point is now that the diagonal elements in  $\mathbf{V}$ , which can be interpreted as the *non probability-conserving* rates (in contrast to  $\mathbf{W}$ ) to stay in the same state during a single transition step (= one multiplication by  $\mathbf{V}$ ), are also truly positive by definition,  $\mathbf{V}_{XX} > 0$ . This means that any transition  $X \leftarrow X'$  as defined by  $\mathbf{V}$  is in fact realized with a certain positive rate by *exactly*  $m$  steps, and this implies the primitiveness for  $\mathbf{V}$  which means that  $(\mathbf{V}^m)_{XX'} > 0$  for any two states  $X, X'$ .

The important point of this property is that it allows us to apply the Perron-Frobenius theorem [133, 134] to  $\mathbf{V}$ . This theorem states that  $\mathbf{V}$  has only one left and one corresponding right eigenvector that can be normalized to have only positive components, and that the corresponding eigenvalue  $\lambda_p$  – the Perron root – is non-degenerate, truly positive and equal to the spectral radius. In other words, any other eigenvalue  $\lambda_{\mathbf{V},x}$  of  $\mathbf{V}$  obeys  $\text{Re}(\lambda_{\mathbf{V},x}) < \lambda_p$ .

In our case, we know from the definition (A.19) that  $\mathbf{e}^T = (1, 1, \dots, 1)$  is a left eigenvector of  $\mathbf{V}$  with strictly positive components and eigenvalue  $\lambda_{\max}$ . By

the Perron-Frobenius theorem,  $\lambda_{\max}$  must be the non-degenerate Perron root. The corresponding right eigenvector is hence unique up to a prefactor, and this prefactor can be chosen such that the vector only has positive components. We again already know from Eq. (A.19) and the Perron-Frobenius theorem that  $\mathbf{P}_z$  is, up to a prefactor, the only right eigenvector of  $\mathbf{V}$  to the eigenvalue  $\lambda_{\max}$ . Therefore, it can be written as

$$\mathbf{P}_z = \alpha \mathbf{P}_p \quad , \quad \alpha \in \mathbb{C}^{\neq 0}, \quad (\text{A.20})$$

where  $\mathbf{P}_p$  is a right eigenvector to the Perron root which has only positive components,  $\mathbf{P}_{p,X} > 0$ , and hence obeys  $e^T \cdot \mathbf{P}_p > 0$ . Moreover, since  $\mathbf{P}_z$  is trace-normalized,  $e^T \cdot \mathbf{P}_z = 1$ , multiplying Eq. (A.20) by  $e^T$  on both sides implies  $\alpha = 1/(e^T \cdot \mathbf{P}_p) > 0$ . The right zero eigenvector  $\mathbf{P}_z$  to the transition matrix  $\mathbf{W}$  is thus not only trace-normalized, but furthermore only has positive components,  $\mathbf{P}_{z,X} = \alpha \mathbf{P}_{p,X} > 0$ . In other words,  $\mathbf{P}_z$  is a representation of a legitimate physical state with positive<sup>1</sup> probabilities which are properly normalized to 1.

Finally, it is clear from Eq. (A.19) that the eigenvalues  $\lambda_{\mathbf{W},x}$  of  $\mathbf{W}$  are obtained from the eigenvalues  $\lambda_{\mathbf{V},x}$  of  $\mathbf{V}$  by a shift of  $-\lambda_{\max} < 0$ :

$$\lambda_{\mathbf{W},x} = \lambda_{\mathbf{V},x} - \lambda_{\max}. \quad (\text{A.21})$$

Since  $\lambda_{\max}$  is the non-degenerate eigenvalue of  $\mathbf{V}$  with the largest real part, Eq. (A.21) and  $\lambda_{\max} > 0$  dictate that the zero eigenvalue  $\lambda_{\mathbf{W},z} = \lambda_{\max} + (-\lambda_{\max}) = 0$  is the non-degenerate eigenvalue of  $\mathbf{W}$  with the largest real part, meaning  $\text{Re}(\lambda_{\mathbf{W},x}) < 0$  for any other eigenvalue  $\lambda_{\mathbf{W},x} \neq 0$ . This proves that  $\mathbf{P}_z = \lim_{t \rightarrow \infty} \mathbf{P}(t)$  is the unique, physical stationary state of the dynamics, independently of the initial state of the system.

We stress that our argument relies on the assumption that all possible transitions exclusively occur as a sequence of state transitions with truly positive rates  $\Gamma f^\pm > 0$ . This only holds for the *probabilities* of the given class of systems in the Born-Markov limit for which the transition matrix is given by Eq. (A.17), and only if the temperatures are positive,  $T_r > 0$ . If, for example, the probabilities coupled to the coherences, these couplings could be described by complex transition rates for which the Perron-Frobenius theorem cannot be applied. Similarly, if  $T_r = 0$ ,<sup>2</sup> some transition rates would be 0, breaking the primitiveness of the above defined matrix  $\mathbf{V}$ . In fact, the Born-Markov treatment of the single-level Anderson model [61] already shows a vanishing spin rate  $\gamma_\sigma = 0$  for  $T = 0$  and certain level positions  $\epsilon$ , and hence a *non-unique* stationary state.

<sup>1</sup>Interestingly, this also shows that the state represented by  $\mathbf{P}_z$  cannot be strictly pure. However, the probabilities can be peaked, allowing to *approximate* the state as pure.

<sup>2</sup>Note that  $T = 0$  is not a physical limit in the Born-Markov approximation!



# Appendix B

## Current kernels

In this appendix, we sketch the derivation of the expression Eq. (2.22) for the particle current into a specific reservoir, and furthermore show Eq. (2.29) to hold for the heat current into the reservoirs in the Born-Markov limit. We again assume the reader to be familiar with the diagrammatic techniques shown in [27, 62, 76, 116–118].

### B.1 Particle current

For the particle current, we first note the following easy to verify commutator relations

$$\begin{aligned} [N^r, H^R] &= [N^r, H] = 0 \\ [N^r, H^T] &= [N^r, H^{T,r}] = -[N, H^{T,r}], \end{aligned} \quad (\text{B.1})$$

where  $H^{T,r}$  is the part of the full tunnel Hamiltonian  $H^T$  [Eq. (2.4)] which couples only to reservoir  $r$ . Importantly, the second commutator relation reflects the fact that the tunneling conserves the particle number. This property allows us, together with  $H^{\text{tot}} = H + H^R + H^T$  and the general mathematical properties of commutators in traces, to write the particle current (2.20) as

$$\begin{aligned} I_N^r(t) &= \partial_t \text{Tr} \text{Tr}_R [N^r \rho^{\text{tot}}(t)] = -i \text{Tr} \text{Tr}_R [N^r L^{\text{tot}} \rho^{\text{tot}}(t)] \\ &= -i \text{Tr} \text{Tr}_R [[N^r, H^{\text{tot}}] \rho^{\text{tot}}(t)] = -i \text{Tr} \text{Tr}_R [[N^r, H^{T,r}] \rho^{\text{tot}}(t)] \\ &= i \text{Tr} \text{Tr}_R [[N, H^{T,r}] \rho^{\text{tot}}(t)] = -\text{Tr} [N \text{Tr}_R [-iL^{T,r} \rho^{\text{tot}}(t)]]. \end{aligned} \quad (\text{B.2})$$

Using diagrammatic perturbation theory as explained in the references cited above, this then leads to Eq. (2.22). Furthermore, it becomes clear how the kernel  $\mathcal{W}^r$  in (2.22) is defined. Namely, the full coupling kernel  $\mathcal{W}$  entering the generalized master equation (2.19) arises when evaluating

$$\partial_t \rho(t) = \text{Tr}_R [-iL^T \rho^{\text{tot}}(t)]. \quad (\text{B.3})$$

For the current, we need to evaluate almost the same expression, except that the leftmost tunneling Liouvillian in the trace is given by  $L^{T,r}$ , only describing the

tunneling to the single reservoir  $r$ . Therefore, the resulting integral kernel  $\mathcal{W}^r$  must be understood as the coupling to a single reservoir  $r$ , but renormalized by the presence of the other reservoirs if higher orders in the coupling are taken into account. In the Born-Markov approximation and in the single-channel limit, see App. A, the reservoir resolved coupling can, however, be written as a matrix which simply equals the matrix for the coupling kernel [Eq. (A.17)] except for a fixed reservoir index  $r$ :

$$\mathbf{W}_{XX'}^r = \sum_{\nu,\sigma} \left\{ \Gamma_{r\nu\sigma}(\Delta E_{X'}^{+(l_r\sigma)}) f_r^+(\Delta E_{X'}^{+(l_r\sigma)}) \sum_{X_\gamma} [\delta_{X'+(l_r,\sigma)}^{X_\gamma} (\delta_{X'+(l_r,\sigma)}^X - \delta_X^{X'})] \right. \\ \left. + \Gamma_{r\nu\sigma}(\Delta E_{X'}^{-(l_r\sigma)}) f_r^-(\Delta E_{X'}^{-(l_r\sigma)}) \sum_{X_\gamma} [\delta_{X'-(l_r,\sigma)}^{X_\gamma} (\delta_{X'-(l_r,\sigma)}^X - \delta_X^{X'})] \right\}. \quad (\text{B.4})$$

In the following section, we will use this form of the reservoir resolved kernel.

## B.2 Heat current in the Born-Markov, single-channel limit

Let us now turn to the expression for the heat current in the Born-Markov limit. We again focus on systems in the single-channel limit (each spin resolved reservoir couples spin-conservingly to only one single-particle state in the open system) and for which the particle number states are the many-body energy eigenstates of the open system Hamiltonian. We also again stress that these restrictions are fulfilled by the two quantum dot setups studied in paper I and II.

We start from the definition of the energy current into the reservoir  $r$  given in Eq. (2.21). Using

$$[H^r, H^R] = [H^r, H] = 0 \quad , \quad [H^r, H^T] = [H^r, H^{T,r}] \quad (\text{B.5})$$

we follow a procedure analogous to Eq. (B.2) to arrive at

$$I_E^r(t) = \partial_t \text{Tr} \text{Tr}_R [H^r \rho^{\text{tot}}(t)] = \text{Tr} \text{Tr}_R [-i [H^r, H^{T,r}] \rho^{\text{tot}}(t)]. \quad (\text{B.6})$$

Since the tunnel barriers themselves can store energy, the energy current is not conserved, and we cannot replace  $H^r$  by  $-H$  in the commutator on the right hand side of the above expression; instead, we have to explicitly calculate the commutator. Using the definitions and notation established in Sec. A.1, a straightforward calculation yields

$$\hat{I}_E^r(t) = -i [H^r(t), H^{T,r}] = -i \sum_{j,i} \epsilon_i \delta_{r_i r} \eta_i T_{j;i} d_j c_i. \quad (\text{B.7})$$

To evaluate Eq. (B.6), we have to express (B.7) in terms of the fermionic superoperators shown in (A.4). For this, it turns out to be more convenient to rewrite Eq. (B.7) into a symmetric form using an anti-commutator  $\{\bullet, \bullet\}$ , which is always possible since  $\text{Tr Tr}_R [O\rho] = \text{Tr Tr}_R [\frac{1}{2} \{O, \rho\}]$ . One finds

$$\frac{1}{2} \{\hat{\mathbb{I}}_E^r, \bullet\} = \frac{-i}{2} \sum_{\substack{q_j, q_i \\ j, i}} \epsilon_i \delta_{r_i r} \eta_i T_{j; i} \delta_{q_j \bar{q}_i} G_j^{q_j} J_i^{q_i} \bullet. \quad (\text{B.8})$$

Using this expression, one can now evaluate the contribution to Eq. (B.6) in the lowest order in the coupling. One finds this contribution to be the same as for the coupling kernel [Eq. (A.8)], apart from an additional factor 1/2, the fact that the reservoir index is fixed to  $r$ , that the expression in the sum is multiplied by  $\epsilon_{r\mathbf{k}\nu\sigma}$ , and that the Keldysh index of the left open system superfermion is given by  $q = -$  instead of  $q = +$ :

$$\begin{aligned} \mathcal{W}_{1,E}^r(\Delta t) &= -\frac{1}{2} \sum_{\substack{\eta, \mathbf{k}, \nu \\ \sigma, q}} (\text{Re}(\tau_{l_r\sigma; r\mathbf{k}\nu\sigma}) + i \cdot \eta \text{Im}(\tau_{l_r\sigma; r\mathbf{k}\nu\sigma})) \\ &\quad \times (\text{Re}(\tau_{l_r\sigma; r\mathbf{k}\nu\sigma}) - i \cdot \eta \text{Im}(\tau_{l_r\sigma; r\mathbf{k}\nu\sigma})) \\ &\quad \times \eta \epsilon_{r\mathbf{k}\nu\sigma} e^{i\eta \epsilon_{r\mathbf{k}\nu\sigma} \Delta t} [f_r^\eta(\epsilon_{r\mathbf{k}\nu\sigma}) - q f_r^{\bar{\eta}}(\epsilon_{r\mathbf{k}\nu\sigma})] G_{\bar{\eta}l_r\sigma}^- e^{-iL\Delta t} G_{\eta l_r\sigma}^q \\ &= \frac{-1}{4\pi} \sum_{\substack{\eta, \nu \\ \sigma, q}} \int_{-\infty}^{\infty} dE \eta E \cdot \Gamma_{r\nu\sigma}(E) [f_r^\eta(E) - q f_r^{\bar{\eta}}(E)] G_{\bar{\eta}l_r\sigma}^- e^{i[\eta E - L]\Delta t} G_{\eta l_r\sigma}^q. \end{aligned} \quad (\text{B.9})$$

Note that we have used  $\text{Im}(\Gamma) = 0$  [Eq. (A.9)].

Since we require the trace  $\sum_X (XX | \mathcal{W}_{1,E}^r | \bullet)$ , we calculate the matrix element  $(XX | \mathcal{W}_{1,E}^r | X_\alpha X_\beta)$ . Performing a calculation analogous to Eq. (A.12) yields

$$\begin{aligned} (XX | G_{\bar{\eta}l_r\sigma}^- e^{-iL\Delta t} G_{\eta l_r\sigma}^q | X_\alpha X_\beta) &= \frac{\delta_{X_\beta}^{X_\alpha}}{2} \sum_{X_\gamma} \left\{ e^{-i\Delta E_{X_\alpha}^{\eta(l_r, \sigma)} \Delta t} \delta_{X_\alpha + \eta(l_r, \sigma)}^{X_\gamma} [\delta_{X_\alpha}^X + \delta_{X_\gamma}^X] \right. \\ &\quad \left. + q e^{-i\Delta E_{\bar{\eta}(l_r, \sigma)}^{X_\alpha} \Delta t} \delta_{X_\alpha - \eta(l_r, \sigma)}^{X_\gamma} [\delta_{X_\alpha}^X + \delta_{X_\gamma}^X] \right\}. \end{aligned} \quad (\text{B.10})$$

In comparison to Eq. (A.12), we find a  $+$  instead of a  $-$  in front of the  $q$  as well as between the Kronecker deltas in the square brackets.

Next, taking matrix elements in Eq. (B.9), we use Eq. (B.10) and subsequently

sum over  $q$  and  $\eta$ . We obtain

$$\begin{aligned}
& (XX|\mathcal{W}_{1,E}^r(\Delta t)|X_\alpha X_\beta) \\
&= -\frac{\delta_{X_\beta}^{X_\alpha}}{2\pi} \sum_{\substack{\nu,\sigma \\ X_\gamma}} \int_{-\infty}^{\infty} dE \Gamma_{r\nu\sigma}(E) \cdot E \\
&\quad \left\{ f_r^+(E) \delta_{X_{\alpha+(l_r,\sigma)}}^{X_\gamma} \left( \delta_{X_{\alpha+(l_r,\sigma)}}^X + \delta_X^{X_\alpha} \right) \cos \left( (\Delta E_{X_\alpha}^{+(l_r,\sigma)} - E) \Delta t \right) \right. \\
&\quad \left. - f_r^-(E) \delta_{X_{\alpha-(l_r,\sigma)}}^{X_\gamma} \left( \delta_{X_{\alpha-(l_r,\sigma)}}^X + \delta_X^{X_\alpha} \right) \cos \left( (\Delta E_{X_\alpha}^{-(l_r,\sigma)} - E) \Delta t \right) \right\}. \tag{B.11}
\end{aligned}$$

This again shows that we only need to consider the secular terms of the kernel. We therefore introduce the matrix  $(\mathbf{W}_E^r)_{XX'} = (XX|\mathcal{W}_{1,E}^r|X'X')$ , and continue by calculating the zero frequency Laplace transform of this matrix. Following the steps carried out from Eq. (A.15) to Eq. (A.17), we arrive at

$$\begin{aligned}
(\mathbf{W}_E^r)_{XX'} &= - \sum_{\nu,\sigma} \left\{ \frac{\Delta E_{X'}^{+(l_r,\sigma)} \Gamma_{r\nu\sigma}(\Delta E_{X'}^{+(l_r,\sigma)}) f_r^+(\Delta E_{X'}^{+(l_r,\sigma)})}{2} \right. \\
&\quad \times \sum_{X_\gamma} \left[ \delta_{X'+(l_r,\sigma)}^{X_\gamma} \left( \delta_{X'+(l_r,\sigma)}^X + \delta_X^{X'} \right) \right] \\
&\quad - \frac{\Delta E_{X'}^{-(l_r,\sigma)} \Gamma_{r\nu\sigma}(\Delta E_{X'}^{-(l_r,\sigma)}) f_r^-(\Delta E_{X'}^{-(l_r,\sigma)})}{2} \\
&\quad \left. \times \sum_{X_\gamma} \left[ \delta_{X'-(l_r,\sigma)}^{X_\gamma} \left( \delta_{X'-(l_r,\sigma)}^X + \delta_X^{X'} \right) \right] \right\}. \tag{B.12}
\end{aligned}$$

This is the explicit form of the energy current kernel that can be used to calculate the heat current for the single-level quantum dot in Sec. 4.4. However, we have already claimed in Sec. 2.6.1 that the energy current in the Born-Markov limit is conserved, allowing us to rewrite the heat current as a current *out of the open system* [Eq. (2.29)]. With the explicit expression (B.4), this is now straightforward to prove.

The main trick is to use that we only need to calculate the trace over the current kernel times the probabilities  $P_X(t) = (XX|\rho(t))$  entering the reduced density operator, that is, terms of the general form

$$\sum_{X'} \left[ \sum_X (\mathbf{W}_E^r)_{XX'} \right] P_{X'}. \tag{B.13}$$

We use this explicitly by combining Eq. (B.12) with Eq. (B.4):

$$\begin{aligned}
& \sum_X [(-\mathbf{W}_E^r)_{XX'} - E_X (\mathbf{W}^r)_{XX'}] \\
&= \sum_{X,\nu,\sigma} \left\{ \sum_{X_\gamma} \delta_{X'+(l_r,\sigma)}^{X_\gamma} \frac{\Gamma_{r\sigma}(\Delta E_{X'}^{+(l_r,\sigma)})}{2} f_r^+(\Delta E_{X'}^{+(l_r,\sigma)}) \right. \\
&\quad \times \left[ \delta_{X'+(l_r,\sigma)}^X \left( \Delta E_{X'}^{+(l_r,\sigma)} - 2E_X \right) + \delta_X^{X'} \left( \Delta E_{X'}^{+(l_r,\sigma)} + 2E_X \right) \right] \\
&\quad - \sum_{X_\gamma} \delta_{X'-(l_r,\sigma)}^{X_\gamma} \frac{\Gamma_{r\sigma}(\Delta E_{X'}^{-(l_r,\sigma)})}{2} f_r^-(\Delta E_{X'}^{-(l_r,\sigma)}) \\
&\quad \times \left[ \delta_{X'-(l_r,\sigma)}^X \left( \Delta E_{X'}^{-(l_r,\sigma)} + 2E_X \right) + \delta_X^{X'} \left( \Delta E_{X'}^{-(l_r,\sigma)} - 2E_X \right) \right] \left. \right\} \\
&= \sum_{\nu,\sigma} \left\{ \sum_{X_\gamma} \delta_{X'+(l_r,\sigma)}^{X_\gamma} \frac{\Gamma_{r\sigma}(\Delta E_{X'}^{+(l_r,\sigma)})}{2} f_r^+(\Delta E_{X'}^{+(l_r,\sigma)}) \right. \\
&\quad \times \left[ -E_{X'+(l_r,\sigma)} - E_{X'} + E_{X'+(l_r,\sigma)} + E_{X'} \right] \\
&\quad - \sum_{X_\gamma} \delta_{X'-(l_r,\sigma)}^{X_\gamma} \frac{\Gamma_{r\sigma}(\Delta E_{X'}^{-(l_r,\sigma)})}{2} f_r^-(\Delta E_{X'}^{-(l_r,\sigma)}) \\
&\quad \times \left[ E_{X'} + E_{X'-(l_r,\sigma)} - E_{X'} - E_{X'-(l_r,\sigma)} \right] \left. \right\} \\
&= 0, \tag{B.14}
\end{aligned}$$

where  $E_X$  are the energies of the many-body energy eigenstates  $|X\rangle$ . In other words, we find

$$\sum_X (\mathbf{W}_E^r)_{XX'} \bullet = - \sum_X E_X (\mathbf{W}^r)_{XX'} \bullet, \tag{B.15}$$

which together with Eq. (B.13) proves the simplified heat current formula (2.29). Physically, this means that for the systems of interest here and in paper I and II, the energy current is conserved in the Born-Markov limit.



# Appendix C

## Influence of the fermion-parity mode

In Sec. 3.3 in Eq. (3.15), we claim that any correlator  $(O^\dagger|(-\mathbf{1})^N)$  of an operator  $O$  can only be non-zero if  $O$  is *linearly dependent* on the product of all occupation number operators  $N_j$  of single-particle states  $|j\rangle = |l_j\sigma\rangle$  [Sec. 2.1] defining the open system:

$$O \stackrel{!}{=} \alpha \cdot \prod_j N_j + O^{\text{rest}} \quad , \quad \alpha \in \mathbb{R}^{\neq 0}, \quad (\text{C.1})$$

with the remaining part  $O^{\text{rest}}$  defined to be linearly independent of  $\prod_j N_j$ . In this appendix, we prove this relation. For a convenient notation, we here write field operators for the open system states as

$$d_j^{\eta_j} = \begin{cases} d_j^\dagger & \eta_j = +1 \\ d_j & \eta_j = -1 \end{cases}. \quad (\text{C.2})$$

The occupation number states are in the following denoted as  $|\{n_j\}\rangle$ , with  $n_j := n_{l_j\sigma_j}$  being the particle number in state  $j = (l_j, \sigma_j)$ .

First, we note that due to the anticommutation relation for field operators acting on the open system,

$$\{d_j^{\eta_j}, d_{j'}^{\eta_{j'}}\} = \delta_{jj'} \delta_{\eta_j(-\eta_{j'})}, \quad (\text{C.3})$$

we can expand any linear operator  $A$  acting on the many-body Fock space of the open system which *does not* have the form (C.1) into a sum of operators which are all a product of the following two operators: one term  $A_{\neq j}$  which is a product of field operators that *do not* create or annihilate a particle in the state  $j = (l_j, \sigma_j)$ , and another operator which is either the identity or one fermionic operator  $d_j^{\eta_j}$ , either creating ( $\eta = +$ ) or annihilating ( $\eta = -$ ) an electron in the single-particle state  $j = (l_j, \sigma_j)$ :

$$A = \sum_{\{j\}} \beta_j A_{\neq j} \cdot (\alpha_j d_j^{\eta_j} + 1 - \alpha_j) \quad , \quad \alpha_j = 0, 1, \quad (\text{C.4})$$

where the sum goes *at least*<sup>1</sup> once over all states  $j$ . In the following, we prove

<sup>1</sup>We allow for multiple summands for each state  $j$  with different coefficients  $\beta_j$ , such that we also include any possible linear combination 1 and  $d_j^{\eta_j}$ .

Eq. (C.1) by showing that

$$\left([A_{\neq j} \cdot (\alpha d_j^{\eta_j} + 1 - \alpha)\right]^\dagger |(-\mathbb{1})^N\rangle = 0 \quad (\text{C.5})$$

for each summand in the sum (C.4). Using

$$\langle \{n_m\} | \bullet | \{n_m\} \rangle = \langle \{n_m\}, n_j = 0 | (n_j d_j + 1 - n_j) \bullet (n_j d_j^\dagger + 1 - n_j) | \{n_m\}, n_j = 0 \rangle, \quad (\text{C.6})$$

the splitting  $(-\mathbb{1})^N = (-\mathbb{1})^{N_j} (-\mathbb{1})^{\sum_{m \neq j} N_m}$ , and the anticommutation relation (C.3), we find

$$\begin{aligned} & \left([A_{\neq j} \cdot (\alpha d_j^{\eta_j} + 1 - \alpha)\right]^\dagger |(-\mathbb{1})^N\rangle \\ &= \sum_{\{n_m\}} \langle \{n_m\} | A_{\neq j} \cdot (\alpha d_j^{\eta_j} + 1 - \alpha) (-\mathbb{1})^N | \{n_m\} \rangle \\ &= \sum_{\{n_m\}} \langle \{n_m\}, n_j = 0 | \left[ (n_j d_j + 1 - n_j) A_{\neq j} (-\mathbb{1})^{\sum_{m \neq j} N_m} \right. \\ & \quad \left. \times (\alpha d_j^{\eta_j} + 1 - \alpha) (-\mathbb{1})^{N_j} (n_j d_j^\dagger + 1 - n_j) \right] | \{n_m\}, n_j = 0 \rangle \\ &= \sum_{\{n_m\}_{m \neq j}} \langle \{n_m\}, n_j = 0 | A_{\neq j} (-\mathbb{1})^{\sum_{m \neq j} N_m} \\ & \quad \times \sum_{n_j} \left[ (\sigma n_j d_j + 1 - n_j) (\alpha d_j^{\eta_j} + 1 - \alpha) (-\mathbb{1})^{N_j} (n_j d_j^\dagger + 1 - n_j) \right] \\ & \quad \times | \{n_m\}, n_j = 0 \rangle, \end{aligned} \quad (\text{C.7})$$

where the factor  $\sigma \in \{\pm 1\}$  is the result of commuting  $d_j$  with  $A_{\neq j}$  [Eq. (C.3)], and  $\alpha$  is chosen to be 0 or 1 [Eq. (C.4)].

Next, let us simplify the sum over  $n_j$ . Using the fermionic anticommutation relations and  $(-\mathbb{1})^{N_j} = 1 - 2N_j$ , we find

$$\begin{aligned} & \sum_{n_j} \left[ (\sigma n_j d_j + 1 - n_j) (\alpha d_j^{\eta_j} + 1 - \alpha) (-\mathbb{1})^{N_j} (n_j d_j^\dagger + 1 - n_j) \right] \\ &= (\alpha d_j^{\eta_j} + 1 - \alpha) (-\mathbb{1})^{N_j} + \sigma d_j (\alpha d_j^{\eta_j} + 1 - \alpha) (-\mathbb{1})^{N_j} d_j^\dagger \\ &= \eta_j \alpha d_j^{\eta_j} + (1 - \alpha) [1 - \sigma - (2 - \sigma) N_j]. \end{aligned} \quad (\text{C.8})$$

Substituting this back into Eq. (C.7) and using

$$\langle \{n_m\}, n_j = 0 | A_{\neq j} d_j^{\eta_j} | \{n_m\}, n_j = 0 \rangle = \langle \{n_m\}, n_j = 0 | A_{\neq j} N_j | \{n_m\}, n_j = 0 \rangle = 0, \quad (\text{C.9})$$

for any choice of  $A_{\neq j}$ , one obtains

$$\begin{aligned} & \left([A_{\neq j} \cdot (\alpha d_j^{\eta_j} + 1 - \alpha)\right]^\dagger |(-\mathbb{1})^N\rangle \\ &= \sum_{\{n_m\}_{m \neq j}} \langle \{n_m\}, n_j = 0 | A_{\neq j} (-\mathbb{1})^{\sum_{m \neq j} N_m} (1 - \alpha) (1 - \sigma) | \{n_m\}, n_j = 0 \rangle. \end{aligned} \quad (\text{C.10})$$

For  $\alpha = 1$ , this obviously vanishes. For  $\alpha = 0$  and  $\sigma = -1$ , corresponding to an odd number of field operators in  $A_{\neq j}$ , the correlator  $(A_{\neq j}^\dagger |(-\mathbf{1})^N)$  vanishes merely as a consequence of the cyclic property of the trace. However, as apparent from Eq. (C.10), it also vanishes for  $\sigma = 1$ . We have therefore derived that

$$([A_{\neq j} \cdot (\alpha_j d_j^n + 1 - \alpha)]^\dagger |(-\mathbf{1})^N) = 0. \quad (\text{C.11})$$

With  $N_j(-\mathbf{1})^{N_j} = -N_j$ , it becomes clear that in order for  $(O^\dagger |(-\mathbf{1})^N)$  to be non-zero, the operator  $O$  needs to contain one creation and one annihilation operator forming the occupation number operator  $N_j = d_j^\dagger d_j$ . Repeating the same argument for  $A_{\neq i}$  with all other states  $i \equiv (l_i, \sigma_i) \neq j$  and finally using  $(\mathbf{1} |(-\mathbf{1})^N) = 0$ , one can conclude that the Eq. (C.1) must hold for the correlator  $(O^\dagger |(-\mathbf{1})^N)$  to be non-zero.



# References

- [1] T. A. Fulton and G. J. Dolan, “Observation of single-electron charging effects in small tunnel junctions”, *Phys. Rev. Lett.* **59**, 109–112 (1987) (cit. on pp. 1, 3, 5, 6).
- [2] J. H. F. Scott-Thomas, S. B. Field, M. A. Kastner, H. I. Smith, and D. A. Antoniadis, “Conductance Oscillations Periodic in the Density of a One-Dimensional Electron Gas”, *Phys. Rev. Lett.* **62**, 583–586 (1989) (cit. on pp. 1, 5).
- [3] U. Meirav, M. A. Kastner, and S. J. Wind, “Single-electron charging and periodic conductance resonances in GaAs nanostructures”, *Phys. Rev. Lett.* **65**, 771–774 (1990) (cit. on pp. 1, 5).
- [4] A. T. Johnson, L. P. Kouwenhoven, W. de Jong, N. C. van der Vaart, C. J. P. M. Harmans, and C. T. Foxon, “Zero-dimensional states and single electron charging in quantum dots”, *Phys. Rev. Lett.* **69**, 1592–1595 (1992) (cit. on pp. 1, 5).
- [5] E. B. Foxman, P. L. McEuen, U. Meirav, N. S. Wingreen, Y. Meir, P. A. Belk, N. R. Belk, M. A. Kastner, and S. J. Wind, “Effects of quantum levels on transport through a Coulomb island”, *Phys. Rev. B* **47**, 10020–10023 (1993) (cit. on pp. 1, 5).
- [6] J. Weis, R. J. Haug, K. v. Klitzing, and K. Ploog, “Competing channels in single-electron tunneling through a quantum dot”, *Phys. Rev. Lett.* **71**, 4019–4022 (1993) (cit. on pp. 1, 5).
- [7] M. Kastner, “The single electron transistor and artificial atoms”, *Ann. Phys.* **9**, 885–894 (2000) (cit. on pp. 1, 5, 58).
- [8] M. Büttiker, A. Prêtre, and H. Thomas, “Dynamic conductance and the scattering matrix of small conductors”, *Phys. Rev. Lett.* **70**, 4114–4117 (1993) (cit. on pp. 1, 3, 13, 40).
- [9] M. Büttiker, H. Thomas, and A. Prêtre, “Mesoscopic capacitors”, *Phys. Lett. A* **180**, 364–369 (1993) (cit. on pp. 1, 3).
- [10] A. Prêtre, H. Thomas, and M. Büttiker, “Dynamic admittance of mesoscopic conductors: Discrete-potential model”, *Phys. Rev. B* **54**, 8130–8143 (1996) (cit. on pp. 1, 3).

- 
- [11] J. Gabelli, G. Fève, J.-M. Berroir, B. Plaçais, A. Cavanna, B. Etienne, Y. Jin, and D. C. Glattli, “Violation of Kirchhoff’s laws for a coherent RC circuit”, *Science* **313**, 499 (2006) (cit. on pp. 1, 5).
- [12] G. Fève, A. Mahé, J.-M. Berroir, T. Kontos, B. Plaçais, D. C. Glattli, A. Cavanna, B. Etienne, and Y. Jin, “An On-Demand Coherent Single-Electron Source”, *Science* **316**, 1169–1172 (2007) (cit. on pp. 1, 5, 6).
- [13] A. Mahé, F. D. Parmentier, E. Bocquillon, J.-M. Berroir, D. C. Glattli, T. Kontos, B. Plaçais, G. Fève, A. Cavanna, and Y. Jin, “Current correlations of an on-demand single-electron emitter”, *Phys. Rev. B* **82**, 201309 (2010) (cit. on pp. 1, 2, 5).
- [14] D. Loss and D. P. DiVincenzo, “Quantum computation with quantum dots”, *Phys. Rev. A* **57**, 120–126 (1998) (cit. on p. 1).
- [15] M. Field, C. G. Smith, M. Pepper, D. A. Ritchie, J. E. F. Frost, G. A. C. Jones, and D. G. Hasko, “Measurements of Coulomb blockade with a noninvasive voltage probe”, *Phys. Rev. Lett.* **70**, 1311–1314 (1993) (cit. on pp. 1, 6).
- [16] R. J. Schoelkopf, P. Wahlgren, A. A. Kozhevnikov, P. Delsing, and D. E. Prober, “The Radio-Frequency Single-Electron Transistor (RF-SET): A Fast and Ultrasensitive Electrometer”, *Science* **280**, 1238–1242 (1998) (cit. on pp. 1, 6).
- [17] W. Lu, Z. Ji, L. Pfeiffer, K. W. West, and A. J. Rimberg, “Real-time detection of electron tunnelling in a quantum dot”, *Nature* **423**, 422–425 (2003) (cit. on pp. 1, 6, 28).
- [18] T. Fujisawa, T. Hayashi, Y. Hirayama, H. D. Cheong, and Y. H. Jeong, *Appl. Phys. Lett.* **84**, 2343–2345 (2004) (cit. on pp. 1, 6, 28).
- [19] J. Elzerman, R. Hanson, L. Willems van Beveren, B. Witkamp, L. Vandersypen, and L. Kouwenhoven, “Single-shot read-out of an individual electron spin in a quantum dot”, *Nature* **430**, 431–435 (2004) (cit. on pp. 1, 5, 6, 27, 28).
- [20] S. Gustavsson, R. Leturcq, M. Studer, I. Shorubalko, T. Ihn, K. Ensslin, D. Driscoll, and A. Gossard, “Electron counting in quantum dots”, *Surf. Sci. Rep.* **64**, 191–232 (2009) (cit. on pp. 1, 6, 27, 28).
- [21] C. Barthel, M. Kjærgaard, J. Medford, M. Stopa, C. M. Marcus, M. P. Hanson, and A. C. Gossard, “Fast sensing of double-dot charge arrangement and spin state with a radio-frequency sensor quantum dot”, *Phys. Rev. B* **81**, 161308 (2010) (cit. on pp. 1, 6, 57).
- [22] J. Güttinger, J. Seif, C. Stampfer, A. Capelli, K. Ensslin, and T. Ihn, “Time-resolved charge detection in graphene quantum dots”, *Phys. Rev. B* **83**, 165445 (2011) (cit. on pp. 1, 6, 27, 28).

- 
- [23] E. Bocquillon, F. D. Parmentier, C. Grenier, J.-M. Berroir, P. Degiovanni, D. C. Glattli, B. Pla çais, A. Cavanna, Y. Jin, and G. Fève, “Electron Quantum Optics: Partitioning Electrons One by One”, *Phys. Rev. Lett.* **108**, 196803 (2012) (cit. on pp. 1, 2).
- [24] J. P. Pekola, O.-P. Saira, V. F. Maisi, A. Kemppinen, M. Möttönen, Y. A. Pashkin, and D. V. Averin, “Single-electron current sources: Toward a refined definition of the ampere”, *Rev. Mod. Phys.* **85**, 1421–1472 (2013) (cit. on pp. 1, 5, 6, 27, 28).
- [25] F. Battista, “Single particle sources and quantum heat fluctuations”, *Contemp. Phys.* **55**, 286–301 (2014) (cit. on p. 1).
- [26] H.-P. Breuer and F. Petruccione, *The Theory of Open Quantum Systems* (Oxford University Press, 2002) (cit. on pp. 2, 20, 31).
- [27] H. Schoeller, “A perturbative nonequilibrium renormalization group method for dissipative quantum mechanics”, English, *Eur. Phys. Journ. Special Topics* **168**, 179–266 (2009) (cit. on pp. 2, 22, 31, 36, 79).
- [28] C. Karrasch, S. Andergassen, M. Pletyukhov, D. Schuricht, L. Borda, V. Meden, and H. Schoeller, “Non-equilibrium current and relaxation dynamics of a charge-fluctuating quantum dot”, *EPL* **90**, 30003 (2010) (cit. on pp. 2, 31).
- [29] S. Andergassen, M. Pletyukhov, D. Schuricht, H. Schoeller, and L. Borda, “Renormalization group analysis of the interacting resonant-level model at finite bias: Generic analytic study of static properties and quench dynamics”, *Phys. Rev. B* **83**, 205103 (2011) (cit. on pp. 2, 31).
- [30] H.-P. Breuer, “Foundations and measures of quantum non-Markovianity”, *J. Phys. B: At., Mol. Opt. Phys.* **45**, 154001 (2012) (cit. on p. 2).
- [31] E.-M. Laine, H.-P. Breuer, J. Piilo, C.-F. Li, and G.-C. Guo, “Nonlocal Memory Effects in the Dynamics of Open Quantum Systems”, *Phys. Rev. Lett.* **108**, 210402 (2012) (cit. on p. 2).
- [32] O. Kashuba and H. Schoeller, “Transient dynamics of open quantum systems”, *Phys. Rev. B* **87**, 201402 (2013) (cit. on pp. 2, 31).
- [33] O. Kashuba, D. M. Kennes, M. Pletyukhov, V. Meden, and H. Schoeller, “Quench dynamics of a dissipative quantum system: A renormalization group study”, *Phys. Rev. B* **88**, 165133 (2013) (cit. on pp. 2, 31).
- [34] D. M. Kennes, O. Kashuba, M. Pletyukhov, H. Schoeller, and V. Meden, “Oscillatory Dynamics and Non-Markovian Memory in Dissipative Quantum Systems”, *Phys. Rev. Lett.* **110**, 100405 (2013) (cit. on pp. 2, 31).
- [35] S. Wißmann, H.-P. Breuer, and B. Vacchini, “Generalized trace-distance measure connecting quantum and classical non-Markovianity”, *Phys. Rev. A* **92**, 042108 (2015) (cit. on p. 2).

- 
- [36] R. Schmidt, M. F. Carusela, J. P. Pekola, S. Suomela, and J. Ankerhold, “Work and heat for two-level systems in dissipative environments: Strong driving and non-Markovian dynamics”, *Phys. Rev. B* **91**, 224303 (2015) (cit. on p. 2).
- [37] S. Das and G. S. Agarwal, “Decoherence effects in interacting qubits under the influence of various environments”, *J. Phys. B: At., Mol. Opt. Phys.* **42**, 205502 (2009) (cit. on pp. 2, 13).
- [38] E. Ferraro, M. Scala, R. Migliore, and A. Napoli, “Non-Markovian dissipative dynamics of two coupled qubits in independent reservoirs: Comparison between exact solutions and master-equation approaches”, *Phys. Rev. A* **80**, 042112 (2009) (cit. on pp. 2, 13).
- [39] L. Aolita, F. de Melo, and L. Davidovich, “Open-system dynamics of entanglement: a key issues review”, *Rep. Prog. Phys.* **78**, 042001 (2015) (cit. on pp. 2, 13).
- [40] R.-P. Riwar, J. Splettstoesser, and J. König, “Zero-frequency noise in adiabatically driven interacting quantum systems”, *Phys. Rev. B* **87**, 195407 (2013) (cit. on p. 2).
- [41] T. J. Suzuki and T. Kato, “Effects of Coulomb interaction on photon-assisted current noise through a quantum dot”, *Phys. Rev. B* **91**, 165302 (2015) (cit. on p. 2).
- [42] P. Streda, “Quantised thermopower of a channel in the ballistic regime”, *J. Phys.: Condens. Matter* **1**, 1025 (1989) (cit. on pp. 2, 9).
- [43] C. W. J. Beenakker and A. A. M. Staring, “Theory of the thermopower of a quantum dot”, *Phys. Rev. B* **46**, 9667–9676 (1992) (cit. on pp. 2, 9).
- [44] A. A. M. Staring, L. W. Molenkamp, B. W. Alphenaar, H. van Houten, O. J. A. Buyk, M. A. A. Mabeoone, C. W. J. Beenakker, and C. T. Foxon, “Coulomb-Blockade Oscillations in the Thermopower of a Quantum Dot”, **22**, 57 (1993) (cit. on pp. 2, 9).
- [45] L. D. Hicks and M. S. Dresselhaus, “Effect of quantum-well structures on the thermoelectric figure of merit”, *Phys. Rev. B* **47**, 12727–12731 (1993) (cit. on pp. 2, 9).
- [46] L. D. Hicks and M. S. Dresselhaus, “Thermoelectric figure of merit of a one-dimensional conductor”, *Phys. Rev. B* **47**, 16631–16634 (1993) (cit. on pp. 2, 9).
- [47] G. D. Mahan and J. O. Sofo, “The best thermoelectric”, *P. Natl. Acad. Sci. USA* **93**, 7436–7439 (1996) (cit. on pp. 2, 9).
- [48] F. Giazotto, T. T. Heikkilä, A. Luukanen, A. M. Savin, and J. P. Pekola, “Opportunities for mesoscopics in thermometry and refrigeration: Physics and applications”, *Rev. Mod. Phys.* **78**, 217–274 (2006) (cit. on pp. 2, 9).

- 
- [49] Y. Dubi and M. Di Ventra, “*Colloquium* : Heat flow and thermoelectricity in atomic and molecular junctions”, *Rev. Mod. Phys.* **83**, 131–155 (2011) (cit. on pp. 2, 9).
- [50] B. Sothmann, R. Sánchez, and A. N. Jordan, “Thermoelectric energy harvesting with quantum dots”, *Nanotechnology* **26**, 032001 (2015) (cit. on pp. 2, 9–11, 47, 49, 53, 66).
- [51] M. Moskalets and M. Büttiker, “Heat production and current noise for single- and double-cavity quantum capacitors”, *Phys. Rev. B* **80**, 081302 (2009) (cit. on pp. 2, 11, 13, 40, 47).
- [52] M. Esposito, R. Kawai, K. Lindenberg, and C. van den Broeck, “Finite-time thermodynamics for a single-level quantum dot”, *EPL* **89**, 20003 (2010) (cit. on pp. 2, 11, 13, 40, 47).
- [53] J. S. Lim, R. López, and D. Sánchez, “Dynamic thermoelectric and heat transport in mesoscopic capacitors”, *Phys. Rev. B* **88**, 201304 (2013) (cit. on pp. 2, 11, 13, 40, 47).
- [54] S. Juergens, F. Haupt, M. Moskalets, and J. Splettstoesser, “Thermoelectric performance of a driven double quantum dot”, *Phys. Rev. B* **87**, 245423 (2013) (cit. on pp. 2, 11, 13, 40, 47).
- [55] F. Battista, M. Moskalets, M. Albert, and P. Samuelsson, “Quantum Heat Fluctuations of Single-Particle Sources”, *Phys. Rev. Lett.* **110**, 126602 (2013) (cit. on pp. 2, 11, 13, 40, 47).
- [56] M. F. Ludovico, J. S. Lim, M. Moskalets, L. Arrachea, and D. Sánchez, “Dynamical energy transfer in ac-driven quantum systems”, *Phys. Rev. B* **89**, 161306 (2014) (cit. on pp. 2, 11, 13, 40, 47).
- [57] H. Zhou, J. Thingna, P. Hänggi, J.-S. Wang, and B. Li, “Boosting thermoelectric efficiency using time-dependent control”, *Sci. Rep.* **5**, 14870 (2015) (cit. on pp. 2, 11, 13, 40, 47).
- [58] J. D. Fletcher, P. See, H. Howe, M. Pepper, S. P. Giblin, J. P. Griffiths, G. A. C. Jones, I. Farrer, D. A. Ritchie, T. J. B. M. Janssen, and M. Kataoka, “Clock-Controlled Emission of Single-Electron Wave Packets in a Solid-State Circuit”, *Phys. Rev. Lett.* **111**, 216807 (2013) (cit. on pp. 2, 3, 11, 13, 40, 47).
- [59] S. Gasparinetti, K. L. Viisanen, O.-P. Saira, T. Faivre, M. Arzeo, M. Meschke, and J. P. Pekola, “Fast Electron Thermometry for Ultrasensitive Calorimetric Detection”, *Phys. Rev. Applied* **3**, 014007 (2015) (cit. on pp. 2, 3, 11, 13, 40, 47).
- [60] A. Beckel, A. Kurzmann, M. Geller, A. Ludwig, A. D. Wieck, J. König, and A. Lorke, “Asymmetry of charge relaxation times in quantum dots: The influence of degeneracy”, *EPL* **106**, 47002 (2014) (cit. on pp. 2, 6).

- [61] L. D. Contreras-Pulido, J. Splettstoesser, M. Governale, J. König, and M. Büttiker, “Time scales in the dynamics of an interacting quantum dot”, *Phys. Rev. B* **85**, 075301 (2012) (cit. on pp. 2, 6–8, 11, 13, 27, 39, 40, 51, 57, 77).
- [62] R. B. Saptsov and M. R. Wegewijs, “Fermionic superoperators for zero-temperature nonlinear transport: Real-time perturbation theory and renormalization group for Anderson quantum dots”, *Phys. Rev. B* **86**, 235432 (2012) (cit. on pp. 2, 7, 8, 11, 20, 22, 36, 39, 69–71, 79).
- [63] L. Schreiber and T. Leonhardt, *Lehrstuhl für Experimentalphysik und II. Physikalisches Institut, RWTH Aachen*, (2014) <https://www.rwth-aachen.de/cms/Quantuminfo/Forschung/Institut-fuer-Quantentechnologie/~eyea/Bluhm-SiGe/?lidx=1> (visited on 01/05/2016) (cit. on p. 4).
- [64] M. A. Reed, J. N. Randall, R. J. Aggarwal, R. J. Matyi, T. M. Moore, and A. E. Wetsel, “Observation of discrete electronic states in a zero-dimensional semiconductor nanostructure”, *Phys. Rev. Lett.* **60**, 535–537 (1988) (cit. on p. 3).
- [65] J. Alsmeier, E. Batke, and J. P. Kotthaus, “Voltage-tunable quantum dots on silicon”, *Phys. Rev. B* **41**, 1699–1702 (1990) (cit. on p. 3).
- [66] A. Lorke, J. P. Kotthaus, and K. Ploog, “Coupling of quantum dots on GaAs”, *Phys. Rev. Lett.* **64**, 2559–2562 (1990) (cit. on p. 3).
- [67] P. Guéret, N. Blanc, R. Germann, and H. Rothuizen, “Confinement and single-electron tunneling in Schottky-gated, laterally squeezed double-barrier quantum-well heterostructures”, *Phys. Rev. Lett.* **68**, 1896–1899 (1992) (cit. on p. 3).
- [68] B. Meurer, D. Heitmann, and K. Ploog, “Single-electron charging of quantum-dot atoms”, *Phys. Rev. Lett.* **68**, 1371–1374 (1992) (cit. on pp. 3, 5).
- [69] M. T. Björk, C. Thelander, A. E. Hansen, L. E. Jensen, M. W. Larsson, L. R. Wallenberg, and L. Samuelson, “Few-Electron Quantum Dots in Nanowires”, *Nano Lett.* **4**, 1621–1625 (2004) (cit. on pp. 4, 8).
- [70] L. J. Geerligs, V. F. Anderegg, P. A. M. Holweg, J. E. Mooij, H. Pothier, D. Esteve, C. Urbina, and M. H. Devoret, “Frequency-locked turnstile device for single electrons”, *Phys. Rev. Lett.* **64**, 2691–2694 (1990) (cit. on p. 5).
- [71] H. Pothier, P. Lafarge, C. Urbina, D. Esteve, and M. H. Devoret, “Single-Electron Pump Based on Charging Effects”, *EPL* **17**, 249 (1992) (cit. on p. 5).
- [72] L. P. Kouwenhoven, A. T. Johnson, N. C. van der Vaart, C. J. P. M. Harmans, and C. T. Foxon, “Quantized current in a quantum-dot turnstile using oscillating tunnel barriers”, *Phys. Rev. Lett.* **67**, 1626–1629 (1991) (cit. on p. 5).

- 
- [73] A. Fujiwara, N. M. Zimmerman, Y. Ono, and Y. Takahashi, “Current quantization due to single-electron transfer in Si-wire charge-coupled devices”, *Appl. Phys. Lett.* **84**, 1323–1325 (2004) (cit. on p. 5).
- [74] J. J. Sakurai, *Modern quantum mechanics* (Addison-Wesley, 1994) (cit. on pp. 6, 50, 75).
- [75] J. Splettstoesser, M. Governale, J. König, and M. Büttiker, “Charge and spin dynamics in interacting quantum dots”, *Phys. Rev. B* **81**, 165318 (2010) (cit. on pp. 6–8, 13, 27, 40, 51).
- [76] R. B. Saptsov and M. R. Wegewijs, “Time-dependent quantum transport: Causal superfermions, exact fermion-parity protected decay modes, and Pauli exclusion principle for mixed quantum states”, *Phys. Rev. B* **90**, 045407 (2014) (cit. on pp. 7, 8, 20, 22, 36, 39, 69–71, 79).
- [77] G. C. Wick, A. S. Wightman, and E. P. Wigner, “The Intrinsic Parity of Elementary Particles”, *Phys. Rev.* **88**, 101–105 (1952) (cit. on pp. 7, 35).
- [78] Y. Aharonov and L. Susskind, “Charge Superselection Rule”, *Phys. Rev.* **155**, 1428–1431 (1967) (cit. on pp. 7, 35).
- [79] R. Streater and A. Wightman, *PCT, spin and statistics, and all that*, Landmarks in Physics (Princeton University Press, 2000) (cit. on pp. 7, 35).
- [80] N. N. Bogolubov, A. A. Logunov, A. I. Oksak, and I. T. Todorov, *General principles of quantum field theory*, In Russian. English translation: Kluwer Academic Publishers, Dordrecht, 1989 (Nauka, Moscow, 1989) (cit. on pp. 7, 35).
- [81] C. Lotze, M. Corso, K. J. Franke, F. von Oppen, and J. I. Pascual, “Driving a Macroscopic Oscillator with the Stochastic Motion of a Hydrogen Molecule”, *Science* **338**, 779–782 (2012) (cit. on pp. 9, 47).
- [82] O. Abah, J. Roßnagel, G. Jacob, S. Deffner, F. Schmidt-Kaler, K. Singer, and E. Lutz, “Single-Ion Heat Engine at Maximum Power”, *Phys. Rev. Lett.* **109**, 203006 (2012) (cit. on pp. 9, 47).
- [83] J.-P. Brantut, C. Grenier, J. Meineke, D. Stadler, S. Krinner, C. Kollath, T. Esslinger, and A. Georges, “A Thermoelectric Heat Engine with Ultracold Atoms”, *Science* **342**, 713–715 (2013) (cit. on pp. 9, 47).
- [84] A. Bermudez, M. Bruderer, and M. B. Plenio, “Controlling and Measuring Quantum Transport of Heat in Trapped-Ion Crystals”, *Phys. Rev. Lett.* **111**, 040601 (2013) (cit. on pp. 9, 47).
- [85] R. Sánchez and M. Büttiker, “Optimal energy quanta to current conversion”, *Phys. Rev. B* **83**, 085428 (2011) (cit. on pp. 9, 10, 66).

- 
- [86] B. Sothmann, R. Sánchez, A. N. Jordan, and M. Büttiker, “Rectification of thermal fluctuations in a chaotic cavity heat engine”, *Phys. Rev. B* **85**, 205301 (2012) (cit. on pp. 9, 10, 66).
- [87] A. N. Jordan, B. Sothmann, R. Sánchez, and M. Büttiker, “Powerful and efficient energy harvester with resonant-tunneling quantum dots”, *Phys. Rev. B* **87**, 075312 (2013) (cit. on pp. 9, 10, 66).
- [88] F. Hartmann, P. Pfeffer, S. Höfling, M. Kamp, and L. Worschech, “Voltage Fluctuation to Current Converter with Coulomb-Coupled Quantum Dots”, *Phys. Rev. Lett.* **114**, 146805 (2015) (cit. on pp. 9, 10, 66).
- [89] H. Thierschmann, R. Sánchez, B. Sothmann, F. Arnold, C. Heyn, W. Hansen, H. Buhmann, and L. W. Molenkamp, “Three-terminal energy harvester with coupled quantum dots”, *Nat. Nanotechnol.* **10**, 854–858 (2015) (cit. on pp. 9, 10, 49, 66).
- [90] C. Van den Broeck, “Thermodynamic Efficiency at Maximum Power”, *Phys. Rev. Lett.* **95**, 190602 (2005) (cit. on p. 9).
- [91] M. Esposito, K. Lindenberg, and C. Van den Broeck, “Universality of Efficiency at Maximum Power”, *Phys. Rev. Lett.* **102**, 130602 (2009) (cit. on p. 9).
- [92] R. López and D. Sánchez, “Nonlinear heat transport in mesoscopic conductors: Rectification, Peltier effect, and Wiedemann-Franz law”, *Phys. Rev. B* **88**, 045129 (2013) (cit. on p. 9).
- [93] D. Sánchez and R. López, “Scattering Theory of Nonlinear Thermoelectric Transport”, *Phys. Rev. Lett.* **110**, 026804 (2013) (cit. on p. 9).
- [94] J. Meair and P. Jacquod, “Scattering theory of nonlinear thermoelectricity in quantum coherent conductors”, *J. Phys.: Condens. Matter* **25**, 082201 (2013) (cit. on p. 9).
- [95] S. F. Svensson, E. A. Hoffmann, N. Nakpathomkun, P. M. Wu, H. Xu, H. A. Nilsson, D. Sánchez, V. Kashcheyevs, and H. Linke, “Nonlinear thermovoltage and thermocurrent in quantum dots”, *New. J. Phys.* **15**, 105011 (2013) (cit. on p. 9).
- [96] R. S. Whitney, “Nonlinear thermoelectricity in point contacts at pinch off: A catastrophe aids cooling”, *Phys. Rev. B* **88**, 064302 (2013) (cit. on p. 9).
- [97] R. S. Whitney, “Thermodynamic and quantum bounds on nonlinear dc thermoelectric transport”, *Phys. Rev. B* **87**, 115404 (2013) (cit. on p. 9).
- [98] O. Entin-Wohlman, Y. Imry, and A. Aharony, “Three-terminal thermoelectric transport through a molecular junction”, *Phys. Rev. B* **82**, 115314 (2010) (cit. on p. 11).

- 
- [99] O. Entin-Wohlman and A. Aharony, “Three-terminal thermoelectric transport under broken time-reversal symmetry”, *Phys. Rev. B* **85**, 085401 (2012) (cit. on p. 11).
- [100] J.-H. Jiang, O. Entin-Wohlman, and Y. Imry, “Thermoelectric three-terminal hopping transport through one-dimensional nanosystems”, *Phys. Rev. B* **85**, 075412 (2012) (cit. on p. 11).
- [101] J.-H. Jiang, M. Kulkarni, D. Segal, and Y. Imry, “Phonon thermoelectric transistors and rectifiers”, *Phys. Rev. B* **92**, 045309 (2015) (cit. on p. 11).
- [102] T. Ruokola and T. Ojanen, “Theory of single-electron heat engines coupled to electromagnetic environments”, *Phys. Rev. B* **86**, 035454 (2012) (cit. on p. 11).
- [103] Y. Wang, C. Huang, T. Liao, and J. Chen, “Magnon-driven quantum dot refrigerators”, *Phys. Lett. A* **379**, 3054–3058 (2015) (cit. on p. 11).
- [104] L. Onsager, “Reciprocal Relations in Irreversible Processes. I.”, *Phys. Rev.* **37**, 405–426 (1931) (cit. on p. 11).
- [105] M. Esposito, M. A. Ochoa, and M. Galperin, “Quantum Thermodynamics: A Nonequilibrium Green’s Function Approach”, *Phys. Rev. Lett.* **114**, 080602 (2015) (cit. on pp. 11, 23).
- [106] M. Esposito, M. A. Ochoa, and M. Galperin, “Nature of heat in strongly coupled open quantum systems”, *Phys. Rev. B* **92**, 235440 (2015) (cit. on pp. 11, 23).
- [107] M. Büttiker, H. Thomas, and A. Prêtre, “Current partition in multiprobe conductors in the presence of slowly oscillating external potentials”, *English, Z. Phys. B Con. Mat.* **94**, 133–137 (1994) (cit. on pp. 13, 40).
- [108] N. Ubbelohde, F. Hohls, V. Kashcheyevs, T. Wagner, L. Fricke, B. Kästner, K. Pierz, H. W. Schumacher, and R. J. Haug, “Partitioning of on-demand electron pairs”, *Nat. Nanotechnol.* **10**, 46–49 (2015) (cit. on pp. 13, 40, 47).
- [109] S. Diehl, A. Micheli, A. Kantian, B. Kraus, H. Buchler, and P. Zoller, “Quantum states and phases in driven open quantum systems with cold atoms”, *Nat. Phys.* **4**, 878–883 (2008) (cit. on p. 13).
- [110] U. Schneider, L. Hackermuller, J. P. Ronzheimer, S. Will, S. Braun, T. Best, I. Bloch, E. Demler, S. Mandt, D. Rasch, and A. Rosch, “Fermionic transport and out-of-equilibrium dynamics in a homogeneous Hubbard model with ultracold atoms”, *Nat. Phys.* **8**, 213–218 (2012) (cit. on p. 13).
- [111] M. Knap, D. A. Abanin, and E. Demler, “Dissipative Dynamics of a Driven Quantum Spin Coupled to a Bath of Ultracold Fermions”, *Phys. Rev. Lett.* **111**, 265302 (2013) (cit. on p. 13).

- 
- [112] F. Hebenstreit, D. Banerjee, M. Hornung, F.-J. Jiang, F. Schranz, and U.-J. Wiese, “Real-time dynamics of open quantum spin systems driven by dissipative processes”, *Phys. Rev. B* **92**, 035116 (2015) (cit. on p. 13).
- [113] J. Rammer and H. Smith, “Quantum field-theoretical methods in transport theory of metals”, *Rev. Mod. Phys.* **58**, 323–359 (1986) (cit. on pp. 17, 18).
- [114] J. Dalibard, Y. Castin, and K. Mølmer, “Wave-function approach to dissipative processes in quantum optics”, *Phys. Rev. Lett.* **68**, 580–583 (1992) (cit. on p. 17).
- [115] C. W. Gardiner, A. S. Parkins, and P. Zoller, “Wave-function quantum stochastic differential equations and quantum-jump simulation methods”, *Phys. Rev. A* **46**, 4363–4381 (1992) (cit. on p. 17).
- [116] H. Schoeller and G. Schön, “Mesoscopic quantum transport: Resonant tunneling in the presence of a strong Coulomb interaction”, *Phys. Rev. B* **50**, 18436–18452 (1994) (cit. on pp. 20, 22, 36, 79).
- [117] J. König, J. Schmid, H. Schoeller, and G. Schön, “Resonant tunneling through ultrasmall quantum dots: Zero-bias anomalies, magnetic-field dependence, and boson-assisted transport”, *Phys. Rev. B* **54**, 16820–16837 (1996) (cit. on pp. 20, 22, 36, 79).
- [118] M. R. Wegewijs, *Lecture notes in Nanoscale transport: Quantum field theory in Liouville space*, July 2012 (cit. on pp. 22, 23, 79).
- [119] R. K. Wangsness and F. Bloch, “The Dynamical Theory of Nuclear Induction”, *Phys. Rev.* **89**, 728–739 (1953) (cit. on p. 22).
- [120] C. Timm, “Tunneling through molecules and quantum dots: Master-equation approaches”, *Phys. Rev. B* **77**, 195416 (2008) (cit. on p. 22).
- [121] H. Schoeller and F. Reininghaus, “Real-time renormalization group in frequency space: A two-loop analysis of the nonequilibrium anisotropic Kondo model at finite magnetic field”, *Phys. Rev. B* **80**, 045117 (2009) (cit. on p. 22).
- [122] G. Cohen, E. Gull, D. R. Reichman, A. J. Millis, and E. Rabani, “Numerically exact long-time magnetization dynamics at the nonequilibrium Kondo crossover of the Anderson impurity model”, *Phys. Rev. B* **87**, 195108 (2013) (cit. on p. 22).
- [123] C. Karlewski and M. Marthaler, “Time-local master equation connecting the Born and Markov approximations”, *Phys. Rev. B* **90**, 104302 (2014) (cit. on p. 22).
- [124] P. W. Anderson, “Model for the Electronic Structure of Amorphous Semiconductors”, *Phys. Rev. Lett.* **34**, 953–955 (1975) (cit. on pp. 28, 51).

- 
- [125] J. V. Koski, V. F. Maisi, J. P. Pekola, and D. V. Averin, “Experimental realization of a Szilard engine with a single electron”, *P. Natl. Acad. Sci. USA* **111**, 13786–13789 (2014) (cit. on p. 47).
- [126] T. Ihn, S. Gustavsson, U. Gasser, B. Küng, T. Müller, R. Schleser, M. Sigrist, I. Shorubalko, R. Leturcq, and K. Ensslin, “Quantum dots investigated with charge detection techniques”, *Solid State Commun.* **149**, 1419–1426 (2009) (cit. on p. 58).
- [127] P. Strasberg, G. Schaller, T. Brandes, and M. Esposito, “Thermodynamics of a Physical Model Implementing a Maxwell Demon”, *Phys. Rev. Lett.* **110**, 040601 (2013) (cit. on p. 66).
- [128] G. E. Crooks, “Entropy production fluctuation theorem and the nonequilibrium work relation for free energy differences”, *Phys. Rev. E* **60**, 2721–2726 (1999) (cit. on p. 66).
- [129] C. Jarzynski, “Nonequilibrium Equality for Free Energy Differences”, *Phys. Rev. Lett.* **78**, 2690–2693 (1997) (cit. on p. 66).
- [130] S. Mukamel, “Quantum Extension of the Jarzynski Relation: Analogy with Stochastic Dephasing”, *Phys. Rev. Lett.* **90**, 170604 (2003) (cit. on p. 66).
- [131] G. E. Crooks, “On the Jarzynski relation for dissipative quantum dynamics”, *J. Stat. Mech: Theory Exp.* **2008**, P10023 (2008) (cit. on p. 66).
- [132] M. Esposito, U. Harbola, and S. Mukamel, “Nonequilibrium fluctuations, fluctuation theorems, and counting statistics in quantum systems”, *Rev. Mod. Phys.* **81**, 1665–1702 (2009) (cit. on p. 66).
- [133] O. Perron, “Zur Theorie der Matrizen”, German, *Math. Ann.* **64**, 248–263 (1907) (cit. on p. 76).
- [134] G. Frobenius, “Über Matrizen aus nicht negativen Elementen”, German, *Sitzungsber. Königl. Preuss. Akad. Wiss.*, 456–477 (1912) (cit. on p. 76).